Rain follows the forest: Land use policy, climate change, and adaptation*

Florian Grosset-Touba, Anna Papp, and Charles A. Taylor†

August 12, 2026

Abstract

Human actions can alter the climate via land use. We analyze the 1930s Great Plains Shelterbelt, a large-scale forestation program across the US Midwest. The program increased precipitation and decreased temperatures for decades. We measure these changes in downwind counties where no trees were planted, isolating the effects of climate from those of afforestation and enabling us to study adaptation. Improved growing conditions allowed farmers to expand corn acreage and adopt water-intensive practices. In a period of farm consolidation, this altered the structure of the agricultural sector, contributing to the survival of small farms but less farm machine usage. The findings demonstrate the endogeneity of climate to land use change and the long-term impacts of tree planting on agricultural development.

*This paper greatly benefited from comments by Francis Annan, Douglas Almond, Price Fishback, Eyal Frank, Robert Heilmayer, Rick Hornbeck, Solomon Hsiang, Gary Libecap, Kyle Meng, Ben Olken, Wolfram Schlenker, Jeffrey Shrader, Aaron Smith, Marco Tabellini, Andrew Waxman, Andrew Wilson, Brian Wright, and various seminar participants. Aidan McCullen, Yixian Liu, Elisée Amewouame and Baptiste Guybert provided excellent research assistance. AI tools were used to support this research. We are grateful to Dr Meagan Snow for sharing digitized Shelterbelt data. All errors and omissions are our own.

†Grosset-Touba: CREST, ENSAE, Institut Polytechnique de Paris (florian.grosset-touba@ensae.fr); Papp: University of California, Santa Barbara (corresponding author: apapp@bren.ucsb.edu); Taylor: Harvard University (ctaylor@hks.harvard.edu).

"It is true, in like manner, of resources devoted to afforestation, since the beneficial effect on climate often extends beyond the borders of the estate owned by the person responsible for the forest." A.C. Pigou in describing when 'uncompensated services are rendered' in *The Economics of Welfare* (1932)

1 Introduction

Governments have pledged 500 million hectares of land for tree planting by 2050 under the Paris Agreement, an area equivalent to India, Turkey, and South Africa combined (Self et al. 2023). Private initiatives are on a similar scale, such as the World Economic Forum's One Trillion Trees campaign. While reducing net carbon emissions is the main motivation, trees are also planted to cool and shade cities, and to mitigate soil erosion, dust storms, and landslides in rural areas.

Another potential outcome of large-scale tree planting has been proposed by the natural science literature, but garnered less attention in public discourse: a change in the regional climate, driven by the impact of trees on energy and water fluxes. Atmospheric models predict changes in precipitation and temperature where trees are planted, as well as in downwind areas (Bonan 2008).[1] This potential policy-induced change in the local climate implies that large-scale tree planting could also affect economic outcomes through both mechanical effects (e.g., more favorable weather increases crop yields) and responses from individuals and firms (e.g., climate adaptation). These economic effects can manifest locally where trees are planted, but also in locations downwind that are not directly affected by the policy but experience a policy-induced change in climate nonetheless.

In this paper, we examine the causal impact of a large-scale tree-planting program on both climate and economic outcomes. We empirically test the qualitative climate predictions from atmospheric models in response to afforestation, and estimate the resulting magnitudes, focusing on regional effects in areas not directly afforested. We then study the consequences of this policy-induced climate change on agricultural development, and assess the role of climate adaptation.

[1] Precipitation is predicted to increase both locally and downwind. For temperature, the net local effect depends on land characteristics and latitude. Trees can increase evapotranspiration, which reduces temperatures. But since trees are generally darker than the land they are planted on (e.g., cropland or grassland), they can decrease albedo and surface reflection, thus raising temperatures. Comparing forests with nearby open land, satellite evidence shows that this balance varies with latitude: tropical forests cool strongly year-round, temperate forests show a small net cooling annually, and boreal forests can cause net warming (Li et al. 2015). This local channel is distinct from the global cooling due to carbon sequestration, which we do not estimate.

We focus on the Great Plains Shelterbelt in the United States. Planned in response to the Dust Bowl, this government-funded program aimed to reduce soil erosion and dust storms in the US Midwest. Announced in 1934 and implemented from 1935 to 1942, the program led to the planting of 220 million trees. The trees were grown in windbreaks, which consisted of numerous strips of trees planted between fields and farms, occupying less than 0.5% of the total area of the affected counties despite the program's scale. The resulting 'belt' of trees bisected the US from north to south, spanning 1,850km and crossing six states from North Dakota to Texas.

The largest afforestation effort of its time, the Great Plains Shelterbelt is now rivaled in scope by multiple tree-planting projects worldwide. While it was implemented over 85 years ago, we note that the socioeconomic conditions of the US Midwest in the 1940s are comparable to many lower and middle-income countries where similar programs are being designed and implemented today. We therefore focus on this specific program for its unique characteristics. The historical context provides the long time frame required for a direct study of the drivers and consequences of climate change, i.e., changes in the *distribution* of weather events over time. By combining USDA census data with information on climate and land use, we can empirically consider a rich set of outcomes over a long period. Our main sample spans 1930–1965, and we extend the analysis to 2002 to examine long-run persistence, presenting event studies that span 70 years.

The short and delimited policy implementation period allows for simple and clean identification strategies. We use a difference-in-differences strategy that exploits prevailing winds, which is the primary physical mechanism by which trees planted in a given location affect climate in nearby areas where the program is not implemented. We construct a wind exposure measure using hourly ERA5 reanalysis data to approximate a given location's exposure to winds arriving from areas afforested under the Shelterbelt. In our main specification, we exploit cross-sectional variation in average wind exposure. As a robustness check, we also exploit temporal variation in wind patterns, estimating a two-way fixed effects model that identifies effects purely from year-to-year changes in wind direction and speed. We augment the simple difference-in-differences specification with a set of baseline controls to compare areas with similar baseline climates.

We demonstrate that our results are robust to potential threats to identification, including the Dust Bowl and medium-term climate fluctuations, spatially-differential climate trends, strategic location of tree planting, treatment timing, endogeneity of the wind patterns themselves, spatial correlation in inference, interference across counties, and irrigation. We assess our identifying assumptions through balance and baseline pre-trend tests, an "honest" difference-in-differences analysis (Rambachan and Roth 2023), and binary-treatment and synthetic difference-in-differences specifications. We further show that our results hold under an instrumental variable strategy, long differences, alternative controls and fixed effects, alternative constructions of the wind exposure measure, and two alternative gridded climate datasets.

In this paper, we exclusively focus on effects outside the Shelterbelt, where no trees were planted. This spatial separation allows us to isolate the climate spillover channel—operating through increased precipitation and reduced extreme heat—from the direct, local effects of afforestation (e.g., changes in shade, soil quality, or erosion). Li (2021) studies these local effects, comparing afforested units with their direct neighbors, and finds a shift away from crops and towards pasture, likely driven by the benefits of shade for cattle.

We first show that large-scale tree planting substantially alters the climate in downwind non-afforested counties. To assess effect size, we compare counties in the 75th percentile of exposure to summer winds blowing through the Shelterbelt afforested areas to those in the 25th percentile. All estimates we report below are therefore relative differences—how outcomes evolved in high-exposure counties relative to comparable low-exposure ones—rather than absolute changes. We find that precipitation increased by 3.9%, or 2.8mm per month, during the summer months, and maximum temperature decreased by 0.5% (-0.16°C) as well (Table 1). Extreme heat, which has a strong negative impact on yields, decreased even more dramatically, with degree days above 29°C falling 5.7% in counties more exposed to winds from the Shelterbelt. The direction of these effects is consistent with atmospheric model predictions.

Having established that the Shelterbelt project induces climate change, our second step involves estimating the consequences of this climate change on the economy and assessing the role of adaptation. As in the first step, we continue to limit our analysis to areas near, but not directly afforested under the Shelterbelt project, to isolate the effect of climate change from other changes potentially associated with Shelterbelt participation. We focus on agriculture—both crops and livestock—a sector highly exposed to climate and representative of a large share of the economy of the post-war US Midwest.

We find that the production of corn, the key crop in the US Midwest, increased in response to this policy-induced climate change in counties downwind from the Shelterbelt relative to counties less exposed. Corn production increased by 35% in counties in the 75th percentile of wind exposure compared to counties in the 25th percentile. This effect is mostly driven by an expansion in the area of corn harvested by 29%, with a more modest increase in yields by 6%.

We explain this large relative increase in corn production primarily as a climate adaptation response by farmers, with a possible additional mechanical contribution from improved growing conditions. We observe a reallocation of cropland away from less water-intensive crops (e.g., wheat) and towards more water-intensive crops (e.g., corn), while total cropland increased by 8%. We also find a reallocation from pasture toward cropland, and growth in pigs and chickens, which require little or no grazing land, while the number of cattle does not change. Both patterns are consistent with farmers exploiting the wetter, cooler conditions that favor crop production.

These changes took place in a period of rapid farm consolidation in the US. By the mid-1960s, the number of farms had roughly halved relative to 1930, and the average farm size more than doubled (Dimitri et al. 2005; see Figure 3 therein). While much of this 'exit from agriculture' was driven by secular trends in agricultural technology—including the use of machines on larger farms—and structural transformation, we investigate whether the downwind effects of the Shelterbelt can explain spatial differences in farm consolidation.

We find that farm consolidation proceeded more slowly in counties downwind from the Shelterbelt: the total number of farms declined less and the share of small farms rose, relative to control counties. Two readings fit this pattern. The improved climate may have lowered the size at which a farm could operate efficiently, or it may have spared small farms from exposure to bad years with extreme weather events. County aggregates cannot separate the two, but the historical record suggests the second. Consolidation on the Plains had long occurred through drought-driven failure and foreclosure, and it fell hardest on the small farms that lacked enough production to cover costs and service mortgage debt. That vulnerability tracked climate: between 1890 and 1920 average farm size more than doubled in western Kansas following a series of intense droughts but rose by less than a fifth in the wetter east (Libecap and Hansen 2002). While the climate shift we estimate is modest on average, it would reduce exposure to the extreme heat and drought that drive crop loss in bad years. Reduced crop failure and associated farmer exit (Hornbeck 2012) is a channel we cannot separately identify.[2] The survival of relatively more small farms in exposed counties, even as consolidation swept the region, shows that a policy-induced change in climate can alter the structure of the agricultural sector, not only the level of output.

This reduced farm consolidation, together with crop switching, led to changes in the choice of inputs used in the production process. Areas exposed to the improved climate exhibit

[2] Crop insurance did not become widespread in the US until the Federal Crop Insurance Act of 1980.

higher relative spending on fertilizer—consistent with the switch from wheat to corn, which typically requires more fertilizer to maximize yields. They also exhibit lower relative spending on hired machines and hired labor—consistent with a story of lower returns to mechanization on smaller farms. But we also find lower farm values (3.1% lower overall value of agricultural land and buildings) relative to areas less exposed to winds from the Shelterbelt. While the climate became more favorable for crop production, the slower pace of consolidation left more and smaller farms on fewer acres in farms. Most of this lower aggregate value reflects the decline in acres rather than a fall in land prices. Overall, our results indicate that improving the climate through land use policy has significant consequences for long-term agricultural development.

Our study advances our understanding of the interactions between climate and the economy, both substantively and methodologically. First, we contribute to an emerging literature on the endogeneity of local climate to land use. While economists generally assume local climate is exogenous to local outcomes, a growing body of evidence shows this is not the case.[3]

Recent work in this vein includes Braun and Schlenker (2023), who find that the historical expansion of irrigation in the US affected temperature, both locally and in downwind areas. In the Amazonian context, deforestation has been linked to downwind precipitation change (Araujo et al. 2023) and subsequent farmer responses in terms of land use and agricultural productivity (Araujo 2024).[4] Taken together, these recent papers confirm the external validity of the endogeneity of climate to land use changes in a range of settings, and the potential follow-on socioeconomic impacts. However, neither paper maps to an explicit policy choice contemplated by governments around the world in response to climate change: large-scale tree planting.[5]

Next, we describe the methodological implications that extend from our findings on climate endogeneity. The response of agricultural production to changes in the climate is a key parameter to assessing the economic consequences of climate change, with implications for

[3] This idea has long been explored in the natural science literature. Atmospheric models are used to describe the response of local and regional climate to changes in land use (Devaraju et al. 2015). Other studies estimate the reduced-form climate effect of various land use changes, including irrigation (e.g., Lobell et al. 2008; DeAngelis et al. 2010; Mueller et al. 2016; Braun and Schlenker 2023), crop choice (Loarie et al. 2011; Georgescu et al. 2011), and forestation (Smith et al. 2023; Alkama and Cescatti 2016; Peng et al. 2014). Many of these studies are either observational or compare trends in areas with land use change to adjacent unchanged areas, and, therefore, cannot identify spillover effects.

[4] A large body of natural science work has investigated the local and regional climate impacts of deforestation (Spracklen and Garcia-Carreras 2015), generally finding that it reduces precipitation.

[5] Relatedly, Xing et al. (2026) evaluate a large urban afforestation program in Beijing, finding downwind improvements in air quality together with increased pollen exposure. We differ in outcome and setting: we estimate how tree planting changes the regional climate itself—precipitation and extreme heat—and trace the agricultural adaptation that follows.

food security, structural transformation, migration, and trade flows. As detailed below, we propose a reduced-form approach to estimating this response using a policy-induced change in the long-run climate to measure productivity effects, inclusive of adaptive responses. This resulting elasticity comprises both i) the direct mechanical effect of weather shocks drawn from a different distribution (i.e., climate change) and ii) the effects of adaptation to the new climate.

In terms of the direct impact of climate change, our findings have implications for the vast body of work that uses climate as a source of identifying variation. While debates on the economic effects of climate can be traced back centuries (Montesquieu 1750), the credibility revolution in economics and growing concerns about anthropogenic climate change have spurred a revival of studies focusing on climate impacts. Many outcomes are affected by annual weather shocks (see Dell et al. 2012 for a seminal paper, and for reviews Dell et al. 2014 and Carleton and Hsiang 2016). However, identifying the effects of climate change from short-term weather shocks presents challenges (Hsiang 2016; Kolstad and Moore 2020; Lemoine 2024).[6]

One approach to assessing adaptation involves accounting for how responses to climate shocks vary across space by average climate (Butler and Huybers 2013; Heutel et al. 2021; Auffhammer 2022; Hultgren et al. 2025), the idea being that if the same extreme heat event causes less deaths in a warm climate than a cold climate, that difference is (partly) due to adaptation. This useful and intuitive approach still faces concerns about potential confounders across geographies, as well as the "weather-vs-climate" issue discussed above. Another way to get at adaptation is through "long differences": estimating the correlation between long-term changes in climate and outcomes of interest (Burke and Emerick 2016). Identification then relies on the assumption that long-term trends in climate are exogenously determined across spatial units. Our results highlight the potential for reverse causality-driven bias when using spatial variation in climate trends to assess impacts on economic outcomes—given that these climate trends themselves may be driven by endogenously-determined policies—and thereby invite increased caution when using climate trends as a source of identifying variation.

By demonstrating that local climate change can be policy-induced, our study provides a natural direction to advance this literature. We can use standard empirical tools, such as difference-in-differences or regression discontinuity design, to assess whether policies have the potential to affect the climate and to subsequently study the consequences of this policy-

[6] The effect of weather shocks can be larger than climate change if adaptation is less costly over the long run than over the short run (e.g., if fixed cost investments are required). The converse is possible if short-run adaptation strategies like irrigation become more costly over time (Hornbeck and Keskin 2014).

induced climate change. Importantly, exploiting such policy changes enables researchers to argue more convincingly for causal identification of climate effects, particularly in locations downwind or otherwise not directly affected by the policy.[7]

In an agricultural context, existing research provides valuable insights on how economic agents respond to productivity shocks, including soil erosion from the US Dust Bowl (Hornbeck 2012) and permanent reductions in groundwater in India (Blakeslee et al. 2020). Economic agents, however, may respond differently to climate change—that we conceptualize, following Hsiang (2016), as a permanent change in the distribution of transitory productivity shocks—than to single, either permanent or transitory, productivity shocks. There is a robust body of work on US crop yield responses and adaptation to climate change, with mixed results.[8] Most of our current knowledge of mechanisms for agricultural adaptation to climate comes from observational studies.[9]

Our work relates to studies on adaptation to medium-to-long-term fluctuations in the monsoon regime in India (Kala 2017; Taraz 2017; Liu et al. 2023). These generally combine agricultural and economic data over several decades with five- to ten-year changes in the timing and intensity of monsoons to provide causal evidence on crop and labor adaptation. Our study advances this literature by providing direct causal evidence of significant farmer adaptation to a long-term change in continental climate across a range of dimensions, and estimates how these responses moderate the overall impact of climate change (relative to no adaptation). Our paper also builds on work studying the Great Plains Shelterbelt over the long term, and its effect on local agriculture practices and outcomes (Li 2021; Howlader 2023).

Our paper also speaks to a challenge faced by climate modelers. Hindcast evaluations of global climate models can accurately reproduce historical global-mean warming (Hsiang and Kopp 2018; Hausfather et al. 2020), but skill deteriorates at sub-continental scales where ocean variability, aerosols, topography, and land use change introduce large uncertainties (Hawkins and Sutton 2009). In the US Corn Belt, for example, observed summer temperatures are about 1°C cooler than model ensemble means, a discrepancy linked to irrigation

[7] Our findings also have implications for our understanding of place-based policies involving localized changes in productivity (Kline and Moretti 2014; Bustos et al. 2016; Bustos et al. 2020; Asher et al. 2022; Hornbeck and Moretti 2024). Our study, which shows that land use policy can induce climate change across an area far beyond where the policy is implemented, demonstrates economic spillovers through a third potential channel–besides capital and labor reallocation–involving climate change.

[8] See, for instance, Schlenker and Roberts 2009; Butler and Huybers 2013; Annan and Schlenker 2015; Burke and Emerick 2016; Malikov et al. 2020; Yu et al. 2021.

[9] Such adaptive channels include crop choice (Kurukulasuriya and Mendelsohn 2008; Sloat et al. 2020; Cui 2020; Burlig et al. 2026), ecological practices (Schulte et al. 2017), and irrigation (Taylor 2026).

and cropland intensification (Mueller et al. 2016). Cooling anomalies have also been observed in the Indo-Gangetic Plain and North China Plain. In light of these examples, our results suggest that incorporating land use dynamics—including changes in agriculture and forest cover—may help narrow spatial temperature biases and improve future climate projections.

In summary, we find that the Great Plains Shelterbelt—in part inspired by a climate shock itself—induced a significant change in regional climate. This policy-driven climate change, in turn, affected economic outcomes for decades in locations downwind from the policy itself. We also find strong evidence of climate adaptation by farmers. The geographic scale of these effects is large, covering an area twice the size of California.

Recent global enthusiasm for tree planting for climate change mitigation raises many questions about how to best design such projects. There are valid concerns about large-scale tree planting, including the scale of the land required, the timing and permanence of CO_2 reductions, potential ecological impacts, and mixed track records of past programs (Veldman et al. 2019). Our study of the Great Plains Shelterbelt—which used a distinctive windbreak design rather than dense monoculture plantations—speaks to conditions under which tree planting may yield agricultural co-benefits. These findings are most relevant to countries still highly dependent on agriculture and to global breadbasket regions with similar soil and climate characteristics to the US Great Plains, though we caution that benefits depend critically on program design and local context.

2 Background

The Great Plains Shelterbelt Project, also known as the Prairie States Forestry Project, was a Great Depression-era effort to plant forest buffers and windbreaks in the US Midwest. It was the largest afforestation program to date, with over 220 million trees planted between 1935 and 1942. This short implementation period, combined with a defined target area, makes this program an ideal candidate to identify the causal effects of large-scale tree planting on climate and agricultural development.

Franklin D. Roosevelt (FDR) conceived the Shelterbelt idea while running for president in 1932, upon observing on the campaign trail the damages from the destructive Dust Bowl (Droze 1977). FDR had a long-running interest in forestry and experience with reforestation projects as Governor of New York, and believed that an investment in forestry might improve the climate and agriculture of the Great Plains. As president, he commissioned a report recommending the planting of trees in strips 132 feet wide, or "shelterbelts" that protect homes, crops, and livestock from the wind and destructive dust storms.[10] FDR's plan called for a shelterbelt approximately 1,150 miles long and 100 miles wide, running from North Dakota to Texas. Its western limit lay within a precipitation boundary of 16 inches annually in the north and 22 in the south, the higher southern threshold allowing for greater evaporation, beyond which foresters judged planted trees unlikely to survive (U.S. Forest Service 1935).

FDR signed an executive order in 1934, and the first tree was planted in 1935 in Oklahoma. The Forest Service administered the project with labor from the Works Progress Administration, and planting continued until 1942, when funding cuts associated with the war effort brought it to a stop (Droze 1977). Planting took the form of shelterbelts rather than blocks of forest, as intended, with site conditions determining where belts went. Only part of the zone could support trees: in its survey, the Forest Service classified 56% of the zone's 114,700 square miles as suitable for tree growth, 39% as difficult to plant, and 5% as entirely unsuitable due to claypan soils or alkali basins (U.S. Forest Service 1935). Each belt had to sit on plantable soil and be oriented against the damaging winds prevailing in each locality, so unbroken north-south strips were never the intent.

Implementation and politics also mattered. The original intention was for the government to purchase land outright, but budget constraints forced a shift first to leasing arrangements and then to cooperative agreements where farmers donated easements in exchange for free seedlings and technical support. Farmers often objected to surrendering strips at the planned acquisition width of 165 feet, leading project leaders to accept narrower belts (typically 10 rows of trees). Participation was voluntary, and farmers facing higher crop prices converted less land to shelterbelts (Howlader 2023). The zone itself was repeatedly redrawn during the Forest Service's survey, extended, contracted, and deflected as soil and climate conditions dictated (U.S. Forest Service 1935).

The realized plantings were therefore more scattered than the planned zone suggests. This is why we measure treatment from where trees were actually planted rather than from the planned zone. Appendix Figure S1 shows both. Below, we describe how our empirical strategy addresses potential concerns about the endogeneity of farmer uptake and tree planting location, including prior exposure to the Dust Bowl and strategic location choice (Section 5.3).

Early on, there was interest in the Great Plains project's potential influence on local climate. When first reporting on the initiative, the *New York Times* described it as an "experiment in

[10] Another common conservation tool involved rotating portions of fields into 'fallowed strips' that are not plowed in a given year and thus secure the soil and provide a small windbreak (Hansen and Libecap 2004).

climate control to combat the ravages of drought" ("The New York Times" 1934), and Snow (2019) presents the controversy around the program as a battle between 'ecological foresters' who believed that policy decisions influence local climate and environmental conditions and 'determinist geographers' who saw climate as static.

Specific implementation procedures were key to the program's success. For the most part, seedlings from nurseries were planted instead of seeds to increase survival rates. In total, over 30 species of trees and shrubs were selected—tall and short trees, fast and slow growing trees, hardwoods, and conifers—mainly native species but also key introduced varieties such as Chinese elm (Read 1958), selected to ensure species diversity and ecological resilience in a way that mimicked naturally-occurring forests. In considering the program's impact on the water cycle, we note that field plantings were established without irrigation, relying instead on moisture conservation techniques (though nurseries could be irrigated).

Not all planted shelterbelts survived. Because ownership remained with farmers under the cooperative agreements, maintenance varied considerably. As agricultural markets recovered during World War II, some farmers began to view their shelterbelts as wasted acreage and removed them to expand crop production (Droze 1977). Nevertheless, substantial tree cover persists to the present day, as documented by Snow (2019).

3 Data

Our main analysis is based on a county-by-year panel dataset, constructed from four types of data: digitized historical maps of Shelterbelt plantings, wind data to construct our Shelterbelt wind exposure metric, temperature and precipitation data for our climate outcomes, and agricultural census data for our economic outcomes. In our main analysis, we focus on the period from 1930 to 1965.[11] We also present event-study results until 2002, and show robustness to different start years.

Shelterbelt data: We digitize maps of "areas of concentrated Shelterbelt planting" from Read (1958) and overlay them with county boundaries. This is our best available source of data contemporaneous with the tree-planting program, as there are no official statistics on the area of trees planted in each county. We use the digitized shapefiles directly in our wind exposure construction (described in detail in Appendix Section S.2). As we are interested

[11] We start in 1930 due to concerns about data quality and availability before that time (Knappenberger et al. 2001; Kunkel et al. 2007). We end in 1965 to limit the overlap with other agricultural changes, including the expansion of irrigation and urbanization, which could be influenced by tree planting and could influence the climate themselves.

in studying the non-local effects of tree planting, we drop directly afforested Shelterbelt counties in our main analyses. To do this, we classify a county as a Shelterbelt county if over 5% of its total area is covered by this concentrated planting (the 5% cutoff corresponds to the 20th percentile among counties with non-zero tree planting).[12] Figure 1 shows the location of the concentrated Shelterbelt planting areas.

We validate our Shelterbelt measure with an alternative source of data. Snow (2019) digitized the actual Shelterbelt plantings that survived several years to decades after planting, from the United States Geological Survey (USGS) Topographic Map Quadrangles.[13] We calculate each county's area covered by the Shelterbelt from her digitized shapefiles to compare with our main measure. Appendix Figure S2 plots the two measures side-by-side and shows the consistency in geographic coverage. The correlation is high at 0.86. The total footprint of the areas of concentrated Shelterbelt planted is 10.3 million hectares (Read 1958). Based on the windbreak shapefiles from Snow (2019), about 1% of this area is actually covered by trees.

Wind data: Wind is an essential driver of atmospheric transport and regional climate change in relation to afforestation. Trees release water into the atmosphere through evapotranspiration. This atmospheric water vapor travels with wind, increasing precipitation in downwind areas. The same process also affects temperature: the latent heat absorbed during evapotranspiration cools the air locally, and this cooler air mass can be advected downwind. We therefore construct a measure of counties' exposure to winds from the Shelterbelt to determine which counties are most likely to have their climate and economic influenced by the Shelterbelt project.

We measure prevailing winds using the ERA-5 reanalysis data from the European Centre for Medium-Range Weather Forecasts (Hersbach et al. 2023). We choose this dataset as it provides hourly wind fields on a 0.25-degree latitude-longitude grid back to 1940. We use the three wind components provided by ERA5: horizontal u-wind (east-west dimension), horizontal v-wind (north-south dimensions), and vertical pressure velocity ω.[14]

Using the ERA5 reanalysis data, we create a time-invariant approximate measure of how exposed each county is to winds blowing from the Shelterbelt in the summer. Here we

[12] For simplicity, we refer to counties below the 5% threshold as counties with no tree planting.

[13] USGS undertook the detailed mapping of the conterminous US through the production, by hand, of over 55,000 quadrangle maps covering about 64 square miles each, from 1947 to 1992. Snow 2019 identifies in each map the vegetative areas with the characteristic shape and scale of Shelterbelt plantings (e.g., linear features that run east/west or north/south) and extracts the corresponding polygons. She validates this procedure by comparing the final digitized Shelterbelt acreage totals to official project totals by state.

[14] Here we denote vertical pressure velocity by ω to distinguish it from the wind exposure measure w.

describe the intuition behind the construction of our measure, while in Appendix Section S.2 we provide more details. To start, we identify ERA5 grid points that overlap areas of concentrated Shelterbelt planting (with a 5km buffer), yielding the set of origin locations from which we trace trajectories. For each day and each origin point in the concentrated areas of Shelterbelt planting, we release imaginary particles at the 800 hPa level (approximately 2 km altitude) during hours when evapotranspiration from trees is highest (roughly between mid-morning and mid-afternoon)[15] and advance it for 24 hours in one-hour steps. At each step, we bilinearly interpolate the local wind to the particle's location, move it horizontally and update its vertical pressure level. This produces a three-dimensional 24-hour trajectory.

For each trajectory, we assign each hourly position to a county. A county's raw wind exposure is the total number of hourly trajectory points that fall within its boundaries over the chosen aggregation window. We adjust for county land area and rescale exposures to be between 0 and 1. The resulting continuous wind exposure metric $w_i \in [0, 1]$ summarizes the frequency with which air that has passed through Shelterbelt regions is carried over each county i. Figure 2 illustrates this construction and maps the resulting measure across our sample.

For our main measure, we focus on summer months given the importance of climatological conditions during that period for agricultural production. Our main wind exposure measure is time-invariant and aggregates trajectories for all summer (June - August) days in 1940, the earliest available year prior to the end of the Shelterbelt program. We also create annual, monthly, and daily versions where we aggregate separately for each year, each year-month, and each year-day. Additionally, we repeat these steps for other seasons and longer time periods (1940 - 1965) for further analyses.

Temperature and precipitation data: We construct a county-by-year panel of precipitation and temperature based on daily weather station data, using a methodology inspired by Schlenker and Roberts (2006). We start from the Global Historical Climatology Network daily (GHCNd) dataset provided by the US National Oceanographic and Atmospheric Administration (NOAA). We create a balanced panel of stations reporting between 1930 and 1965 to ensure that changes in the measured climate are not driven by changes in the underlying set of measuring stations. We collect data on precipitation and minimum and maximum temperatures and calculate daily degree days at various thresholds for each station. We spatially interpolate this station data to obtain a gridded dataset at a 0.1 degree

[15] We use 800 hPa as this is well within the atmospheric boundary layer where moisture gets mixed and transported regionally; seminal papers like Spracklen et al. (2012) often use this level as well. Regardless, we run robustness checks with particles released at 1000 hPa (ground level) as well. We release particles at 10am, 2pm, and 6pm Central Time, based on diurnal temperature and evapotranspiration patterns measured in, for example, Hamberg et al. (2022).

resolution, and average the resulting measures at the county-by-day level. Finally, we compute the total precipitation, average daily maximum temperature, average daily minimum temperature, and total number of daily degree days at various thresholds for each month. To aggregate this county-by-month dataset to county-by-year, we take the average of these measures over the summer months (June through August). Details on the construction of this dataset are available in Appendix S.3.

We consider degree days as a climatological outcome, since they have been shown to be a relevant measure of temperature when studying impacts on crops or physiology, often performing better than maximum or mean temperature. Degree days have been widely used in economics following work by Schlenker and Roberts (2006; 2009), who demonstrated that yields increase gradually with temperature up to a critical threshold, and decrease sharply with any further temperature increase. For corn, our main crop of interest, the critical threshold is 29°C. We therefore include 29°C degree days as one of our main climate outcome variables.

Standard gridded weather datasets with historical coverage, such as PRISM and NOAA's NClimDiv, either are based on inconsistent station coverage or do not include degree days. PRISM uses all available stations, while NClimDiv provides data at the monthly level (daily data is necessary to compute degree days manually). These limitations led us to construct our main weather dataset directly from the raw daily station data. Still, we verify the robustness of our results for all climate outcomes using PRISM and on precipitation, mean and maximum temperature using the standard NClimDiv dataset. We find both to be robust (Appendix Table S6).

Economic data: We focus on agriculture, the most important sector in the US Midwest during our study period. We use agricultural censuses, conducted roughly every five years by the US Department of Agriculture and digitized by Haines et al. (2018). We prefer using agricultural census data over the USDA's annual surveys because of their spatial coverage. As shown in Appendix Figure S17, we are able to build a balanced panel of the census data that covers most counties of interest in our region. The agricultural survey data is only available for a subset of states and counties, primarily in the northern US that were surveyed prior to 1940. Key states like Kansas and Texas only began data collection in the 1960s. Thus, we would lack baseline data for these important other areas if we did not use the census data.

Other data: County-level elevation and ruggedness (standard deviation of elevation) are derived from the USGS 3D Elevation Program (3DEP) 10-meter digital elevation model via

Google Earth Engine. Soil type classifications are from the USDA NRCS Global Soil Regions product. The shapefile for the Ogallala aquifer is from USGS (Qi 2010). Dust Bowl erosion severity measures are from Hornbeck 2012.

4 Empirical approach

4.1 Overview

Our empirical analysis exploits the timing and geographic location of Shelterbelt tree planting in conjunction with prevailing wind patterns. In a first step, we seek to test whether the Shelterbelt project changed the climate in areas downwind from where trees were planted. In a second step, we ask whether this policy-induced change in the climate influenced agricultural development in the region, through direct and adaptation channels.

Throughout, we focus on counties that are not directly afforested (i.e., not covered by more than 5% area of concentrated Shelterbelt planting) but have a centroid within 300km of the centroid of a Shelterbelt-afforested county. This allows us to clearly isolate the role of a change in the climate, rather than the full combined local effect of planting trees that includes changes in shade and soil quality, among others.

We use the same empirical strategy for the two steps of the analysis. Given the clear temporal and geographic boundaries of the Shelterbelt program, our primary analysis relies on a difference-in-differences framework: comparing the change in climate and economic outcomes—–before and after the program—–across counties more or less exposed to winds blowing from the Shelterbelt. Our preferred specification augments the classic difference-in-differences with a set of controls, in order to compare areas with similar baseline climates. Ex-post, we find our main results to be qualitatively similar whether we use controls, subsets of our controls only, or no controls at all in our specification (Appendix Figures S14 and S15, Panel A).

We explicitly address a number of potential confounds and find our results to be robust to these potential threats. Specifically, we address the timing of the tree planting effects, the strategic choice of tree planting location, the correlation of wind patterns with spatially-differentiated climate trends, the Dust Bowl, irrigation, and the potential endogeneity of wind patterns.

Below, we provide more details on our preferred empirical specification. In the next section, we present our results on the climate impacts of the Shelterbelt (5.1) and its economic consequences (5.2). Finally, we demonstrate that these results are valid and robust (5.3).

4.2 Main specification

Our main empirical strategy is to use a difference-in-differences model with a continuous treatment measure:

$$y_{it} = \beta(w_i \times P_t) + \gamma(\mathbf{X}_i \times Y_t) + \delta_{st} + \nu_i + \epsilon_{it} \tag{1}$$

where y_{it} is the outcome of interest at the county-year level, w_i is the wind exposure measure ($w_i \in [0, 1]$) described in Section 3, and P_t is an indicator variable equal to one for years after 1942.[16] $\mathbf{X}_i$ is a vector of controls, described below, interacted with year fixed effects Y_t.

We also include county ν_i and state-by-year δ_{st} fixed effects. Using fixed effects at the state-by-year level, instead of year as in classic TWFE specifications, allows us to ensure that potentially differential historical trends in climate or agricultural development across states that could correlate with wind exposure would not bias our results. Ex-post, we find that using year fixed effects rather than state-by-year fixed effects produces similar results (Appendix Figures S14 and S15, Panel B).

To address potential concerns about spatial correlation influencing statistical inference, we implement Conley standard errors (100km distance cutoff) for our main estimates. Tables 1-7 include Conley standard errors and p-values alongside clustered standard errors. All climate estimates remain statistically significant. All agricultural activities estimates also remain statistically significant, with the exception of the share of large farms, which loses statistical significance but falls not too far from conventional significance levels.

The effects we identify when estimating our coefficient of interest β are equilibrium effects. For instance, it is possible that planting trees affects the downwind climate, which in turn induces people to change their land use in these downwind areas. This land use change can in itself have a local effect on the climate. This does not threaten the internal validity of our

[16] The Shelterbelt project was conducted from 1935 to 1942. Implementation started slowly, with most trees planted in the final years of the project. (See Appendix Figure S3 for the timing.) We can expect the impact of tree planting to increase over time, as trees grow. We therefore make the conservative choice of using 1943 as the first year of the treatment period. If treatment effects happened earlier, our estimation would underestimate the true effect. We also implement a long differences strategy to side-step this uncertainty about the exact start of the treatment.

approach: we only need to interpret the estimated coefficients as the resulting equilibrium effects of large-scale tree-planting in a given area.

A related concern is interference across units: if improved growing conditions raise output in more exposed counties, the resulting price or factor-market responses could alter farmers' decisions in less exposed counties, which serve as our comparison group. This concern does not apply to the climate results, which operate through physical processes. For the economic outcomes, corn and wheat prices were set in national markets rather than locally, so any price response to higher output downwind would have been shared by more and less exposed counties rather than concentrated in one group. From the early 1950s, federal nonrecourse loans also set a floor under both crops, so additional supply was more likely to be taken into government stocks than to depress the price farmers received (Bowers et al. 1984). Factor markets, by contrast, operate locally, but the pattern of estimates is difficult to reconcile with labor or capital reallocating toward more exposed counties: these counties retained more small farms, used less machinery, and exhibited lower land values, the opposite of what such an inflow would produce. More generally, our estimates identify relative differences between more and less exposed counties—the distributional consequences of the program in downwind areas—rather than its aggregate effects, which is a general feature of DiD specifications.

4.3 Identifying assumptions

As in the simplest difference-in-differences framework, the post-treatment period is defined to be the same for all units: we do not have a staggered treatment. However, we use a continuous (rather than binary) treatment variable: wind exposure w_i. This case has been extensively studied by Callaway et al. (2024). If one assumes that the marginal effect of wind exposure on the outcomes of interest is constant (e.g., moving from 0.1 to 0.2 wind exposure has the same effect on temperature as moving from 0.2 to 0.3), then interpreting β in Equation 1 is straightforward: it is the marginal effect of wind exposure. To aid interpretation since w_i is a re-scaled measure going from 0 to 1, we provide in our main tables and figures the difference in wind exposure between the 25th and 75th percentiles of that measure, among our sample counties. In the text of the paper, we also report results as the effects of going from the 25th to the 75th percentile of wind exposure, assuming constant marginal effects.

If one does not want to assume that the marginal effect is constant, the interpretation of β is difficult—even under a "strong parallel trends" assumption (cf. Theorem 3.4 in Callaway et al. 2024): β becomes a weighted average of marginal effects, with undesirable properties of the weights. The proposed solution from Callaway et al. (2024) is to implement non-parametric methods to flexibly recover marginal effects. However, given our sample size and the noisy historical data, this is hardly feasible in our setting.

We therefore also present results from a simple binary DiD specification, for which interpretation is straightforward. The specification is described in Appendix S.4.3, with results presented in Appendix Tables S1 and S2 alongside the continuous DiD results for easy comparison. For 30 of the 32 outcomes we consider, the results are qualitatively similar across the binary and continuous specifications. For the remaining two, the binary specification yields either a null estimate or an estimate of the opposite sign.[17]

Both the continuous DiD with constant marginal effects and the binary DiD specifications require the classic parallel trends assumption to hold. While it cannot be tested, we can provide suggestive evidence by testing for differential trends in the pre-treatment period. Out of our four climate variables, precipitation and average temperature exhibit trends that are small but statistically significant at the 5% level over the 1930-1942 baseline period (Appendix Table S1, Panel B, Columns 1–2). We formally assess whether these pre-trends qualitatively influence our results by implementing the "Honest DiD" methodology developed by Rambachan and Roth (2023), with additional details provided in Appendix Section S.4.2. While the results are noisy due to the use of historical data inducing low precision when estimating the pre-trends, we find the results to be directionally similar in our main DiD specification (Column 3) and the Honest DiD (Column 4). In addition, we implement a synthetic DiD following Arkhangelsky et al. (2021); see Section 5.3 for an overview and Appendix Section S.4.3 for details. There, we create a synthetic control group by constructing parallel pre-trends to our treated group, and once again find the effects to be similar to our main DiD specification (Table S1, Panel C). Taken together, these results indicate that the limited pre-trends we observe for our climate outcomes are unlikely to be a threat to the validity of our main estimates.

For the economic outcomes, we have at most three data points (the 1930, 1935 and 1940 agricultural censuses) for each county in the baseline period. This makes it difficult to meaningfully test for pre-trends, or apply corrective methods. For each outcome, we thus extend the baseline period to earlier years, where possible. The results are reported in Appendix Table S2, for both 1930 as a start year and the earlier option. Most agricultural

[17] For wheat acreage, the simple binary specification has opposite sign than the continuous one. However, it exhibits significant pre-trends in the binary specification and the synthetic DiD restores a significant negative effect, as in the simple continuous DiD. For land in farms, the binary DiD estimate is close to zero, but the synthetic DiD shows a less precise decrease.

outcomes we consider, unfortunately, exhibit some differential trends at baseline (Column 3). However, as for the climate outcomes, we formally assess whether these pre-trends qualitatively influence our results, by implementing Honest DiD and synthetic DiD methods (Columns 4 and 7, respectively). Reassuringly, from the 21 agricultural outcomes displaying significant effects in our headline specification for which these methods can be applied, 19 are robust.[18]

4.4 Biophysical context and methodological positioning

Land-atmosphere interactions have long been studied, and several strands of natural science literature provide context for our empirical approach. First, calibrated climate models have shown that forest cover alters surface energy and water fluxes: evapotranspiration and roughness cool and moisten the boundary layer while albedo can offset these effects, with net sign and magnitude varying by biome and latitude (Bonan 2008). Comparisons across models find the temperature effect more consistent than the precipitation effect—especially outside the tropics (Pitman et al. 2009; Pitman et al. 2012). However, it is difficult to parameterize narrow, heterogeneous plantings like shelterbelts in these models.

Second, field-based measurements, isotopic tracers (which track water molecules from evaporation to precipitation), and air-mass trajectory analyses (Spracklen et al. 2012) identify upwind locations that supply downwind rainfall, i.e., precipitationsheds, and document increased rainfall when air traverses vegetated upwind regions—but these analyses are generally diagnostic rather than causal and rarely isolate the specific impacts of land use change.

Third, large-scale observational studies using satellite data provide broad coverage (Li et al. 2015; Alkama and Cescatti 2016; Duveiller et al. 2018; Su et al. 2023), but typically focus on local effects rather than downwind spillovers, and face challenges regarding reverse causality between vegetation cover and local climate (i.e., vegetation responds to shifts in climate) and in translating satellite-derived land-surface temperature (LST) to near-ground

[18] For 14 of the 21 outcomes, the honest DiD results align in both sign and statistical significance with the headline DiD results, indicating that the baseline differential pre-trends are not large enough to meaningfully influence our results. For three additional outcomes, the honest DiD confidence sets become wide and include zero; but they remain directionally similar to the headline DiD results and the synthetic DiD results are consistent with the headline ones. As such, we consider them as robust as well. Further, two outcomes (area of pastureland and aggregate land values) have confidence sets from the honest DiD that do not point in the direction of the headline DiD results—of the opposite sign for pastureland, and centered on zero for aggregate land values—but the synthetic DiD recovers the headline DiD results. For two outcomes, wheat acreage and land in farms, the headline DiD results align neither with the honest DiD nor with the synthetic DiD results. The value of animal products sold per acre of pastureland is observed in a single pre-treatment census, so neither method can be applied to it.

air temperature.

We complement this literature with a quasi-experiment. The Shelterbelt program planted trees in a narrow, geographically fixed zone, leaving counties downwind untreated by trees but exposed to winds that had crossed the planted area. Station records of near-ground temperature and precipitation then identify the downwind effect of forestation within a difference-in-differences design. Relative to the three strands above, the planting is observed rather than simulated, the variation is exogenous rather than inferred, and the effects are measured downwind at the surface rather than locally by satellite.

5 Results

We now present the impacts of Shelterbelt tree-planting on the climate, and the resulting effects on agricultural development. We first show that large-scale tree planting increased precipitation and reduced temperature in downwind areas (5.1). We then discuss the consequences of this policy-induced change in the climate for agricultural development—including productivity and farm consolidation—with a focus on climate adaptation (5.2). Finally, we demonstrate the validity of our identification strategy and robustness of our results (5.3).

5.1 Climate impacts

Our main climate results are reported in Table 1. Using our preferred difference-in-differences specification, we find that the Shelterbelt tree-planting program led to robust changes in the climate of downwind counties, with increases in precipitation and decreases in temperature. Specifically, we find that summer precipitation was 2.8mm higher in counties in the 75$^{\text{th}}$ percentile of Shelterbelt wind exposure relative to counties in the 25$^{\text{th}}$ percentile of wind exposure. This is equivalent to a 3.9% increase relative to the baseline average monthly summer rainfall.[19] We also find summer temperatures decreased: mean and maximum temperatures were 0.5% lower in areas more exposed to winds from afforested areas. Exposure to extreme temperatures that are harmful to crop yields also decreased significantly: average monthly degree days above 29°C declined by 2.1 for an increase in wind exposure from the 25$^{\text{th}}$ to the 75$^{\text{th}}$ percentile, equivalent to a 5.7% decrease relative to the mean.[20]

[19] To illustrate how such figures are computed using Table 1, Panel A, Column 1: multiply the 75th–25th percentile wind-exposure gap (0.21) by the "Wind Exposure:Post 1942" value (1.317), which equals 0.28cm, or 2.8mm. This 0.28cm increase is 3.9% of the sample mean precipitation (7.16cm).

[20] Results are similar in the much smaller sample of county-years with agricultural census data, where our economic outcomes are measured (Appendix Table S12): temperature estimates remain negative and

The effects are largest for extreme temperatures, consistent with increased evapotranspiration from the Shelterbelt trees. Evaporative demand is greatest during high temperatures, which means that the cooling influence of evapotranspiration is expected to be most pronounced on high temperatures (Mueller et al. 2016). While climate more favorable to crop production could itself induce land use responses such as irrigation expansion, which might feed back into local climate, we find that this channel is quantitatively small (Appendix Section S.7.2).

To test the consistency of the climatic response, Figure 3 plots the estimated treatment effects across all four seasons (winter, spring, summer, fall). The results align with biophysical expectations in three key ways. First, we find consistent increases in precipitation and decreases in mean temperature across all seasons (Panels A and B). The coefficients do not flip sign in non-summer months, indicating that the Shelterbelt's influence on moisture retention and general cooling is a persistent feature of the modified landscape. Second, the effects are largest in magnitude during the summer. This seasonality is consistent with the summer months having the highest potential evapotranspiration and maximum canopy density. Third, the effect on extreme heat—degree days above 29°C (Panel D)—is concentrated in summer, as expected since such heat essentially does not occur in other seasons, while the cooling in maximum temperature (Panel C) is evident across multiple seasons.[21]

We next investigate the timing of these effects. Figure 4 reports the results from an annual event study, allowing us to observe precisely when effects start appearing. Due to the noisiness of the data, we also report event study results aggregated by 15-year periods in Figure 5, to better observe the long-term dynamics of the effects. For both precipitation and temperature, the effects emerge rapidly after tree-planting begins in earnest in the early 1940s.[22] For precipitation, the effects persist for three decades after the Shelterbelt tree-planting ends before becoming negative in 1973–1987 and undetectable by 2002. By contrast, for the three temperature variables, effects are quite stable over time and persist through 2002.[23]

highly significant, while the precipitation estimate stays positive but loses statistical significance. This attenuation arises only when the sample is restricted on both counties and years at once; precipitation remains significant in the census-county subsample at full annual frequency ($p = 0.008$, Panel B) and is marginally significant in the full set of 539 counties at census-year frequency ($p = 0.081$, Panel C).

[21] The corresponding point estimates are detailed in Table S5.

[22] Given that the seedlings from nurseries were planted instead of seeds, this is plausible.

[23] We do not have a confident explanation for this divergence, though the two signals need not persist together: the cooling is a surface energy balance response carried in air that has crossed the Shelterbelt, whereas added moisture raises rainfall only where and when larger-scale circulation patterns convert it to precipitation. The divergence in any case falls outside 1930–1964, the window over which our main economic results are estimated.

We are most interested in changes in the long run climate, rather than weather shocks. This motivates our choice of a DiD specification with a time-invariant wind exposure measure for identification. Yet, wind speed and direction vary over time, leading to variation in (daily) wind exposure. We can exploit this feature for identification in a two-way fixed effect regression at the annual/monthly/daily level, run on the post-planting period (our wind data starts in 1940 only). While this alternative approach uses a completely different source of identifying variation than our primary specification, we obtain fully consistent results. Table 2 shows that in the years and months when non-afforested counties are more exposed to winds blowing from the Shelterbelt, they experience higher precipitation and lower temperature.[24] We apply this alternative variation only to climate outcomes. On economic outcomes it would identify responses to weather shocks rather than to a change in climate. That is a different question, and one a large literature already addresses without needing a policy shock, since weather shocks are largely random.

5.2 Economic consequences

Our results so far show that Shelterbelt tree planting affected the regional climate via increased rainfall and reduced temperatures. We now turn to the economic consequences of this engineered change in the climate, which made conditions generally more favorable for crop production. As in the previous analyses, to avoid confounding our estimates with any direct local effect of tree planting, we focus on counties outside the Shelterbelt project area, where no trees were planted but the climate still changed with exposure to Shelterbelt winds. For Tables 3–6, we restrict to a balanced panel of counties with non-missing values for all economic outcome variables across all census years. Table 7 uses a smaller sample because input expenditure data (hired labor, machinery, and fertilizer) are not available in all census years.

Corn production. We first focus on corn, the most important crop in the US Midwest in volume and value. We find that Shelterbelt tree planting greatly increased the production of corn in downwind areas. Table 3, Panel A contains the estimates from our preferred difference-in-differences specification (Equation 1). Column 1 suggests that corn production was 35% higher for counties in the 75$^{\text{th}}$ percentile of wind exposure compared to counties in the 25$^{\text{th}}$ percentile.[25]

[24] The details of this empirical strategy are reported in Appendix S.5.2. The analysis at the daily level needs to account for the temporal dynamics of air moisture, precipitation, and temperature. Still, results are also consistent, as reported in Appendix Figure S13.

[25] Approximated by multiplying the coefficient (1.670) by the 75$^{\text{th}}$–25$^{\text{th}}$ percentile wind-exposure gap (0.21).

An increase in corn production (i.e., bushels) can be driven by an increase in the area harvested of corn (i.e., acres), and by an increase in yield (production per area harvested, or bushels per acre). The Shelterbelt tree planting led to a large and significant increase in the area of corn harvested downwind, by 29% in counties in the 75$^{\text{th}}$ percentile of wind exposure relative to counties in the 25$^{\text{th}}$ percentile (Table 3, Panel A, Column 2). Since the percentage difference between the increase in production and in area harvested equals the increase in yield, as illustrated by Figure 7, this implies that most of the corn production increase was driven by the increase in area harvested. The increase in yields was more modest, at 6%, but still statistically significant (Column 3).

Climate adaptation. The increase in the area of corn harvested could have arisen two ways. Farmers may have planted more corn, a relatively water-intensive crop, and thus shifted land away from dryland crops like wheat and pasture. This would be an adaptive response to wetter conditions. Or a larger share of the corn already planted may have survived to harvest, which would be a mechanical response to a change in growing conditions.

Table 3, Panel B provides evidence of the former, climate adaptation through a change in crop composition. The area of wheat harvested *decreased* by 9% (Column 1) while the area of corn harvested increased by 29% (Panel A, Column 2). The contrasting effects on corn versus wheat indicate active adaptation by farmers: a purely mechanical channel, such as a reduction in failed acres, would raise harvested area across crops rather than shift it from wheat toward corn. The estimated effect on crop failures (Panel B, Column 3) is negative but statistically inconclusive. Crop failure is recorded in only two of the five post-treatment censuses in this window, too few to estimate the effect precisely, so we do not rely on it here. However, in the extended panel, where more censuses are observed, we do find a reduction in crop failures after the 1970s (Figure 5).

Panel C turns to livestock. Cattle numbers did not change significantly (Column 1), while the number of pigs and chickens increased significantly by 17% and 14% respectively (Columns 2–3). These animals can be raised in confined areas on smaller farms and fed with corn, making them complementary to the expansion of corn production.

This adaptation behavior following a change in the climate, away from wheat and towards corn, is fully consistent with agronomic evidence. Precipitation has historically been a major determinant of crop choice in the US: dryland wheat is the main crop grown in areas with annual rainfall under 18 inches (Horner et al. 1957), while dryland corn generally requires over 25 inches annually (Neild and Newman 1987). When precipitation increases due to the influence of the Shelterbelt, we could therefore expect the share of cropland devoted to more water-intensive crops, such as corn, to increase—which is the behavior we observe empirically.

The shift in what farmers grew and raised is mirrored in land use. Table 4 documents the reallocation of farmland induced by the Shelterbelt's climate effects. Cropland area increased by 8% while pastureland decreased by 8% (Columns 2 and 3), indicating reallocation from livestock grazing to crop cultivation. Consistent with cropland expansion, and the reallocation of animal husbandry towards activities requiring less land but more buildings (chickens and pigs), woodland area fell by 9%. The residual 'other land' category, which includes farm buildings, rose by 11% (Columns 4 and 5). Overall, total land in farms declined slightly, by 2% (Column 1).

Our findings directly complement prior work by Li (2021), which studies the *local* effect of the Shelterbelt on agricultural outcomes within afforested areas. Li (2021) finds a shift in production away from crops and towards pasture, arguing that this is driven by local shade effects that increase the returns to pasture and cattle. By contrast, we focus on the *downwind* effects, where climate change is the dominant mechanism. In these areas, generally more favorable growing conditions (more precipitation, less extreme heat) increase the relative returns to water-intensive crops, explaining the shift from wheat towards corn that we document. The differing results are therefore consistent with distinct physical mechanisms operating at different spatial scales.

Farmers also adapted their use of water. Table 3, Panel B, Column 2 shows an increase in irrigated farmland. This is puzzling at first, since more rainfall should reduce the need to irrigate rather than increase it. But the response is concentrated outside the Ogallala aquifer, where counties lacking groundwater irrigate from rivers and streams. In these places, more rainfall makes irrigating from surface water less costly and more feasible. Counties over the aquifer, which could already pump cheaply, show no response (Appendix Table S14, discussed in Appendix Section S.7.2). Thus the Shelterbelt's effect on irrigation ran through the supply of water rather than the need for it.

Agricultural development. The Shelterbelt program had important consequences for the development of US agriculture. The post-war period saw intense concentration in the agricultural sector, with smallholder farms being sold to form larger entities. Over our study period, from 1930 to 1964, the total number of farms in our study region decreased from 819,000 to 468,000 (Appendix Figure S6). We argue that the improved growing conditions induced by Shelterbelt tree planting reduced the extent of this farm consolidation. Table 5 shows that more farms survived (i.e., the number of farms declined significantly less) in counties more exposed to winds from the Shelterbelt (Column 1), along with a corresponding decline in average farm size (Column 2). This effect is driven by small farms (less than 100 acres), whose share increased significantly (Column 3) while the share of medium-sized farms (100-499 acres) remained constant (Column 4). The share of large farms (500+ acres) declined (Column 5), though this estimate is sensitive to using the continuous or binary treatment measure.

This reduced farm consolidation is accompanied by a lower overall value of farmland and buildings (Table 6, Panel A, Column 1). Consistent with the shift toward crops, the value of crops sold increased by 9% while the value of the sales of animals and animal products did not change significantly (Columns 2 and 3). This increase came mainly from the expansion of cropland rather than from higher returns per acre, with the per-acre component small and imprecisely estimated (Panel B, Column 2).

We read this slowdown in consolidation as a change in which farms survived rather than in the size at which farming was efficient, though county aggregates cannot fully separate the two. In the Great Plains, farm scale was economically consequential (Hansen and Libecap 2004), and large operations held real advantages in terms of machinery, fallow capacity, and diversification into livestock. A Shelterbelt-driven climate shift of the size we estimate would not have eroded these advantages, but it would change the probability and frequency of farm failure induced by extreme weather. Small farms carried thinner margins, higher costs per bushel, and were far more likely to be foreclosed after a drought (Hornbeck 2012; Libecap and Hansen 2002). Our estimated reduction in extreme heat bears on the margin that drives crop loss, so the Shelterbelt could have slowed their exit. Production moved toward corn and confined hogs and poultry, with a precise null for cattle, ruling out the grain-and-cattle diversification that large farms used to hedge drought.

The lower aggregate value of farmland and buildings observed in Table 6 aligns with this interpretation. Aggregate value is the number of farms times the average value per farm, so a county ending the period with more farms but lower aggregate value suggests a decline in average farm value. And since the average farm gets smaller (Table 5, Column 2), this implies a shift in composition toward surviving small operations. The headline estimates also split the aggregate decline between fewer acres in farms and a lower value per acre, with the per-acre component negative but imprecisely estimated (Table 6, Panel B, Column 1).

These climate-induced changes also affected input decisions: farms exposed to winds from the Shelterbelt spend significantly less on hired labor and machines, but significantly more on fertilizers (Table 7, Columns 1–3). These effects can be induced either by the new choice of crops since corn typically requires more fertilizer than wheat, or by the smaller size of farms given that machinery and external labor may require a certain scale to be profitable.

Overall, these results indicate a key role played by policy-induced climate change on agricultural development, in areas not directly targeted by the tree-planting policy but downwind from it.

Longer term outcomes. Figure 5 traces our main climate and economic outcomes over time in 15-year windows, on the extended sample running through 2002 rather than the balanced 1930–1964 panel used in Tables 3–6. The Shelterbelt was planted over a short and delimited period, so the climate change it caused is dated rather than gradual. We can therefore follow each outcome for six decades and compare when responses appear and how long they last. The temperature effects hold throughout, while the precipitation effect does not survive beyond three decades (Figure 5, Panels a–d). Among the economic outcomes, some appear immediately and then attenuate. The reduction in land in farms is concentrated in the first two windows and then indistinguishable from zero afterwards (Panel l), and the increase in the number of farms peaks and then fades by the end of the period (Panel m). Others build and hold. The share of small farms rises and stays elevated through 2002, while value per acre is not distinguishable from zero in the first window, turns significantly negative in the second, and deepens before leveling off (Panels n and p).

Two implications follow for how the effects of a change in climate should be measured. First, the horizon determines the answer: a study observing only the first fifteen years would record the acreage response and miss the per-acre value response entirely, which is why our balanced 1930–1964 estimates cannot resolve the split between acreage and per-acre value (Table 6, Panel B, Column 1) while the long panel can. Second, transitory weather shocks identify a different object, since they leave capital investments, crop switching, and future expectations largely fixed and recover only short term responses within a growing season (Hsiang 2016; Kolstad and Moore 2020). What we estimate are the adjustments in response to a long term shift in the climate, and the opposing acreage and value profiles show that those adjustments need not point the same way at every horizon.

5.3 Validity and robustness

We now show that our empirical approach is valid, and our results robust. Specifically, we address the following potential concerns: the timing of the tree planting effects, the strategic choice of tree planting location, the correlation of wind patterns with spatially-differentiated climate trends, the Dust Bowl, irrigation, and the potential endogeneity of wind patterns.

5.3.1 Timing of the effects

In the difference-in-differences specification, we define P_t as an indicator variable equal to one for years after 1942. However, it is ex-ante unclear when trees planted under the Shelterbelt program will start influencing the climate and agricultural development. On the one hand, tree planting started as early as 1935, so some effects may also start then. On the other hand, trees need time to grow, and evapotranspiration is a function of tree biomass, so the effects of tree planting may only start materializing after several years. In both cases, this uncertainty around the specific treatment start time would bias our estimated effects towards 0, relative to the true long-term effects of the program.

To alleviate this potential concern, we implement a long differences strategy and estimate:

$$\Delta y_i = \beta^{LD} w_i + \gamma^{LD} \mathbf{X}_i + \psi_s^{LD} + \Delta\epsilon_i \tag{2}$$

where Δy_i is the change in some outcome y in county i between two periods. For comparability, we focus on the same time period as our main empirical specification: 1930-1965. We take averages of each outcome y over 1930–1935 and 1960–1965 and difference these averages to arrive at Δy_i. As in our main specification, w_i is the wind exposure measure that approximates exposure to summer winds from the afforested Shelterbelt counties. We also include state fixed effects, ψ_s, to control for unobserved state-level trends, as well as the same county-level controls ($\mathbf{X}_i$) as in our main specification (Equation 1).

Figure 6 presents the effects of the Shelterbelt tree planting on the downwind climate (Panel A) and key economic consequences (Panel B), showing together the estimates from our preferred difference-in-difference approach (Equation 1) and the long differences approach (Equation 2). (We also show the instrumental variable approach, described in Section 5.3.2.) For each of these approaches, we present the estimates from the specification with and without the main set of baseline controls. We find similar effects whether we use the difference-in-differences or long differences specifications, which indicates that our results are robust to our choice of 1942 as the cutoff between the baseline and post-treatment periods.

This is also consistent with our event study results, presented in Figure 4. Effects on precipitation and temperature emerge in the late 1930s, after tree planting began, and stabilize by the early 1940s. This validates our choice of 1942—the final year of Shelterbelt planting—as our treatment cutoff.

5.3.2 Strategic choice of tree-planting location

A second threat to identification stems from the potential strategic behavior of Shelterbelt participants. Importantly, our identification strategy does not require that the location of tree planting was random, it requires only that planting decisions were not made with anticipated downwind climate or economic effects in mind. If they took into account the program's potential climate spillovers when deciding where to plant trees, then our parallel trends assumption would be violated: trees might have been planted upwind from areas expected to have some specific future climate or economic trends. Note that this would bias our point estimates away from zero only if the trees were strategically planted upwind from areas expected to already witness a relative improvement in their climatic growing conditions.

We address this potential concern with an instrumental variable strategy. Similar to Li (2021), we use the planned Shelterbelt planting zone. While Li is interested in the local effects of the Shelterbelt program and uses the planned zone as a direct instrument for his main regressor (the actual planted areas), we do not use the planned zone as the instrument itself. Rather, we use it to create a measure of wind exposure to the *planned* Shelterbelt area, which we use to instrument wind exposure to the *actual* Shelterbelt.

The planned planting zone is the 100-mile wide band delimited by the Forest Service, shown in the gray shaded area in Appendix Figure S1. Its placement was unrelated to any potential impacts on downwind areas: the western limit was set by the rainfall threshold below which trees were not expected to survive (Section 2), and the width was fixed without reference to conditions on either side.[26]

The exogeneity of the planned Shelterbelt location rests on why it was drawn: the Forest Service fitted the zone to where trees were expected to survive, without regard to effects beyond the planted area. Counties inside and outside the planned area do differ in baseline climate, as expected given the rainfall-based western boundary. However, these differences disappear once we control for longitude quartiles and our main specification's controls (Appendix Table S3, Panel A).

We reproduce the wind exposure measure construction steps described in Section 3, except we replace the areas of actual concentrated Shelterbelt planting with the areas of planned Shelterbelt planting. The resulting planned wind exposure measure is orthogonal to our sample counties' baseline climate. Precipitation does not vary with wind exposure in the raw

[26] Unfortunately, there is no clear discontinuity in the likelihood of Shelterbelt tree planting around the eastern border, so we cannot use a spatial discontinuity design.

data, while the three temperature variables do not once we include the controls (Appendix Table S3, Panel B). We thus present IV results with and without controls.

We use the planned wind exposure measure (w_i^p) as an instrument for the continuous treatment variable (w_i) in our difference-in-differences model. Figure S12 shows the wind exposure instrument next to the actual wind exposure measure. The instrument is strong, with a robust Kleibergen-Paap (2006) F-statistic of 284.4 (Appendix Table S4, Panel A, Column 5).

We find that the instrumental variable estimates, designed to address a potential strategic choice of Shelterbelt program uptake and tree-planting location, are consistent with our preferred difference-in-differences estimates. With controls, the IV estimates are essentially unchanged relative to the headline OLS results. If anything, the maximum temperature and 29C degree days effects are stronger (Appendix Table S4, Panel B). Without controls, the precipitation estimate is smaller but remains large and statistically significant at the 1% level, while the temperature estimates remain similar (Appendix Table S4, Panel A). This indicates that our preferred estimates are not driven by a strategic selection of tree-planting location.

5.3.3 Spatially-differential climate trends and baseline shocks

It is well established that oceanic oscillations influence the regional climate over the course of years and decades. The most prominent is the El Niño-Southern Oscillation (ENSO), in which warming in the Pacific Ocean produces periodic climate shifts that differentially affect regions across the globe (Zebiak and Cane 1987). Likewise, global warming differentially affects regions across the US. Our estimates of climate impacts downwind from the Shelterbelt could be biased if the spatial patterns of wind exposure happened to be correlated with spatially differential climate trends.

In addition, the Shelterbelt project was conceived and implemented in response to the Dust Bowl—a major climatic episode that spanned much of the 1930s.[27] One might wonder, consequently, whether a reversion to non-shock conditions might have occurred around the time of tree planting. This would bias our estimates if a change in the climate in the Shelterbelt area would affect the climate downwind, even absent trees being planted (for instance, because of increased water vapor in the atmosphere).

[27] Interestingly, climate scientists argue that the Dust Bowl was caused by a combination of oceanic anomalies (which are exogenous to human activities in the US Midwest) and of local human-induced land degradation (Cook et al. 2009).

We now provide five sets of results demonstrating that these potential concerns are not empirically warranted.

First, we include state-by-year fixed effects in our main specification (Equation 1). This specification allows us to compare counties that are spatially close, hence unlikely to be exposed to differential climate trends absent the Shelterbelt tree planting, but that face differential wind exposure—thereby addressing the potential concern. As we expect with this approach, we find that counties with different levels of wind exposure have on average similar baseline climates (Table S1, Panel A).

Second, we go one step further and create a spatial grid, with cells of 2 degrees latitude and 2 degrees longitude. We then replace our state-by-year fixed effects by these gridcell-by-year fixed effects, to compare counties in the same region that are unlikely to face differential large-scale, medium-term climate oscillations and have similar baseline exposure to the Dust Bowl. The results, reported in Figures S14 and S15, are similar to our main results.

Third, we confirm that differential trends or the Dust Bowl are unlikely to bias the validity of our results, by using an alternative strategy to compare counties with similar baseline trends. Instead of including controls in our difference-in-differences specification, we implement a synthetic difference-in-differences specification: we compare the set of counties with above-median wind exposure to a composite set of the counties with below-median wind exposure, weighted such that the two groups have similar baseline trends, on average.[28] We can replicate our main results with the synthetic DiD method over the period 1930-1965. Nonetheless, a longer baseline period is useful to better estimate and match the baseline trends. We therefore also construct samples starting in 1920 and 1910; even though our main sample does not start this early given concerns about the availability and quality of pre-1930 climate and agricultural data (Knappenberger et al. 2001; Kunkel et al. 2007).[29] Both the classic DiD method and the synthetic DiD method offer generally consistent results, whether we consider 1920–1965 or 1930–1965 as the period of analysis (Appendix Table S10 and Figure S16).[30]

Fourth, we verify the robustness of our main results by using alternative time periods that omit the Dust Bowl era. We rerun our analyses separately by dropping the project im-

[28] See Section S.4.3 for more details.

[29] In order to replicate our analysis for 1910 or 1920 through 1965, we repeat the construction of a county-by-year panel of precipitation and temperature from weather stations with daily readings as detailed in Section S.3, except using a balanced panel of stations reporting between 1910 and 1965 instead of 1930 and 1965. We use the same stations for the analyses that start in 1920.

[30] Both sets of results using 1910-1965 are somewhat lower in magnitude, likely due to lower data quality in those early years, but still statistically significant for all but the mean temperature synthetic DiD method.

plementation years (1936 to 1942) and peak Dust Bowl years (1934, 1936, 1939) from our baseline period. Appendix Tables S7 and S8 show the results are generally consistent with our main findings. We also conduct long difference estimates (Equation 2) with alternative time windows. In Panel A of Appendix Table S11, we compare 1925-1930 (instead of 1930–1935) to 1960-1965 to address concerns that the early 1930s were still heavy drought periods. In Panel B, we compare 1930–1935 to 1950–1955 (instead of 1960–1965) to compare two general drought periods in the Great Plains in the pre- and post-planting periods. In both cases, the estimates are qualitatively similar to our main long differences results.

Fifth, we verify the robustness of our climate results by including Dust Bowl measures of erosion levels from Hornbeck 2012, which can be taken as proxy for the local severity of the Dust Bowl episode, as controls in our main specification. As such, we identify the downwind effects from the Shelterbelt tree planting by comparing counties with similar Dust Bowl exposure. The results, presented in Appendix Table S9, show that our results are robust. This was expected given the balance achieved across counties in our main specifications: even without controlling for the Dust Bowl exposure explicitly, our effects are identified by comparing counties with similar climates during our pre-period 1930–1942, which overlaps with the Dust Bowl.

Taken together, this consistent set of results derived from different empirical strategies indicates that our results are not driven by spatially differential climate trends, or by the Dust Bowl episode.

5.3.4 Irrigation

Irrigation strongly increased in the US Midwest after World War II, and prior work has indicated that irrigation also has the potential to affect the climate locally and downwind (e.g., Lobell et al. 2008; DeAngelis et al. 2010; Mueller et al. 2016; Braun and Schlenker 2023). If the Shelterbelt tree-planting happened where irrigation expanded, then our results could be contaminated: there could have been a change in the climate downwind from the Shelterbelt areas, even absent the tree-planting. However, this potential concern is not warranted empirically. We provide here a short overview of the empirical evidence, with more details provided in Appendix Section S.7.

First, historical sources (e.g., Barton 1936) describe precisely the cultivation of the trees planted under the Shelterbelt project, without any mention of irrigation. This lack of irrigation of the Shelterbelt trees themselves is consistent with the lack of available water at the time, and is unlikely to be driving the results we observe.

Second, we do not find the expansion of irrigation over our study period to be positively correlated with the areas of Shelterbelt planting. Specifically, among the Shelterbelt counties, the expansion of irrigated farmland is uncorrelated with the area of concentrated Shelterbelt planting (from the Read 1958 maps), and negatively correlated with the area of Shelterbelt trees (from the Snow 2019 shapefiles): counties with denser tree-planting saw, if anything, a smaller expansion of irrigation (Appendix Figure S18). Only a positive correlation could generate spurious downwind effects; a negative one would, if anything, attenuate our estimates. Looking at all Shelterbelt counties and their neighbors (all counties within 200km of a Shelterbelt county), we also do not find that being a county with Shelterbelt tree-planting is associated with a greater expansion of irrigated farmland (coef. = 0.005, p-value = 0.459).

Since the Shelterbelt trees were not irrigated themselves, and the Shelterbelt planting areas are not positively correlated with the areas of strong irrigation expansion, the potential concern that the substantial expansion of irrigation post-WWII might be confounding our results is not warranted.

5.3.5 Endogeneity and robustness of wind patterns

Our wind exposure measure is constructed from ERA5 reanalysis data, which provides spatially-consistent hourly wind fields starting in 1940. This allows us to construct our main exposure measure using data from 1940 itself, as tree-planting was just starting in earnest and largely addressing concerns about using post-intervention wind patterns. Importantly, prevailing winds have remained stable: constructing an alternative measure from 1965 ERA5 data yields a correlation of 0.97 with our main 1940 measure.

Nevertheless, we verify that our results are robust to the specific construction of the wind exposure measure. Our baseline measure initiates particles at 800 hPa (approximately 2,000 meters altitude, within the boundary layer where moisture is mixed and transported regionally) using wind data from 1940 only, before the Shelterbelt trees were mature enough to influence wind patterns. Figures S14 and S15 (third panel) show that results are similar across four variants of the measure: (i) our baseline (800 hPa, 1940 winds), (ii) 800 hPa using the full 1940–1965 wind data, (iii) 1000 hPa (approximately ground level) using 1940 winds, and (iv) 1000 hPa using 1940–1965 winds. The fact that results are similar whether we use pre-planting winds (1940 only) or the full sample period (1940–1965) confirms that prevailing wind patterns did not change meaningfully as a result of the Shelterbelt tree planting. The robustness checks with different starting altitudes also show that our results are not sensitive to assumptions about the altitude at which moisture travels from forested areas to downwind counties.

As a further check, we test whether our results are consistent with bias from wind pattern changes. We do this using our discretized wind exposure measure and the associated specification given in Equation 5. If we assume that the Shelterbelt changes wind patterns in a way that affects climate in neighboring counties, then a bias would occur if we classify as downwind neighbor areas that now receive precipitation from the new wind regime but did not otherwise. However, this new precipitation would be reallocated towards the downwind neighbors from counties that we classify as other (non-downwind) neighbors: ones that used to receive rain from the wind, but do not anymore due to the new wind pattern. If the Shelterbelt was reallocating precipitation in such a way, we should observe an effect of the intervention on the downwind counties of the same magnitude and opposite direction than the effect on the other non-downwind counties. This implication is directly testable: we do not find a negative treatment effect on other non-downwind neighbor counties, so it is unlikely that there was any material reallocation of precipitation (Figure S11).

6 Conclusion and discussion

While tree planting is often positioned as an important tool in mitigating global climate change, the impacts of massive tree-planting programs on local and regional climate—and the resulting economic effects—are less often examined and discussed. In this paper, we study the Great Plains Shelterbelt project, which planted over 220 million trees in the US between 1935 and 1942, representing what is likely the largest afforestation initiative in history up to that date.

We digitize historical maps of the Shelterbelt project to study the effects of tree planting on climate and economic outcomes like yields. We use a difference-in-differences approach that exploits wind patterns. We compare counties more exposed to large-scale prevailing winds from afforested areas in the Shelterbelt to those less exposed to these winds. We find that rainfall increased and temperature decreased with higher exposure to winds from afforested areas. Our results are robust to various alternate empirical methods, including instrumental variables, long differences, difference-in-differences with binary treatment variables, and synthetic difference-in-differences approaches.

Our climate estimates are in line with the natural science literature. While boreal forests are known to warm the surface, because dark trees absorb more sunlight than the snow they replace, and tropical forests result in net cooling due to evapotranspiration and the mixing generated by their rough canopies, the net impact of temperate forests—such as those in the US Midwest—is debated (Lee et al. 2011; Anderson et al. 2011). Our findings suggest the cooling effect dominates in our agricultural context. Specifically, our estimated decrease in maximum summer temperatures of 0.16°C is broadly consistent in magnitude with the annual mean land-surface cooling of temperate forests observed via satellite, 0.27°C (Li et al. 2015).[31] Our estimated precipitation increase of 3.9% is somewhat conservative relative to estimates for other temperate regions: for example, a European reforestation scenario was empirically estimated to raise summer precipitation by 7.6% (Meier et al. 2021). This difference seems consistent with the Shelterbelt's narrow spatial footprint and our focus on downwind rather than the planted areas themselves.

Are these climate effects realistic given the scale of the Shelterbelt program? One way to test this is to compare the estimated precipitation effect to the water the planted trees could physically transpire. For each non-Shelterbelt county, we multiply the coefficient in Table 1 by the county's wind exposure to obtain a predicted increase in monthly summer precipitation, sum across the three summer months (June–August), and weight by county area. This yields a total increase of approximately 2.1 trillion gallons. Spread over the total sample area, this amounts to 0.57 cm of additional rainfall over the summer, or under 3% of the baseline summer total.[32] Because our estimates identify relative differences across counties, this is an order-of-magnitude plausibility check rather than the program's absolute precipitation impact.

Using the other approach, the program planted 220 million trees with an estimated survival rate of 61% (Read 1958), leaving roughly 134 million surviving trees. USGS estimates that a large oak tree can transpire 40,000 gallons per year.[33] Spread over the same area, the surviving trees could transpire 1.34 trillion gallons if summer accounts for a quarter of annual transpiration, the equivalent of 0.37 cm of water, and twice that if summer accounts for half, as is plausible given that evapotranspiration peaks in the summer months. Our estimated increase of 0.57 cm falls inside that range. The exercise is coarse[34], but the precipitation

[31] Satellite-derived land surface temperature and in-situ near-surface air temperature can diverge (Winckler et al. 2019).

[32] The coefficient in Table 1 is 1.317 cm per month per unit of wind exposure, so county i's predicted summer increase is $3 \times 1.317 \times w_i$ cm, where w_i is its (unitless) wind exposure. Multiplying this depth by county area and summing across the 539 counties gives a volume of 7.9 billion m^3, or 2.1 trillion gallons. Dividing that volume by the total sample area of 1.37 million km^2 gives an area-weighted mean depth of 0.57 cm, against a baseline summer total of 21.5 cm.

[33] https://www.usgs.gov/special-topics/water-science-school/science/evapotranspiration-and-water-cycle

[34] This calculation omits direct evaporation from the soil, interactions with cropland, and differences in transpiration across species, tree age, baseline climate, and time within the growing season. The USGS figure refers to a large mature oak and is therefore generous for the young, mixed-species belts planted here, most of which were elm, ash, cottonwood, honeylocust and redcedar.

impact we find in Section 5.1 is the same order of magnitude as what the planted trees could physically supply.

After establishing the climate effects of the Shelterbelt project, we study the economic consequences of this engineered climate change. Because we focus on counties where no trees were planted, our estimates isolate the effects of the policy-induced change in climate from the direct local effects of afforestation and other local changes associated with the program. We find that corn production increased in areas more exposed to winds from the Shelterbelt but not directly afforested. This increase in corn production is mostly driven by an increase in the area harvested of corn, rather than by corn yields. Such increase, in turn, reflects climate adaptation: farmers switch from less water-intensive crops like wheat to more water-intensive crops like corn.

The policy-induced change in climate has important consequences for the agricultural development of the US Midwest: in a period of intense farm consolidation and mechanization, we find that areas downwind of the Shelterbelt whose growing conditions improved witnessed relatively less consolidation, keeping more small farms. But these areas also mechanized less, evidenced by lower use of farm machinery. The overall value of agricultural land and buildings was 3.1% lower, spread over more farms of smaller average size and fewer acres in farms—a change in the composition of the sector rather than a fall in land prices.

To quantify the economic magnitude of these effects, we compare the change in agricultural land values attributable to Shelterbelt wind exposure against the program's costs. Summing the estimated treatment effect across all non-Shelterbelt counties in our study region, by multiplying each county's baseline land value by the predicted change from Table 6 (Panel A, Column 1), yields an aggregate effect of approximately −\$256 million, or 3.3% of baseline farmland value in these counties—a decline, not an increase. Because value per acre and land in farms sum to aggregate value, this figure decomposes exactly: the per-acre component accounts for roughly a third and is not statistically distinguishable from zero, so most of the decline reflects fewer acres in farms rather than a fall in land prices. The figure measures redistribution across counties rather than a national welfare effect. Our design identifies how exposed counties fared relative to less exposed ones, so any change common to both is differenced out, and the sum of these relative differences need not equal the program's aggregate impact (Section 4).

For scale, the program's direct total cost was approximately \$18.5 million, including both government expenditures and farmers' contributions (Droze 1977). We stress that this calculation prices a single channel in counties downwind of the plantings. It excludes any local effect where trees were planted, and it does not monetize the gains in precipitation, extreme heat, and crop yields documented above, so it should not be read as a complete accounting of the program's return.

Our findings are particularly timely given the global enthusiasm for large-scale tree planting as a means of mitigating climate change—especially in light of estimates that such activities could potentially reduce atmospheric CO_2 levels by 25% (Bastin et al. 2019). Tree planting is a major part of nearly all proposed pathways to 'net zero' emissions, with estimated capital requirements on the scale of hundreds of billions of dollars. The excitement around tree planting is further evidenced by the increasing number of national forestry initiatives used by countries to meet their mitigation targets under the Paris Agreement.[35]

There are good reasons for this enthusiasm. Tree planting is a 'simple technology' enjoying high levels of public approval and public participation. Prior to concerns about climate change, afforestation initiatives like the Great Plains Shelterbelt and China's Three-North Shelterbelt Program were implemented to stabilize soils and reduce erosion and dust storms. Further, forestation efforts can reduce air pollution, particularly in urban settings (Xing et al. 2026). Our paper adds another co-benefit to this list. The increased precipitation and decreased extreme heat that we find during the growing season benefit crop production—particularly in the major cropland regions of the world that face hot summers and limited rainfall—conditions that are worsening under climate change. So in this sense, tree planting can be both a tool for mitigation (by sequestering carbon) and adaptation (by reducing the negative impact of global warming on agriculture).[36]

However, large-scale afforestation is not without controversy, particularly regarding the enormous amount of land required to reduce CO_2 levels at a meaningful scale.[37] Some critics worry that massive afforestation efforts could come at the expense of cropland and thus food security, while others are concerned about the dispossession of land from pastoralists and other traditional groups. Another major concern relates to the timing of the CO_2 reductions,

[35] Recently national initiatives include Pakistan's 10 Billion Trees Tsunami (2018), India's Tree-planting pledges (2017), Mexico's Sowing Life Program (2019), Kazakhstan's Two Billion Tree Project (2020), Turkey's Breath for the Future (2021), Mongolia's One Billion Tree Project (2021).

[36] An active literature in economics focuses on the drivers and consequences of deforestation, especially in the tropics (Burgess et al. 2012; Jayachandran et al. 2017; Burgess et al. 2019; Balboni et al. 2026; Araujo et al. 2026; for a review see Balboni et al. 2023). Our study focuses on tree planting, but the benefits we identify can also represent costs of deforestation. By illustrating the challenges to maintain the current tree cover, this evidence base can help guide the design of afforestation programs.

[37] One estimate of the land required for afforestation to achieve a 'net zero' transition by 2030 is 160 million hectares, larger than France, Spain, and Germany combined (McKinsey Global Institute 2022). Another report estimated an even larger figure of 1.2 *billion* hectares to achieve the carbon sequestration from national climate pledges under the Paris Agreement—an area equivalent to all current global cropland (Dooley et al. 2022).

given that emission reductions are immediate while trees take decades to grow, as well as their permanence in light of the potential for large-scale tree mortality from drought, invasive species (e.g., mountain pine beetle), cyclones, and wildfires (Leverkus et al. 2022). Indeed, some high-profile claims about tree planting's potential have faced significant scientific criticism (Veldman et al. 2019), and many past programs have delivered disappointing results due to poor species selection, inadequate management, or conflicts with local land users.

Many of these very real concerns can be addressed through the careful design of afforestation programs. Not all tree-planting initiatives are equal, and their outcomes and co-benefits will be a function of the land selected, the tree species included, their ongoing management over time, and community engagement. In China, there is evidence of farmers cutting down native trees and replacing them with monocultural plantations (Hua et al. 2018). The program we study, the Great Plains Shelterbelt, was unique in that tree planting occurred in concentrated areas and windbreaks. Over 30 species of trees and shrubs were selected—tall and short trees, fast and slow growing trees, hardwoods, and conifers—most of which were native and thus locally adapted (Read 1958) to ensure species diversity and ecological resilience in a way that mimicked naturally-occurring forests. Clearly, a tree planting program involving monocultures or non-native species could produce outcomes different than what we find—as well as different capital costs.

Relatedly, another valid question concerns the external validity of our results and the extent that the Great Plains is similar to other potential tree planting regions of the world. In terms of economic status, we first note that many countries today are still highly dependent on agriculture, like the US Midwest was in the 1940s.[38] In terms of agronomic conditions, the Great Plains Shelterbelt occurred on mollisol soils, which are common throughout rainfall-limited historic grasslands. As shown in Appendix Figure S5, these soils are also present in the major crop growing regions of China, Russia, Kazakhstan, Ukraine, Turkey, Argentina, Uruguay, Mexico, and Canada—many of the same countries which have proposed large-scale tree planting programs. Thus it is reasonable to think that similar climate and yield effects from tree planting could occur outside the Great Plains context.

To conclude, we find that the Great Plains Shelterbelt altered the climate and growing conditions of a meaningfully large area—a region roughly twice the size of California—over the course of several decades, producing important economic consequences. Our results show that human actions can alter local and regional climates through land use. In addition to the implications for tree planting initiatives and climate policy described above, our paper

[38] Both Mexico and China, for example, have a current GDP per capita and share of the population employed in agriculture similar to the US in 1945 (Appendix Figure S4).

highlights the endogeneity risk in using spatial variation in climate trends to assess local climate change impacts, and the potential bias it can imbue on climate change damage estimates. Future work should investigate how drivers of climate spillovers can be used as instruments for identifying the effect of climate change on economic outcomes.

7 Figures

Figure 1: Shelterbelt Measure

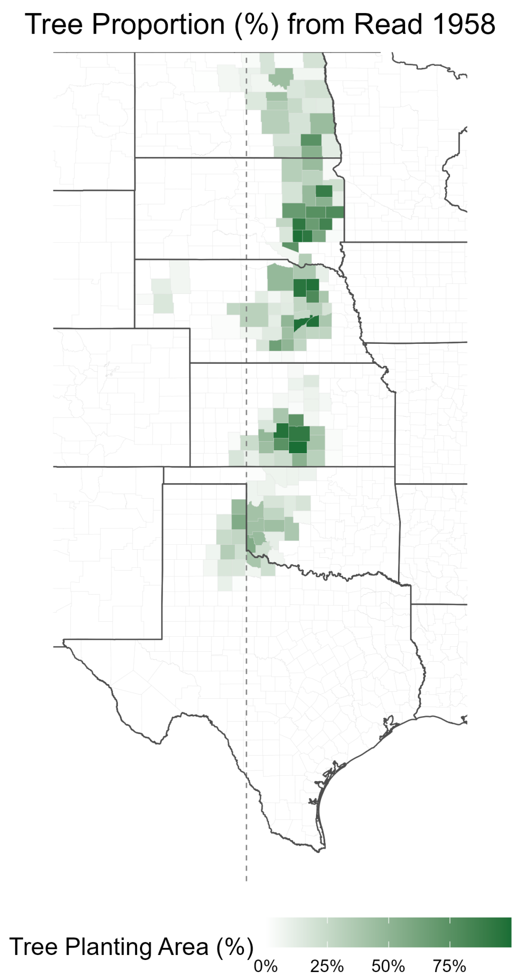

Notes: Figure shows intensive tree planting area (% of county area) based on digitized maps from Read (1958). We calculate the percentage of each county covered by "areas of concentrated Shelterbelt planting". Throughout the paper, we refer to counties with at least 5% tree proportion as Shelterbelt counties.

Figure 2: Shelterbelt wind exposure measure

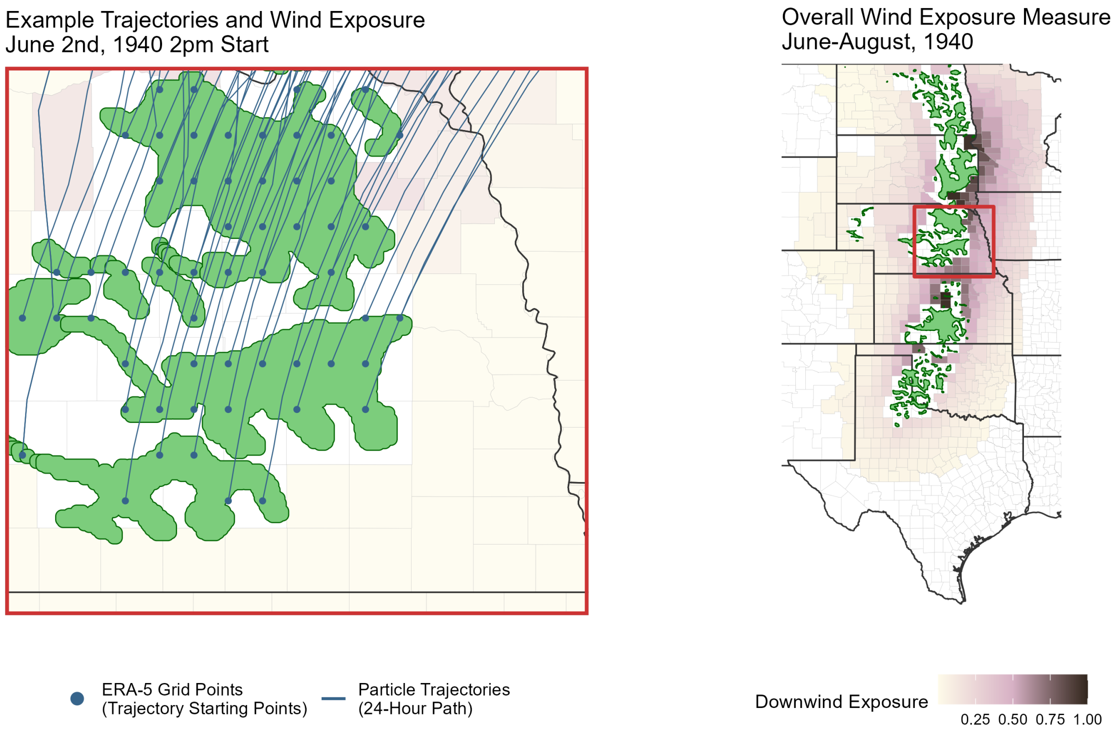

Notes: Figures illustrate the construction of our Shelterbelt wind exposure measure. Shaded green area shows concentrated Shelterbelt planting. Purple shading shows continuous wind exposure measure for non-Shelterbelt counties. The left panel shows details of construction for a subset of the Shelterbelt area. Blue dots represent the starting points of particle trajectories (ERA-5 grid points). Blue lines represent paths of imaginary particles initiated on an example day and hour (June 2nd, 1940, at 2pm) and updated every hour for 24 hours. A path going through a given county means a higher Shelterbelt wind exposure for that county. Aggregating these paths over all counties and summer hours yields our continuous measure of wind exposure. More details on the variable's construction are provided in Appendix S.2. The right panel shows the final continuous wind exposure measure for all counties in the sample.

Figure 3: Climate effects by season

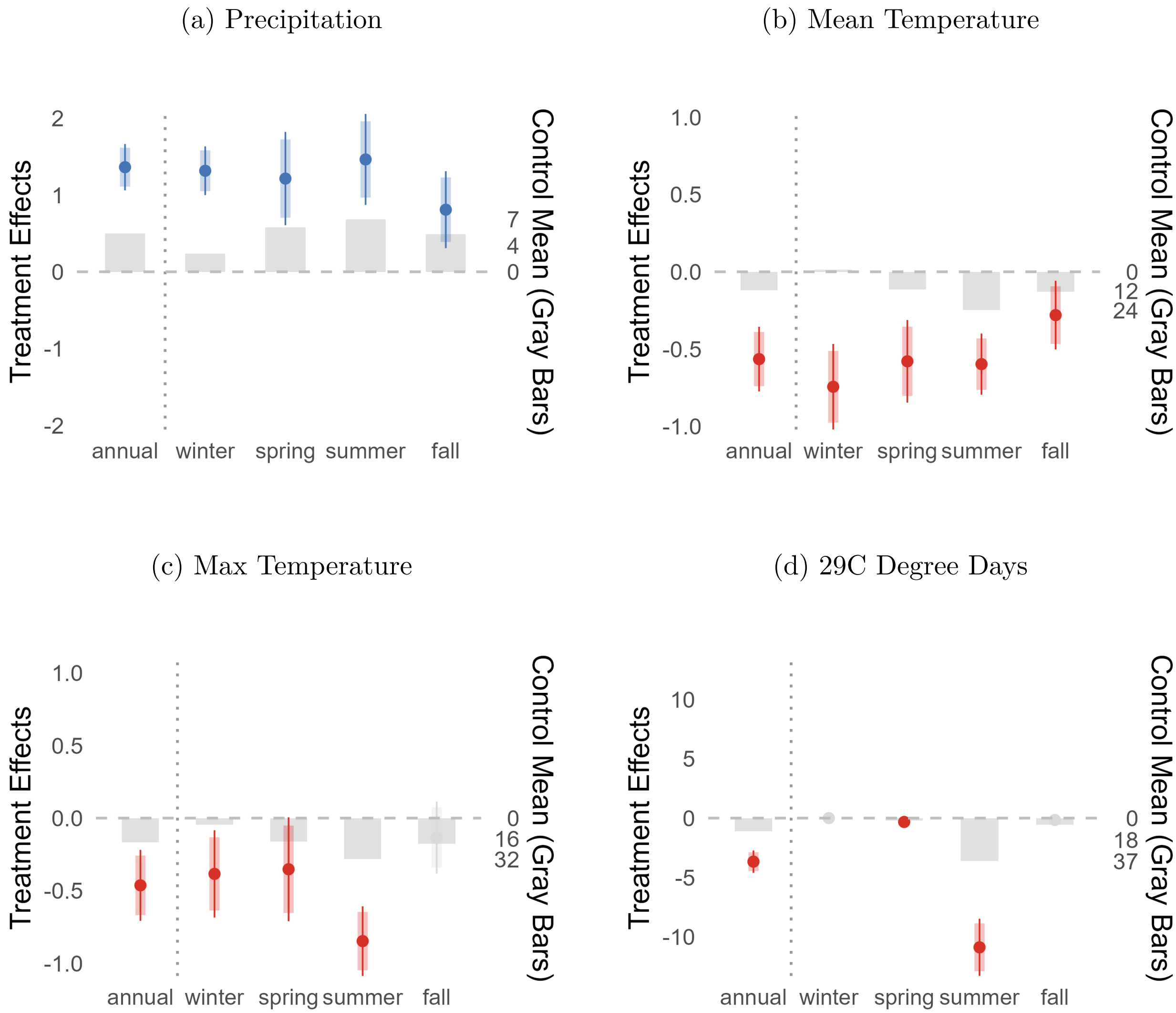

Notes: Figure plots coefficient estimates and 95% (thin line) and 90% (thick line) confidence intervals for the effect of seasonal wind exposure on climate outcomes, estimated using Equation 1. The gray bars represent the control mean of the dependent variable for each specific season. Dependent variables are: (a) precipitation (cm), (b) mean temperature (°C), (c) maximum temperature (°C), and (d) degree days above 29°C. The x-axis categorizes effects by annual (average across all months), winter (Dec-Feb), spring (Mar-May), summer (Jun-Aug), and fall (Sep-Nov). Wind exposure is also season-specific, computed by averaging monthly wind exposure for the months in each season (using the 1940 cross-section). The difference between the 75th and 25th percentile of this season-specific wind exposure measure is 0.26 (annual), 0.24 (winter), 0.24 (spring), 0.30 (summer), and 0.28 (fall). Sample of 539 counties outside the Shelterbelt and with centroids within 300km of the centroids of Shelterbelt counties. Time-invariant topographic controls, interacted by year. County and state-by-year FE are included. Standard errors are clustered at the county level.

Figure 4: Climate effects over time

(a) Mean Summer Temperature

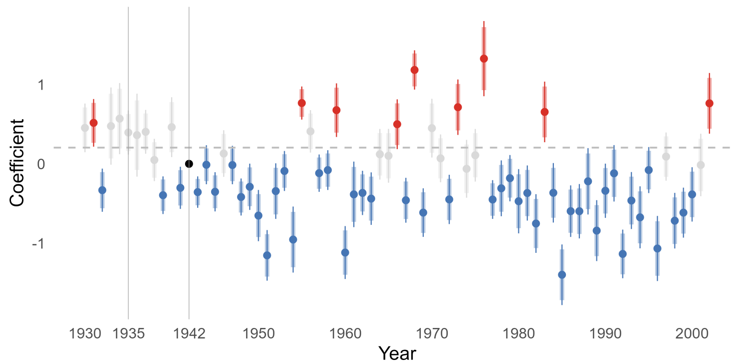

(b) Summer Precipitation

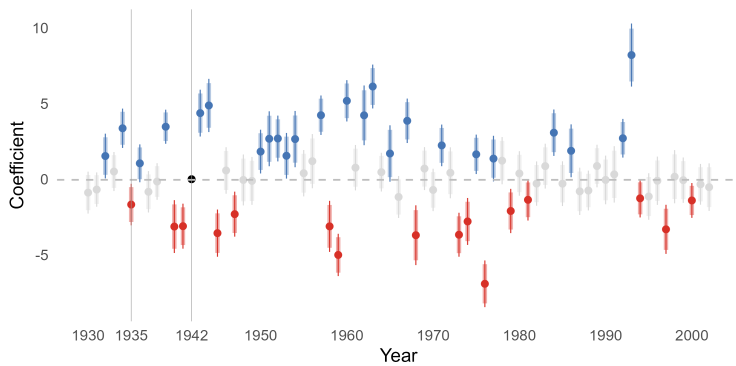

Notes: Figure shows event study specification, at the annual level from 1930 to 2002. The reference year is 1942. The gray vertical lines represent the start and end of the tree-planting period (1935–1942). The dashed horizontal line is set at the level of the baseline average (pre-1942); the coefficients are reported in color if this baseline sample average is not covered by their 90% confidence intervals. The difference between the 75$^{\text{th}}$ and 25$^{\text{th}}$ percentile of the continuous wind exposure measure is 0.21.

Figure 5: Treatment effects over the long term

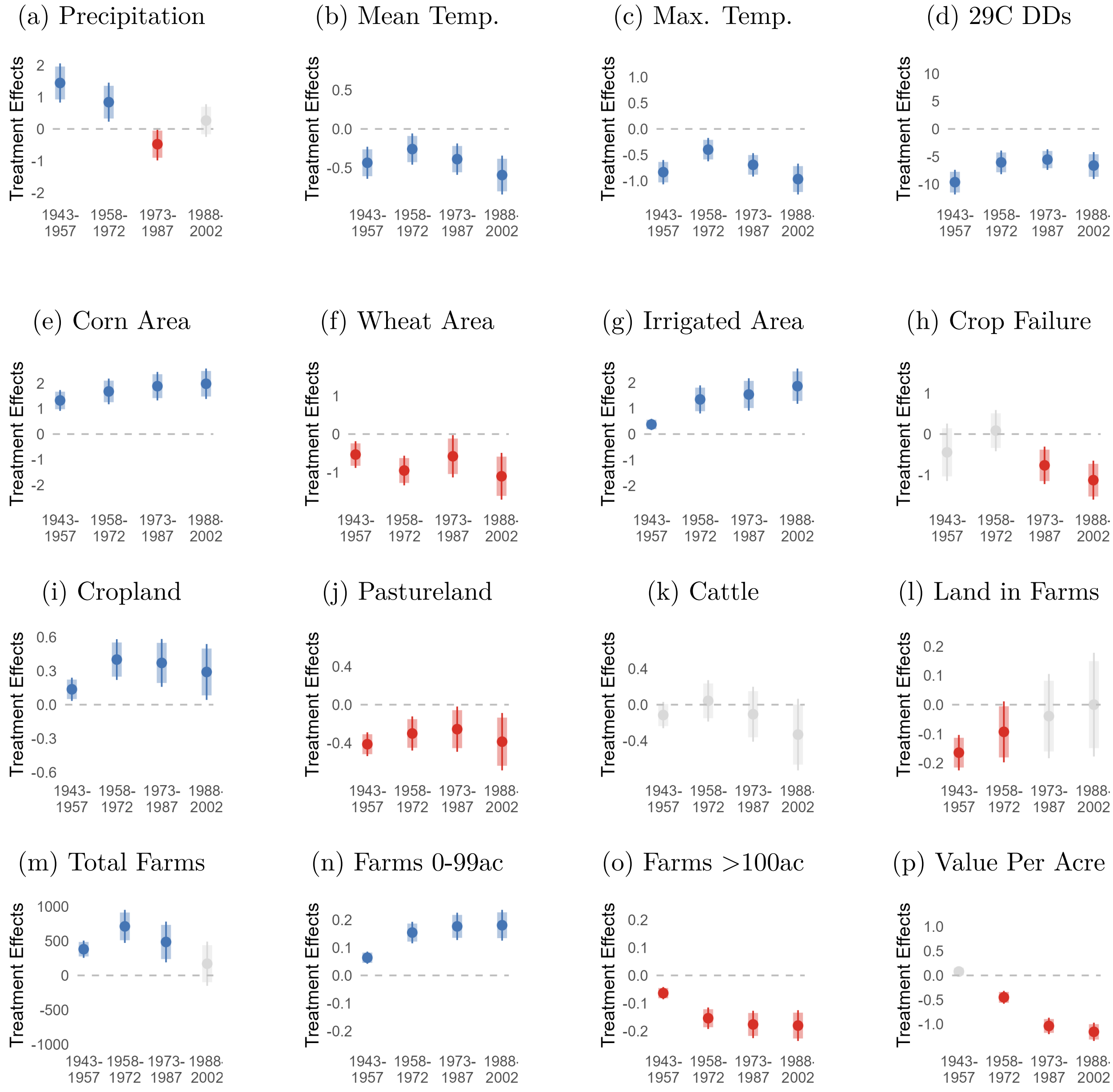

Notes: Figures show event study specification, with outcomes aggregated every 15 years. The reference period is the baseline period, 1930–1942. For the agricultural census outcomes, the period 1943–1957 encompasses the censuses 1945, 1950, 1954 ; the period 1958–1972 encompasses the censuses 1959, 1964, 1969 ; the period 1973–1987 encompasses the censuses 1974, 1978, 1982, 1987; the period 1988–2002 encompasses the censuses 1992, 1997, 2002. Coefficients are shown in grey unless significantly different from 0 at the 90% confidence level. Among significant estimates, blue denotes a positive coefficient and red a negative one, except in the temperature panels b) through d), where red denotes warming. Economic outcomes in Panels e) through l), and p), show logged outcomes. Panel m) shows the number of farms. Economic outcomes in Panels n) and o) show shares, among all farms. These use $\log(x)$ when zero-free and $\log(x+1)$ otherwise (zero counts in Table S13). The difference between the 75^{th} and 25^{th} percentile of the continuous wind exposure measure is 0.21.

Figure 6: Climate and economic results summary

Panel A: Climate outcomes

Panel B: Economic consequences

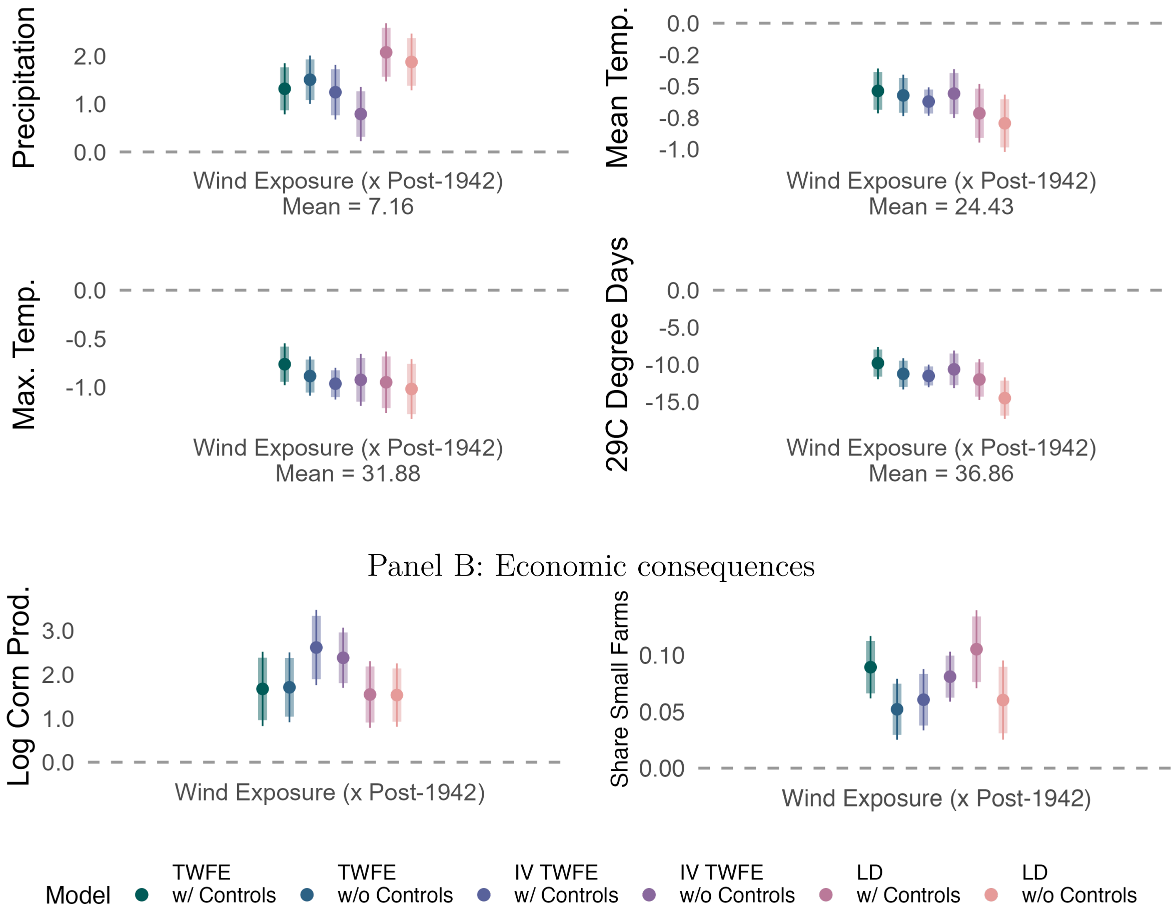

Notes: Figures plot coefficient estimates and 95% (thin line) and 90% (thick line) confidence intervals across three different models: two-way fixed effects (TWFE) (Equation 1), instrumental variables TWFE (Equation 8), and long differences (LD) (Equation 2), each with and without controls. 1930–1965 sample. The main independent variable is wind exposure (w_i), which measures approximate exposure to winds from afforested areas, interacted by a post-treatment dummy for the TWFE models. The difference between the 75$^{\text{th}}$ and 25$^{\text{th}}$ percentile of the continuous wind exposure measure is 0.21. Time-invariant controls include county-level elevation, ruggedness, area over the Ogallala aquifer, and for the IV results, longitude quartiles. County and state-by-year (or state, for LD) FE are included. In Panel A, dependent variables are summer precipitation, mean and maximum temperature, and 29C degree days (June - August averages). In Panel B, dependent variables are log corn production and the share of farms with a size below 100 acres. Logged outcomes use $\log(x)$ when zero-free and $\log(x+1)$ otherwise (zero counts in Table S13).

Figure 7: Effects on corn production, area, and yield

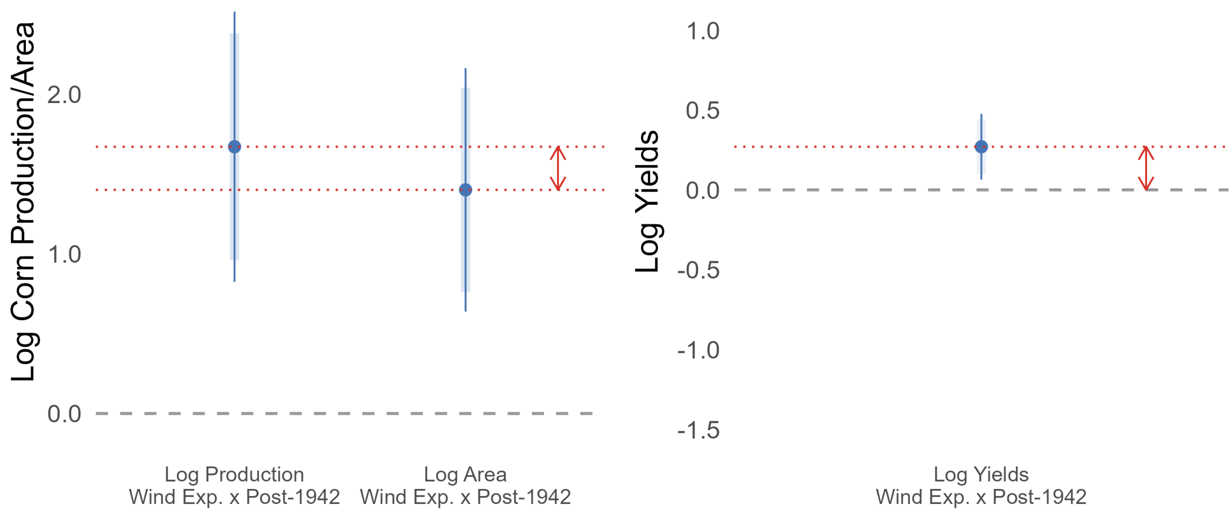

Notes: Figure shows results from estimating Equation 1, for log corn production and area (left panel) and log corn yields (right panel) for 449 counties, with centroids within 300km of the centroids of Shelterbelt counties, dropping directly afforested areas. The main independent variable is wind exposure (w_i), which measures approximate exposure to winds from afforested areas, interacted by a post-treatment dummy. The difference between the 75^{th} and 25^{th} percentile of the continuous wind exposure measure is 0.21. Time-invariant controls include county-level elevation, ruggedness, and area over the Ogallala aquifer. County and state-by-year FE are included. The difference between log production increase and log area increase is equal to the log yield increase. Logged outcomes use $\log(x)$ when zero-free and $\log(x+1)$ otherwise (zero counts in Table S13; no zeros for any of the outcomes in this figure). Coefficient estimates and 95% (thin line) and 90% (thick line) confidence intervals are reported.

8 Tables

Table 1: Impact of Great Plains Shelterbelt on summer county climate, 1930 to 1965

	Dependent variable:			
	Precipitation (cm)	Mean Temp (C)	Max Temp (C)	Degree Days (29C)
	(1)	(2)	(3)	(4)
Wind Exposure:Post 1942	1.317***	−0.538***	−0.763***	−9.809***
	(0.271)	(0.091)	(0.110)	(1.105)
	[<0.001]	[<0.001]	[<0.001]	[<0.001]
Conley SE	(0.449)	(0.130)	(0.155)	(1.622)
Conley p-value	[0.003]	[<0.001]	[<0.001]	[<0.001]
Sample Mean	7.16	24.43	31.88	36.86
Std.Dev.	2.94	2.82	2.92	22.94
Observations	19,404	19,404	19,404	19,404

Notes: Table shows results for estimating Equation 1. Sample of 539 counties outside the Shelterbelt and with centroids within 300km of the centroids of Shelterbelt counties, over 1930-1965. The main independent variable is wind exposure (w_i), which measures approximate exposure to winds from afforested areas, interacted by a post-treatment dummy. The difference between the 75th and 25th percentile of the continuous wind exposure measure is 0.21. Dependent variables are county-year averages over the summer months (June, July, and August). For clarity, for the "Sample Mean" row: (1) precipitation of 7.16cm is the average monthly cumulative rainfall, averaged across June-August; (2) mean temperature of 24.43C is the monthly average of daily mean temperatures, averaged across June-August; (3) max temperature of 31.88C is the monthly average of daily maximum temperatures, averaged across June-August; (4) degree days (29C) of 36.86 is the monthly sum of daily degree days exceeding 29C (i.e., a 32C day would contribute 3 degree days to that month), averaged across June-August. The "Sample Mean" and "Std. Dev." measures are taken in the pre-1942 period. Time-invariant controls, interacted by year, include county-level elevation, ruggedness, and area over the Ogallala aquifer. County and state-by-year FE are included. Standard errors are clustered at the county level, shown in parentheses; p-values shown in brackets (*p<0.1; **p<0.05; ***p<0.01). Conley standard errors and p-values with a cutoff of 100km are also reported. See Appendix Table S12 for results restricting the sample to county-years with agricultural census data available.

Table 2: Impact of Great Plains Shelterbelt wind exposure on weather (within-county variation)

	Dependent variable:			
	Precipitation (cm)	Mean Temp (C)	Max Temp (C)	Degree Days (29C)
	(1)	(2)	(3)	(4)
Panel A: Post-planting TWFE, Year and County Level				
Wind Exposure	22.511***	−3.093***	−5.621***	−65.934***
	(0.942)	(0.226)	(0.307)	(3.632)
	[<0.001]	[<0.001]	[<0.001]	[<0.001]
Conley SE	(1.827)	(0.443)	(0.597)	(7.265)
Conley p-value	[<0.001]	[<0.001]	[<0.001]	[<0.001]
Sample Mean	8.46	23.67	30.84	28.37
Residual Variance Ratio	0.489	0.043	0.08	0.133
Observations	12,397	12,397	12,397	12,397
Panel B: Post-planting TWFE, Year-Month and County Level				
Wind Exposure	19.418***	−1.761***	−3.628***	−42.801***
	(0.765)	(0.145)	(0.199)	(2.592)
	[<0.001]	[<0.001]	[<0.001]	[<0.001]
Conley SE	(1.589)	(0.272)	(0.376)	(5.084)
Conley p-value	[<0.001]	[<0.001]	[<0.001]	[<0.001]
Sample Mean	8.46	23.67	30.84	28.37
Residual Variance Ratio	0.597	0.078	0.128	0.212
Observations	37,191	37,191	37,191	37,191

Notes: Table shows estimation of Equation 9: TWFE regression on the 1943–1965 time period (post tree-planting). Regress climate outcome on time-and-space varying wind exposure, time fixed effects and county fixed effects. The level of the panel (i.e., the level of aggregation of the weather variable and the wind exposure variables, as well as of the time FE) is yearly in Panel A and monthly in Panel B. Residual variance ratio represents the ratio of the residuals from regressing the outcome variable on the fixed effects to the overall variance of the outcome. Coefficients are not directly comparable in magnitude to Table 1: the time-varying wind exposure measure has substantially less residual variation after absorbing county and time fixed effects than the cross-sectional measure used in Table 1 (the residual standard deviation is approximately one-fifth of the static measure's standard deviation), which mechanically inflates the per-unit coefficients. Standard errors are clustered at the county level, shown in parentheses; p-values shown in brackets (*p<0.1; **p<0.05; ***p<0.01). Conley standard errors and p-values with a cutoff of 100km are also reported.

Table 3: Impact of Great Plains Shelterbelt on agricultural activities, 1930 to 1964

	(1)	(2)	(3)
Panel A: Corn production	Log Bushels	Log Area Harvested	Log Yields
Wind Exposure:Post 1942	1.670***	1.400***	0.270**
	(0.430)	(0.388)	(0.105)
	[<0.001]	[<0.001]	[0.011]
Conley SE	(0.591)	(0.521)	(0.138)
Conley p-value	[0.005]	[0.007]	[0.051]
Mean	1507.66	39.47	27.23
Observations	3,592	3,592	3,592
Panel B: Other crop activities	Wheat Harvested (Log Area)	Irrigated Farmland (Log Area)	Crop Failures (Log Area)
Wind Exposure:Post 1942	−0.452***	0.954***	−0.422
	(0.174)	(0.171)	(0.272)
	[0.010]	[<0.001]	[0.122]
Conley SE	(0.257)	(0.249)	(0.423)
Conley p-value	[0.078]	[<0.001]	[0.319]
Mean	2.51	0.24	2.46
Observations	3,592	3,592	2,245
Panel C: Animal husbandry	Cattle (Log No.)	Pigs (Log No.)	Chickens (Log No.)
Wind Exposure:Post 1942	−0.022	0.810***	0.643***
	(0.076)	(0.125)	(0.088)
	[0.769]	[<0.001]	[<0.001]
Conley SE	(0.103)	(0.164)	(0.115)
Conley p-value	[0.828]	[<0.001]	[<0.001]
Mean	10.23	9.2	11.66
Observations	3,592	3,592	3,592

Notes: Table shows results for estimating Equation 1 for 449 counties, with centroids within 300km of the centroids of Shelterbelt counties, dropping directly afforested areas. Dependent variables are from USDA 5-year agricultural censuses (8 censuses between 1930 and 1964; 3,592 county-year observations). Acreage outcomes are measured in thousands of acres. Crop failure is not tabulated in the 1950, 1954, and 1959 censuses. The main independent variable is wind exposure (w_i), which measures approximate exposure to winds from afforested areas, interacted by a post-treatment dummy. Logged outcomes use $\log(x)$ when zero-free and $\log(x+1)$ otherwise (zero counts in Table S13); results are similar with inverse hyperbolic sine. The 75^{th}–25^{th} percentile difference of the wind exposure measure is 0.21. Time-invariant controls, interacted by year, include county-level elevation, ruggedness, and area over the Ogallala aquifer. County and state-by-year FE are included. Standard errors are clustered at the county level shown in parentheses; p-values shown in brackets (*p<0.1; **p<0.05; ***p<0.01). Conley standard errors and p-values with a cutoff of 100km are also reported.

Table 4: Impact of Great Plains Shelterbelt on farmland use, 1930 to 1964

	Dependent variable: Log Acres of				
	Land in Farms	Cropland	Pastureland	Woodland	Other Land
	(1)	(2)	(3)	(4)	(5)
Wind Exposure:Post 1942	-0.099^{***}	0.362^{***}	-0.395^{***}	-0.450^{***}	0.523^{***}
	(0.034)	(0.065)	(0.076)	(0.138)	(0.093)
	[0.005]	[<0.001]	[<0.001]	[0.002]	[<0.001]
Conley SE	(0.048)	(0.090)	(0.105)	(0.181)	(0.107)
Conley p-value	[0.040]	[<0.001]	[<0.001]	[0.013]	[<0.001]
Mean	6.05	5.28	5.07	1.25	2.67
Observations	3,592	3,592	3,143	3,143	3,143

Notes: Table shows results for estimating Equation 1 for 449 counties, with centroids within 300km of the centroids of Shelterbelt counties, dropping directly afforested areas. Dependent variables are from USDA 5-year agricultural censuses (8 censuses between 1930 and 1964). Acreage outcomes are measured in thousands of acres. The four land-use categories are mutually exclusive and, in the census definition, sum to total land in farms: cropland excludes acreage used only for pasture, which pastureland includes; woodland is farm woodland not pastured; and other land is the residual category: farmsteads and farm buildings, roads, ponds, and wasteland. Pastureland, woodland, and other land have no comparable 1940 county total, so those columns are estimated on seven censuses. The main independent variable is wind exposure (w_i), which measures approximate exposure to winds from afforested areas, interacted by a post-treatment dummy. Logged outcomes use $\log(x)$ when zero-free and $\log(x+1)$ otherwise (zero counts in Table S13); results are similar with inverse hyperbolic sine. The 75^{th}–25^{th} percentile difference of the wind exposure measure is 0.21. Time-invariant controls, interacted by year, include county-level elevation, ruggedness, and area over the Ogallala aquifer. County and state-by-year FE are included. Standard errors are clustered at the county level shown in parentheses; p-values shown in brackets (*p<0.1; **p<0.05; ***p<0.01). Conley standard errors and p-values with a cutoff of 100km are also reported.

Table 5: Impact of Great Plains Shelterbelt on farm consolidation, 1930 to 1964

	(1)	(2)	(3)	(4)	(5)
	Farms No.	Avg. Size	Share of Farms (by size, in acres)		
	Any size	(Log Acres)	< 100	100-499	≥ 500
Wind Exposure:Post 1942	424.645***	−0.468***	0.089***	−0.034	−0.055*
	(73.545)	(0.057)	(0.014)	(0.034)	(0.030)
	[<0.001]	[<0.001]	[<0.001]	[0.311]	[0.065]
Conley SE	(91.964)	(0.088)	(0.019)	(0.050)	(0.045)
Conley p-value	[<0.001]	[<0.001]	[<0.001]	[0.493]	[0.228]
Mean	1833.14	5.6	0.26	0.59	0.15
Observations	3,592	3,592	3,592	3,592	3,592

Notes: Table shows results for estimating Equation 1 for 449 counties, with centroids within 300km of the centroids of Shelterbelt counties, dropping directly afforested areas. Dependent variables are from USDA 5-year agricultural censuses (8 censuses between 1930 and 1964). The main independent variable is wind exposure (w_i), which measures approximate exposure to winds from afforested areas, interacted by a post-treatment dummy. The table reports the total number of farms, the log of average farm size (total land in farms divided by the number of farms, in acres), and the share of farms in each size class. Logged outcomes use $\log(x)$ when zero-free and $\log(x+1)$ otherwise (zero counts in Table S13); results are similar with inverse hyperbolic sine. The difference between the 75$^{\text{th}}$ and 25$^{\text{th}}$ percentile of the continuous wind exposure measure is 0.21. Time-invariant controls, interacted by year, include county-level elevation, ruggedness, and area over the Ogallala aquifer. County and state-by-year FE are included. Standard errors are clustered at the county level shown in parentheses; p-values shown in brackets (*p<0.1; **p<0.05; ***p<0.01). Conley standard errors and p-values with a cutoff of 100km are also reported.

Table 6: Impact of Great Plains Shelterbelt on farm values, 1930 to 1964

	(1)	(2)	(3)
Panel A: Aggregate values			
	Land and Buildings	Crops Sold	Animals Sold
Wind Exposure:Post 1942	-0.148^{**}	0.429^{***}	0.015
	(0.060)	(0.149)	(0.087)
	[0.015]	[0.005]	[0.867]
Conley SE	(0.088)	(0.205)	(0.121)
Conley p-value	[0.092]	[0.036]	[0.904]
Mean	16.39	13.59	14.23
Observations	3,592	3,143	3,143

Panel B: Values per acre			
	Per Acre of Farmland	Per Acre of Cropland	Per Acre of Pastureland
Wind Exposure:Post 1942	-0.050	0.065	0.465^{***}
	(0.052)	(0.131)	(0.138)
	[0.341]	[0.621]	[0.001]
Conley SE	(0.075)	(0.170)	(0.205)
Conley p-value	[0.510]	[0.702]	[0.023]
Mean	3.43	1.41	2.53
Observations	3,592	3,143	2,694

Notes: Table shows results for estimating Equation 1 for 449 counties, with centroids within 300km of the centroids of Shelterbelt counties, dropping directly afforested areas. Dependent variables are from USDA 5-year agricultural censuses (8 censuses between 1930 and 1964). Panel A reports aggregate values; Panel B divides each by the acreage on which it is produced. All outcomes are in logs of dollars. Crop and animal sales are missing in 1935, and pastureland has no comparable 1940 county total, so Column 3 of Panel B is estimated on six censuses with a single pre-treatment year. The main independent variable is wind exposure (w_i), which measures approximate exposure to winds from afforested areas, interacted by a post-treatment dummy. Logged outcomes use $\log(x)$ when zero-free and $\log(x+1)$ otherwise (zero counts in Table S13); results are similar with inverse hyperbolic sine. The 75^{th}–25^{th} percentile difference of the wind exposure measure is 0.21. Time-invariant controls, interacted by year, include county-level elevation, ruggedness, and area over the Ogallala aquifer. County and state-by-year FE are included. Standard errors are clustered at the county level shown in parentheses; p-values shown in brackets (*p<0.1; **p<0.05; ***p<0.01). Conley standard errors and p-values with a cutoff of 100km are also reported.

Table 7: Impact of Great Plains Shelterbelt on input choices, 1930 to 1964

	Dependent variable: Log Spending, on		
	Hired Labor	Hired Machines	Fertilizer
	(1)	(2)	(3)
Wind Exposure:Post 1942	-0.502^{***}	-0.406^{***}	6.895^{***}
	(0.111)	(0.119)	(0.638)
	[<0.001]	[0.001]	[<0.001]
Conley SE	(0.142)	(0.159)	(0.777)
Conley p-value	[<0.001]	[0.011]	[<0.001]
Mean	12.08	12.37	6.01
Observations	2,694	2,694	1,632

Notes: Table shows results for estimating Equation 1 for counties with centroids within 300km of the centroids of Shelterbelt counties, dropping directly afforested areas. Dependent variables are from USDA 5-year agricultural censuses (8 censuses between 1930 and 1964). The main independent variable is wind exposure (w_i), which measures approximate exposure to winds from afforested areas, interacted by a post-treatment dummy. Logged outcomes use $\log(x)$ when zero-free and $\log(x+1)$ otherwise (zero counts in Table S13); results are similar with inverse hyperbolic sine. The difference between the 75$^{\text{th}}$ and 25$^{\text{th}}$ percentile of the continuous wind exposure measure is 0.21. Fertilizer spending (Column 3) is not reported in the 1950 or 1959 censuses, so it is estimated on four censuses (1930, 1940, 1954, and 1964; 408 counties), whereas hired labor and hired machinery (Columns 1–2) use the six censuses in which both are reported (1930, 1940, 1950, 1954, 1959, and 1964; 449 counties). Time-invariant controls, interacted by year, include county-level elevation, ruggedness, and area over the Ogallala aquifer. County and state-by-year FE are included. Standard errors are clustered at the county level, shown in parentheses; p-values shown in brackets (*p<0.1; **p<0.05; ***p<0.01). Conley standard errors and p-values with a cutoff of 100km are also reported.

References

Alkama, Ramdane, and Alessandro Cescatti. 2016. “Biophysical climate impacts of recent changes in global forest cover.” *Science* 351 (6273): 600–604.

Anderson, Ray G., Josep G. Canadell, James T. Randerson, Robert B. Jackson, Bruce A. Hungate, Dennis D. Baldocchi, George A. Ban-Weiss, et al. 2011. “Biophysical considerations in forestry for climate protection.” *Frontiers in Ecology and the Environment* 9 (3): 174–182.

Annan, Francis, and Wolfram Schlenker. 2015. “Federal crop insurance and the disincentive to adapt to extreme heat.” *American Economic Review* 105 (5): 262–266.

Araujo, Rafael. 2024. “When clouds go dry: an integrated model of deforestation, rainfall, and agriculture.”

Araujo, Rafael, Juliano Assunção, Marina Hirota, and José A Scheinkman. 2023. “Estimating the spatial amplification of damage caused by degradation in the Amazon.” *Proc. Natl. Acad. Sci. U. S. A.* 120 (46): e2312451120.

Araujo, Rafael, Francisco Costa, and Marcelo Sant’Anna. 2026. “Efficient Conservation of the Brazilian Amazon: Estimates from a Dynamic Model.” *The Review of Economic Studies* 93 (1): 72–105.

Arkhangelsky, Dmitry, Susan Athey, David A. Hirshberg, Guido W. Imbens, and Stefan Wager. 2021. “Synthetic Difference-in-Differences.” *The American Economic Review* 111 (12): 4088–4118.

Asher, Sam, Alison Campion, Douglas Gollin, and Paul Novosad. 2022. “The long-run development impacts of agricultural productivity gains: Evidence from irrigation canals in india.” *Working Paper.*

Auffhammer, Maximilian. 2022. “Climate Adaptive Response Estimation: Short and long run impacts of climate change on residential electricity and natural gas consumption.” *Journal of Environmental Economics and Management* 114:102669.

Balboni, Clare, Aaron Berman, Robin Burgess, and Benjamin A. Olken. 2023. “The economics of tropical deforestation.” *Annual Review of Economics* 15:723–754.

Balboni, Clare, Robin Burgess, and Benjamin A Olken. 2026. “The origins and control of forest fires in the tropics.” *The Review of Economic Studies* 93 (4): 2348–2389.

Barton, Thomas F. 1936. “The Great Plains Tree Shelterbelt Project.” *Journal of Geography* 35 (4): 125–135.

Bastin, Jean-Francois, Yelena Finegold, Claude Garcia, Danilo Mollicone, Marcelo Rezende, Devin Routh, Constantin M Zohner, and Thomas W Crowther. 2019. “The global tree restoration potential.” *Science* 365 (6448): 76–79.

Bhuller, Manudeep, Tarjei Havnes, Edwin Leuven, and Magne Mogstad. 2013. “Broadband Internet: An Information Superhighway to Sex Crime?” *The Review of Economic Studies* 80 (4): 1237–1266.

Blakeslee, David, Ram Fishman, and Veena Srinivasan. 2020. “Way Down in the Hole: Adaptation to Long-Term Water Loss in Rural India.” *The American Economic Review* 110 (1): 200–224.

Bonan, Gordon B. 2008. “Forests and Climate Change: Forcings, Feedbacks, and the Climate Benefits of Forests.” *Science* 320 (5882): 1444–1449.

Bowers, Douglas E., Wayne D. Rasmussen, and Gladys L. Baker. 1984. *History of Agricultural Price-Support and Adjustment Programs, 1933–84: Background for 1985 Farm Legislation.* Agriculture Information Bulletin 485. Washington, DC: U.S. Department of Agriculture, Economic Research Service.

Braun, Thomas, and Wolfram Schlenker. 2023. “Cooling Externality of Large-Scale Irrigation.” *NBER Working Paper,* Working Paper Series, no. 30966.

Burgess, Robin, Francisco J M Costa, and Ben Olken. 2019. “The Brazilian Amazon’s double reversal of fortune.”

Burgess, Robin, Matthew Hansen, Benjamin A Olken, Peter Potapov, and Stefanie Sieber. 2012. "The Political Economy of Deforestation in the Tropics." *The Quarterly Journal of Economics* 127 (4): 1707–1754.

Burke, Marshall, and Kyle Emerick. 2016. "Adaptation to climate change: Evidence from US agriculture." *American Economic Journal: Economic Policy* 8 (3): 106–40.

Burlig, Fiona, Louis Preonas, and Matt Woerman. 2026. *Groundwater and Crop Choice in the Short and Long Run.* Working Paper 28706. National Bureau of Economic Research.

Bustos, Paula, Bruno Caprettini, and Jacopo Ponticelli. 2016. "Agricultural productivity and structural transformation: Evidence from Brazil." *American Economic Review* 106 (6): 1320–1365.

Bustos, Paula, Gabriel Garber, and Jacopo Ponticelli. 2020. "Capital accumulation and structural transformation." *The Quarterly Journal of Economics* 135 (2): 1037–1094.

Butler, Ethan E, and Peter Huybers. 2013. "Adaptation of US maize to temperature variations." *Nature Climate Change* 3 (1): 68–72.

Callaway, Brantly, Andrew Goodman-Bacon, and Pedro H. C. Sant'Anna. 2024. *Difference-in-Differences with a Continuous Treatment.* Working Paper 32117. National Bureau of Economic Research.

Carleton, Tamma A., and Solomon M. Hsiang. 2016. "Social and economic impacts of climate." *Science* 353 (6304): aad9837.

Cook, Benjamin I., Ron L. Miller, and Richard Seager. 2009. "Amplification of the North American "Dust Bowl" drought through human-induced land degradation." *Proceedings of the National Academy of Sciences* 106 (13): 4997–5001.

Cui, Xiaomeng. 2020. "Climate change and adaptation in agriculture: Evidence from US cropping patterns." *Journal of Environmental Economics and Management* 101:102306.

DeAngelis, Anthony, Francina Dominguez, Ying Fan, Alan Robock, M Deniz Kustu, and David Robinson. 2010. "Evidence of enhanced precipitation due to irrigation over the Great Plains of the United States." *Journal of Geophysical Research: Atmospheres* 115 (D15).

Dell, Melissa, Benjamin F Jones, and Benjamin A Olken. 2012. "Temperature Shocks and Economic Growth: Evidence from the Last Half Century." *American Economic Journal: Macroeconomics* 4 (3): 66–95.

———. 2014. "What Do We Learn from the Weather? The New Climate-Economy Literature." *Journal of Economic Literature* 52 (3): 740–798.

Devaraju, N., Govindasamy Bala, and Angshuman Modak. 2015. "Effects of large-scale deforestation on precipitation in the monsoon regions: remote versus local effects." *Proceedings of the National Academy of Sciences* 112 (11): 3257–3262.

Dimitri, Carolyn, Anne Effland, and Neilson C Conklin. 2005. *The 20th Century Transformation of U.S. Agriculture and Farm Policy.* Economic Information Bulletin 3. U.S. Department of Agriculture, Economic Research Service.

Dooley, Kate, Heather Keith, Anne Larson, Georgina Catacora-Vargas, Wim Carton, Kirstine Lund Christiansen, Ojong Enokenwa Baa, Alain Frechette, Sonia Hugh, Nathan Ivetic, et al. 2022. "The Land Gap Report."

Droze, Wilmon H. 1977. *Trees, prairies, and people: A history of tree planting in the Plains States.* Texas Woman's University.

Duveiller, Grégory, Josh Hooker, and Alessandro Cescatti. 2018. "The mark of vegetation change on Earth's surface energy balance." *Nature Communications* 9:679.

Edwards, Eric C., and Steven M. Smith. 2018. "The Role of Irrigation in the Development of Agriculture in the United States." *The Journal of Economic History* 78 (4): 1103–1141.

Fishman, Ram. 2018. "Groundwater depletion limits the scope for adaptation to increased rainfall variability in India." *Climatic change* (Dordrecht) 147 (1-2): 195–209.

Georgescu, Matei, David B Lobell, and Christopher B Field. 2011. "Direct climate effects of perennial bioenergy crops in the United States." *Proceedings of the National Academy of Sciences* 108 (11): 4307–4312.

Goodman-Bacon, Andrew. 2018. "Public Insurance and Mortality: Evidence from Medicaid Implementation." *Journal of Political Economy* 126 (1): 216–262.

Haines, Michael, Price Fishback, and Paul Rhode. 2018. *United States Agriculture Data, 1840 - 2012.*

Hamberg, L. Jonas, Joshua B. Fisher, Jonathan L.W. Ruppert, Jessica Tureček, Dean H. Rosen, and Patrick M.A. James. 2022. "Assessing and modeling diurnal temperature buffering and evapotranspiration dynamics in forest restoration using ECOSTRESS thermal imaging." *Remote Sensing of Environment* 280:113178.

Hansen, Zeynep K, and Gary D Libecap. 2004. "Small farms, externalities, and the Dust Bowl of the 1930s." *Journal of Political Economy* 112 (3): 665–694.

Hausfather, Zeke, Henri F Drake, Tristan Abbott, and Gavin A Schmidt. 2020. "Evaluating the performance of past climate model projections." *Geophysical Research Letters* 47 (1): e2019GL085378.

Hawkins, Ed, and Rowan Sutton. 2009. "The potential to narrow uncertainty in regional climate predictions." *Bulletin of the American Meteorological Society* 90 (8): 1095–1108.

Hersbach, H., B. Bell, P. Berrisford, G. Biavati, A. Horányi, J. Mu noz Sabater, J. Nicolas, et al. 2023. *ERA5 hourly data on single levels from 1940 to present.* Copernicus Climate Change Service (C3S) Climate Data Store (CDS). (Accessed on DD-MMM-YYYY).

Heutel, Garth, Nolan H Miller, and David Molitor. 2021. "Adaptation and the mortality effects of temperature across US climate regions." *Review of Economics and Statistics* 103 (4): 740–753.

Hornbeck, Richard. 2012. "The Enduring Impact of the American Dust Bowl: Short- and Long-Run Adjustments to Environmental Catastrophe." *American Economic Review* 102 (4): 1477–1507.

Hornbeck, Richard, and Pinar Keskin. 2014. "The historically evolving impact of the ogallala aquifer: Agricultural adaptation to groundwater and drought." *American Economic Journal: Applied Economics* 6 (1): 190–219.

Hornbeck, Richard, and Enrico Moretti. 2024. "Estimating who benefits from productivity growth: local and distant effects of city productivity growth on wages, rents, and inequality." *The Review of Economics and Statistics* 106 (3): 587–607.

Horner, GM, WA Starr, and JK Patterson. 1957. "The Pacific Northwest wheat region." *The Yearbook of Agriculture (Washington, DC: US Department of Agriculture),* 475–481.

Howlader, Aparna. 2023. "Determinants and consequences of large-scale tree plantation projects: Evidence from the Great Plains Shelterbelt Project." *Land Use Policy* 132:106785.

Hsiang, Solomon. 2016. "Climate Econometrics." *Annual Review of Resource Economics* 8 (1): 43–75.

Hsiang, Solomon, and Robert E Kopp. 2018. "An economist's guide to climate change science." *Journal of Economic Perspectives* 32 (4): 3–32.

Hua, Fangyuan, Lin Wang, Brendan Fisher, Xinlei Zheng, Xiaoyang Wang, Douglas W Yu, Ya Tang, Jianguo Zhu, and David S Wilcove. 2018. "Tree plantations displacing native forests: The nature and drivers of apparent forest recovery on former croplands in Southwestern China from 2000 to 2015." *Biological Conservation* 222:113–124.

Hultgren, Andrew, Tamma Carleton, Michael Delgado, Diana R Gergel, Michael Greenstone, Trevor Houser, Solomon Hsiang, et al. 2025. "Impacts of climate change on global agriculture accounting for adaptation." *Nature* 642 (8068): 644–652.

Jayachandran, Seema, Joost de Laat, Eric F Lambin, Charlotte Y Stanton, Robin Audy, and Nancy E Thomas. 2017. "Cash for carbon: A randomized trial of payments for ecosystem services to reduce deforestation." *Science* 357 (6348): 267–273.

Kala, Namrata. 2017. "Learning, adaptation, and climate uncertainty: Evidence from Indian agriculture." *MIT Center for Energy and Environmental Policy Research Working Paper,* nos. 2017-023.

Kleibergen, Frank, and Richard Paap. 2006. "Generalized reduced rank tests using the singular value decomposition." *Journal of Econometrics* 133 (1): 97–126.

Kline, Patrick, and Enrico Moretti. 2014. "Local economic development, agglomeration economies, and the big push: 100 years of evidence from the Tennessee Valley Authority." *The Quarterly Journal of Economics* 129 (1): 275–331.

Knappenberger, Paul C., Patrick J. Michaels, and Robert E. Davis. 2001. "Nature of observed temperature changes across the United States during the 20th century." *Climate Research* 17 (1): 45–53.

Kolstad, Charles D, and Frances C Moore. 2020. "Estimating the Economic Impacts of Climate Change Using Weather Observations." *Review of Environmental Economics and Policy* 14 (1): 1–24.

Kunkel, Kenneth E., Michael A. Palecki, Kenneth G. Hubbard, David A. Robinson, Kelly T. Redmond, and David R. Easterling. 2007. "Trend Identification in Twentieth-Century U.S. Snowfall: The Challenges." *Journal of Atmospheric and Oceanic Technology* (Boston MA, USA) 24 (1): 64–73.

Kurukulasuriya, Pradeep, and Robert Mendelsohn. 2008. "Crop switching as a strategy for adapting to climate change." *African Journal of Agricultural and Resource Economics* 2 (1): 1–22.

Lee, Xuhui, Michael L. Goulden, David Y. Hollinger, Alan Barr, T. Andrew Black, Gil Bohrer, Rosvel Bracho, et al. 2011. "Observed increase in local cooling effect of deforestation at higher latitudes." *Nature* 479 (7373): 384–387.

Lemoine, Derek. 2024. "Estimating the Consequences of Climate Change from Variation in Weather." *NBER Working Paper,* Working Paper Series, no. 25008.

Leverkus, Alexandro B, Simon Thorn, David B Lindenmayer, and Juli G Pausas. 2022. "Tree planting goals must account for wildfires." *Science* 376 (6593): 588–589.

Li, Tianshu. 2021. "Protecting the breadbasket with trees? The effect of the great plains shelterbelt project on agriculture." *Land Economics* 97 (2): 321–344.

Li, Yan, Maosheng Zhao, Safa Motesharrei, Qiaozhen Mu, Eugenia Kalnay, and Shuangcheng Li. 2015. "Local cooling and warming effects of forests based on satellite observations." *Nature Communications* 6:6603.

Libecap, Gary D, and Zeynep K Hansen. 2002. "'Rain Follows the Plow' and Dryfarming Doctrine: The Climate Information Problem and Homestead Failure in the Upper Great Plains, 1890–1925." *Journal of Economic History* 62 (1): 86–120.

Liu, Maggie, Yogita Shamdasani, and Vis Taraz. 2023. "Climate Change and Labor Reallocation: Evidence from Six Decades of the Indian Census." *American Economic Journal: Economic Policy* 15 (2): 395–423.

Loarie, Scott R., David B. Lobell, Gregory P. Asner, Qiaozhen Mu, and Christopher B. Field. 2011. "Direct impacts on local climate of sugar-cane expansion in Brazil." *Nature Climate Change* 1 (2): 105–109.

Lobell, David B, Celine J Bonfils, Lara M Kueppers, and Mark A Snyder. 2008. "Irrigation cooling effect on temperature and heat index extremes." *Geophysical Research Letters* 35 (9).

Malikov, Emir, Ruiqing Miao, and Jingfang Zhang. 2020. "Distributional and temporal heterogeneity in the climate change effects on U.S. agriculture." *Journal of Environmental Economics and Management* 104:102386.

McKinsey Global Institute. 2022. *The net-zero transition: what it would cost, what it could bring.* Technical report.

Meier, Ronny, Jonas Schwaab, Sonia I. Seneviratne, Michael Sprenger, Elizabeth Lewis, and Edouard L. Davin. 2021. "Empirical estimate of forestation-induced precipitation changes in Europe." *Nature Geoscience* 14 (7): 473–478.

Montesquieu, Charles de. 1750. *The Spirit of the Laws.* Thomas Nugent.

Mueller, Nathaniel D, Ethan E Butler, Karen A McKinnon, Andrew Rhines, Martin Tingley, N Michele Holbrook, and Peter Huybers. 2016. "Cooling of US Midwest summer temperature extremes from cropland intensification." *Nature Climate Change* 6 (3): 317–322.

National Center for Atmospheric Research Staff. 2014. "The Climate Data Guide: Regridding Overview." Accessed June 8, 2026. https://climatedataguide.ucar.edu/climate-tools/regridding-overview.

Neild, Ralph E, and James E Newman. 1987. *Growing season characteristics and requirements in the Corn Belt.* National Corn Handbook NCH-40, Cooperative Extension Service.

Peng, Shu-Shi, Shilong Piao, Zhenzhong Zeng, Philippe Ciais, Liming Zhou, Laurent Z. X. Li, Ranga B. Myneni, Yi Yin, and Hui Zeng. 2014. "Afforestation in China cools local land surface temperature." *Proceedings of the National Academy of Sciences* 111 (8): 2915–2919.

Pigou, Arthur Cecil. 1932. *The Economics of Welfare.* 4th. London: Macmillan.

Pitman, A. J., N. de Noblet-Ducoudré, F. B. Avila, L. V. Alexander, J.-P. Boisier, V. Brovkin, C. Delire, et al. 2012. "Effects of land cover change on temperature and rainfall extremes in multi-model ensemble simulations." *Earth System Dynamics* 3 (2): 213–231.

Pitman, A. J., N. de Noblet-Ducoudré, F. T. Cruz, E. L. Davin, G. B. Bonan, V. Brovkin, M. Claussen, et al. 2009. "Uncertainties in climate responses to past land cover change: First results from the LUCID intercomparison study." *Geophysical Research Letters* 36:L14814.

Qi, S.L. 2010. *Digital map of aquifer boundary for the High Plains aquifer in parts of Colorado, Kansas, Nebraska, New Mexico, Oklahoma, South Dakota, Texas, and Wyoming.* U.S. Geological Survey Data Series 543.

Rambachan, Ashesh, and Jonathan Roth. 2023. "A More Credible Approach to Parallel Trends." *Review of Economic Studies* 90 (5): 2555–2591.

Read, Ralph A. 1958. "Great Plains shelterbelt in 1954." *Great Plains Agricultural Council.*

Russo, Tess A., and Upmanu Lall. 2017. "Depletion and response of deep groundwater to climate-induced pumping variability." *Nature Geoscience* 10 (2): 105–108.

Schlenker, Wolfram, and Michael J Roberts. 2006. "Nonlinear Effects of Weather on Corn Yields." *Review of Agricultural Economics* 28 (3): 391–398.

———. 2009. "Nonlinear temperature effects indicate severe damages to US crop yields under climate change." *Proceedings of the National Academy of Sciences* 106 (37): 15594–15598.

Schulte, Lisa A, Jarad Niemi, Matthew J Helmers, Matt Liebman, J Gordon Arbuckle, David E James, Randall K Kolka, Matthew E O'Neal, Mark D Tomer, John C Tyndall, et al. 2017. "Prairie strips improve biodiversity and the delivery of multiple ecosystem services from corn–soybean croplands." *Proceedings of the National Academy of Sciences* 114 (42): 11247–11252.

Self, Alister, Rebecca Burdon, Jared Lewis, Peter Riggs, and Kate Dooley. 2023. *Land Gap Report Briefing Note: 2023 Update.* Technical report. Land Gap Report (landgap.org).

Sloat, Lindsey L, Steven J Davis, James S Gerber, Frances C Moore, Deepak K Ray, Paul C West, and Nathaniel D Mueller. 2020. "Climate adaptation by crop migration." *Nature Communications* 11 (1): 1243.

Smith, C, J C A Baker, and D V Spracklen. 2023. "Tropical deforestation causes large reductions in observed precipitation." *Nature* 615 (7951): 270–275.

Snow, Meagan. 2019. "The Shelterbelt "Scheme": Radical Ecological Forestry and the Production of Climate in the Fight for the Prairie States Forestry Project." PhD diss., University of Minnesota.

Spracklen, D. V., S. R. Arnold, and C. M. Taylor. 2012. "Observations of increased tropical rainfall preceded by air passage over forests." *Nature* 489 (7415): 282–285.

Spracklen, D. V., and L. Garcia-Carreras. 2015. "The impact of Amazonian deforestation on Amazon basin rainfall." *Geophysical Research Letters* 42 (21): 9546–9552.

Su, Yongxian, Chaoqun Zhang, Philippe Ciais, Zhenzhong Zeng, Alessandro Cescatti, Jiali Shang, Jing Ming Chen, et al. 2023. "Asymmetric influence of forest cover gain and loss on land surface temperature." *Nature Climate Change* 13 (8): 823–831.

Taraz, Vis. 2017. "Adaptation to climate change: Historical evidence from the Indian monsoon." *Environment and Development Economics* 22 (5): 517–545.

Taylor, Charles A. 2026. "Irrigation and climate change: Long-run adaptation and its externalities." *Journal of the Association of Environmental and Resource Economists* 13 (4): 935–973.

"Tree Belt in West to Fight Droughts." 1934. *The New York Times,* 1.

U.S. Forest Service. 1935. *Possibilities of Shelterbelt Planting in the Plains Region.* Technical report. Prepared under the direction of the Lake States Forest Experiment Station. Washington, DC: U.S. Government Printing Office.

Veldman, Joseph W., Julie C. Aleman, Swanni T. Alvarado, T. Michael Anderson, Sally Archibald, William J. Bond, Thomas W. Boutton, et al. 2019. "Comment on "The global tree restoration potential"." *Science* 366 (6463): eaay7976.

Winckler, Johannes, Christian H. Reick, Sebastiaan Luyssaert, Alessandro Cescatti, Paul C. Stoy, Quentin Lejeune, Thomas Raddatz, Andreas Chlond, Marvin Heidkamp, and Julia Pongratz. 2019. "Different response of surface temperature and air temperature to deforestation in climate models." *Earth System Dynamics* 10 (3): 473–484.

Xing, Jianwei, Zhiren Hu, Fan Xia, Jintao Xu, and Eric Yongchen Zou. 2026. "Urban Forests: Environmental Health Values and Risks." *The Review of Economics and Statistics.*

Yu, Chengzheng, Ruiqing Miao, and Madhu Khanna. 2021. "Maladaptation of U.S. corn and soybeans to a changing climate." *Scientific Reports* 11 (1): 12351.

Zebiak, Stephen E, and Mark A Cane. 1987. "A model el niño southern oscillation." *Monthly Weather Review* 115 (10): 2262–2278.

S Supplementary Appendix - For Online Publication

This Appendix contains the following supplementary materials:

Part A: Data and Methods

- **Section S.1:** Additional background and context
- **Section S.2:** Wind exposure construction details
- **Section S.3:** Climate data construction
- **Section S.4:** Identification assumptions
  - Section S.4.1: Baseline pre-trends
  - Section S.4.2: "Honest" difference-in-differences
  - Section S.4.3: Binary treatment and synthetic difference-in-differences
  - Section S.4.4: Results

Part B: Additional Empirical Approaches and Results

- **Section S.5**: Details on additional empirical approaches
  - **Section S.5.1:** Instrumental variables approach
  - **Section S.5.2:** Panel evidence from within-county variation
- **Section S.6:** Additional results
  - Section S.6.1: Alternative controls, fixed effects, regressors
  - Section S.6.2: Results by season
  - Section S.6.3: Alternative climate data
  - Section S.6.4: Differential climate trends and the Dust Bowl
  - Section S.6.5: Agricultural census subsample results
- **Section S.7:** Irrigation
  - Section S.7.1: Irrigation as potential confound
  - Section S.7.2: Irrigation as an outcome

S.1 Additional background and context

In this section, we present additional information on the history of the Great Plains Shelterbelt project. Figure S1 shows a map of concentrated Shelterbelt planting that we digitize and use to construct our main measure of wind exposure. The resulting county-level measure (share of area covered by concentrated tree planting) is shown in the left panel of Figure S2.

Figure S1: Shelterbelt planned area and realized concentrated planting

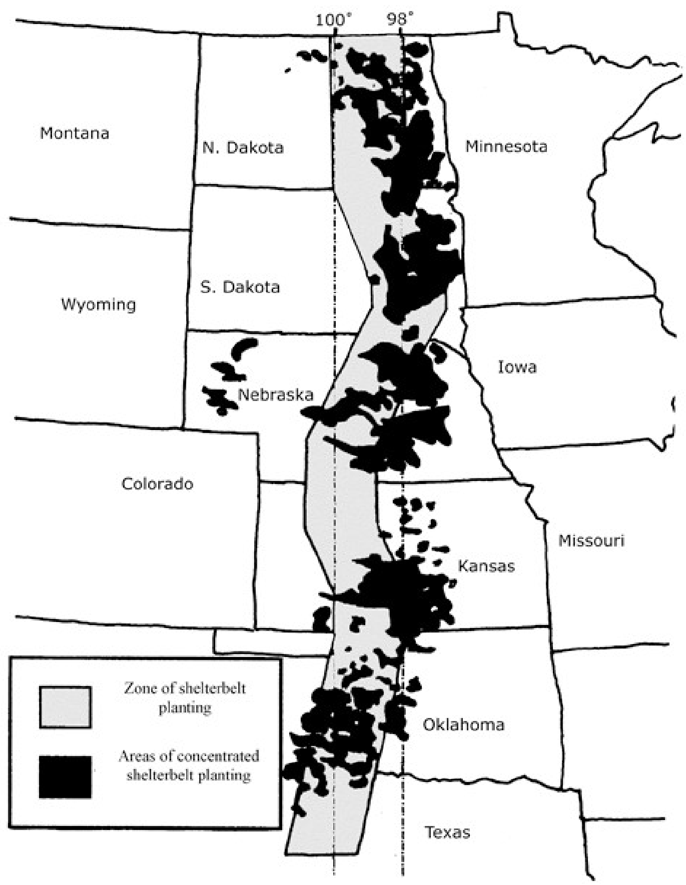

Notes: Map shows planned zone of Shelterbelt planning and areas of concentrated Shelterbelt planning according to Read 1958. Our Shelterbelt definition is based on county areas covered by the areas of concentrated tree planting; and our wind exposure measure is based on the exact location of these "areas of concentrated Shelterbelt planting".

Figure S2 shows the concentration of tree planting at the county level to facilitate comparison with other metrics, but we use the shapefile derived from Figure S1 to construct our wind exposure measure. We also check that this measure of Shelterbelt planting is heavily correlated with an alternate measure of digitized Shelterbelt shapefiles from Snow 2019, which is shown in the right panel of Figure S2.

Figure S2: Shelterbelt measures

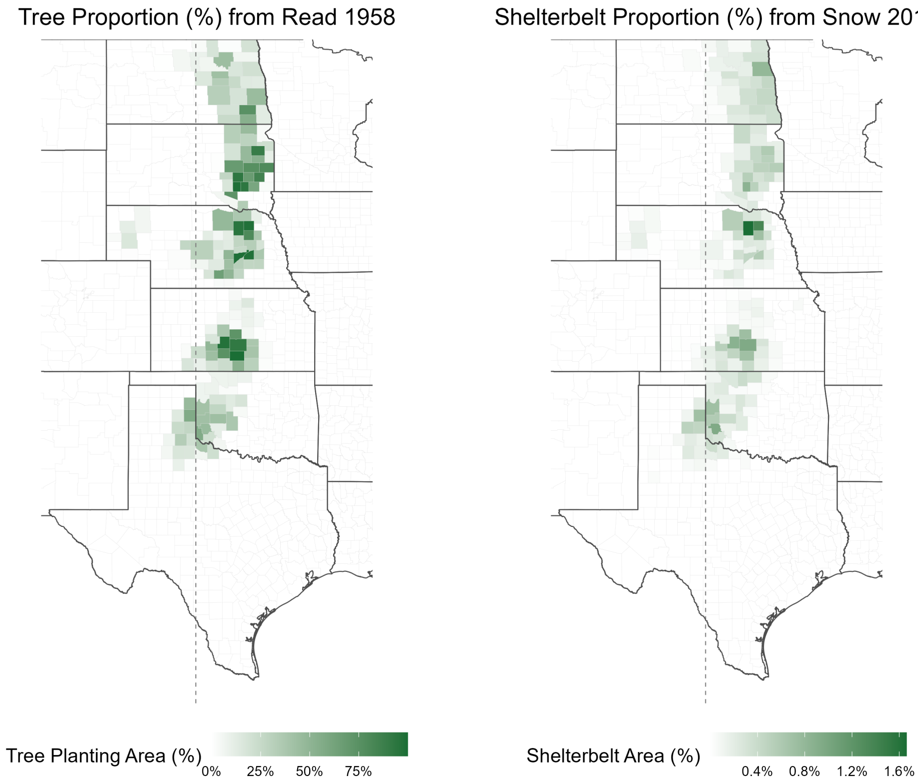

Notes: Figure compares our main measure of Shelterbelt treatment from Read (1958) and the alternate measure from Snow (2019) used for robustness checks. The two measures are similar (correlation 0.86).

Figure S3 shows the approximate numbers of trees planted in each year of the program.

Figure S3: Shelterbelt tree planting over time

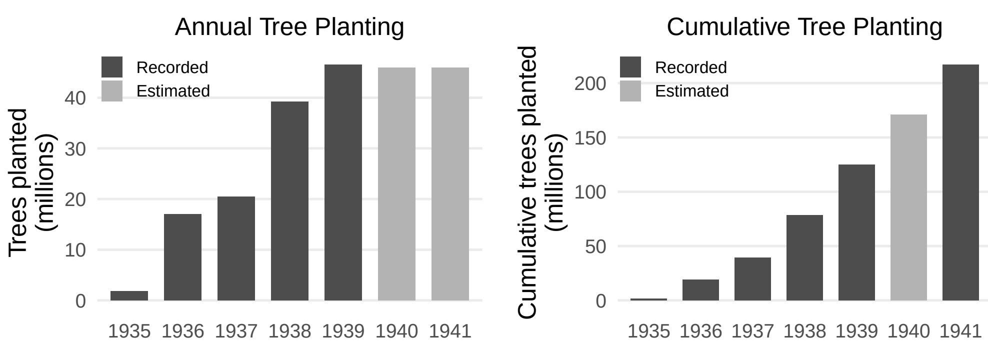

Notes: Left panel plots the number of trees planted in each year; the right panel plots the cumulative number of trees planted. Gray bars indicate estimated values. Cumulative totals are known through 1939 and for 1941, but not for 1940; the annual figures for 1940 and 1941 are therefore estimated by distributing the known 1939–1941 increase. Accordingly, in the left panel 1940 and 1941 are shaded gray, while in the right panel only 1940 is shaded, since the 1941 cumulative total is directly observed.

Figures S4 and S5 offer contextual evidence supporting the external validity of our results and illustrate economic and agronomic parallels between the Great Plains and various contemporary global contexts.

Figure S4: United States in 1945, compared to countries in 2018

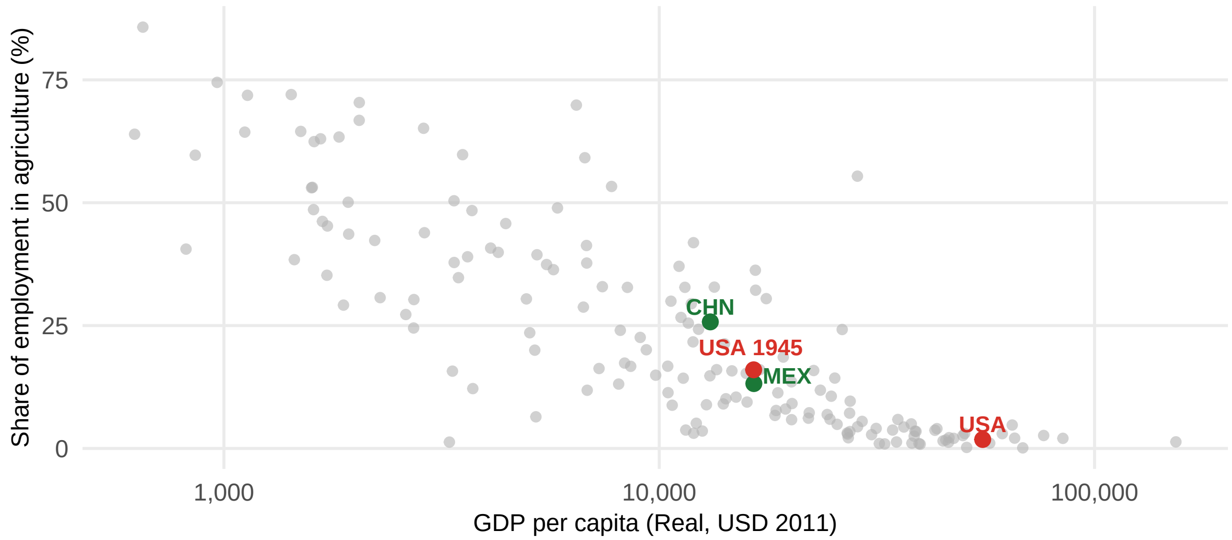

Notes: GDP per capita from the Maddison Project Database (2018 and 1945). Share of employment in agriculture from the US Census (1945, IPUMS, Dimitri et al. 2005) and the World Development Indicators (2018, WB).

Figure S5: Global Distribution of Mollisols and the Great Plains Shelterbelt

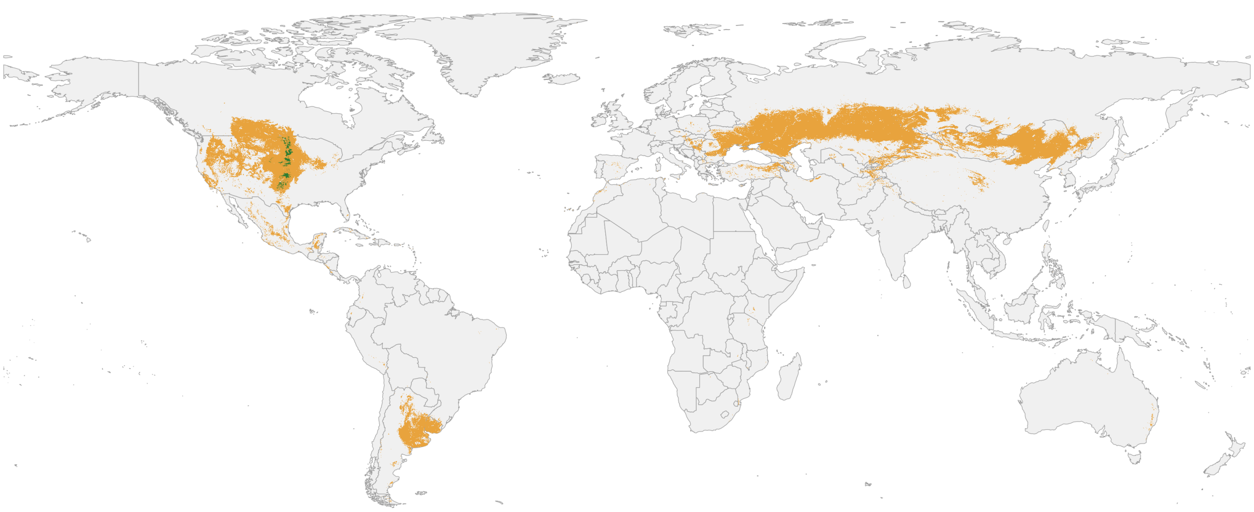

Notes: Mollisols are represented using the World Reference Base (WRB) classifier equivalents, which include Chernozems, Kastanozems, or Phaeozems. These groups align closely with the USDA Soil Taxonomy Mollisols order. The green area indicates the historical outline of the Great Plains Shelterbelt.

Figure S6 shows the evolution of farm count in the agricultural census over the period of our analysis.

Figure S6: Farm count in sample counties from the USDA 5-year agricultural census data, 1930 to 1964

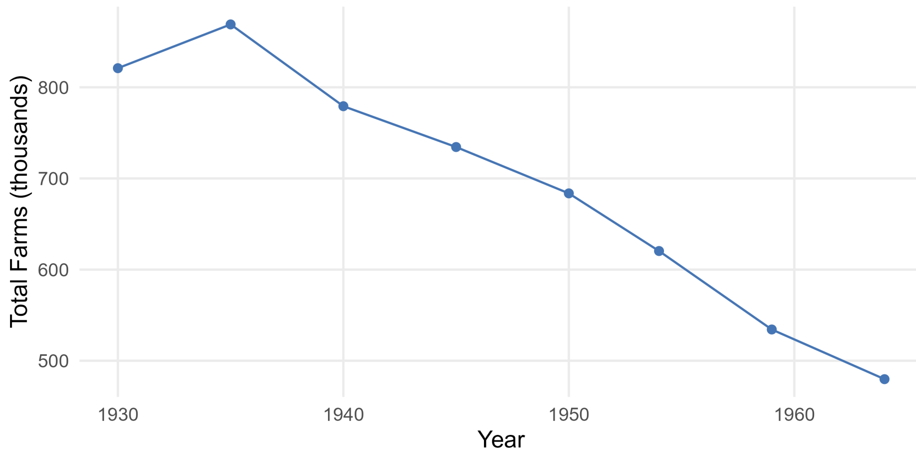

Notes: Figure shows the total farm count in counties in our study area for which we have observations from the agricultural census for every time period between 1930 and 1964.

S.2 Wind exposure construction details

In order to construct our various measures of how exposed county i is to winds from all areas of concentrated Shelterbelt planting, we take the following steps. We use ERA5 reanalysis data from the ECMWF as it is available beginning 1940. This data is gridded at a latitude-longitude of 0.25° and available hourly. Figure S7 summarizes the main steps of our process.

The steps of our process are the following.

1. We overlap the areas of "concentrated Shelterbelt planting" (Figure S1, adding a 5km buffer) with the ERA5 grid. Let g index these 281 points. The first panel of Figure S7 shows a subset of these points for concentrated Shelterbelt planting areas in South Dakota and Nebraska.

2. For each day d and starting point g, we take the following steps:

    a) We initialize imaginary particles at pressure level 800 hPa at several start times on day d. We choose 800 hPa (corresponding to approximately 2km altitude) as this is well within the atmospheric boundary layer where moisture gets mixed and transported regionally. Seminal papers like Spracklen et al. 2012 use this level to initialize particles as well. We also run robustness checks with 1000 hPa, corresponding to approximately 100 meters altitude. We start the process at 10am, 2pm, and 6pm Central Time given the higher evapotranspiration of trees at this time (Hamberg et al. 2022) and to take into consideration changing winds throughout the day.

b) For 24 one-hour periods, we repeat the following for each initialization:

   i) For the given location of the particle, we get the horizontal and vertical wind directions and speeds. When the particle is not exactly at an ERA-5 grid point, we use bilinear interpolation to get these values.

   ii) We update the location of the particle based on both the horizontal and vertical motion of the particle, assuming movement in the same direction for one hour. This results in a new location for the particle after an hour. We update the vertical location of the particle by calculating vertical displacement and then snapping to the nearest standard pressure level.

The above steps trace out the trajectory of winds for a 24-hour period for day d and starting point g. Let this trajectory be t_{gd}. The second panel of Figure S7 shows an example trajectory for an imaginary particle that starts at coordinates 42.5°N, 97.5°W, initiated on June 2nd, 1940 at 2pm CT. The third panel shows all trajectories from this part of the Shelterbelt on this day. Note that while Figure S7 shows two-dimensional trajectories for simplicity, the trajectories we calculate are three-dimensional. The three-dimensional path of an example trajectory is shown in Figure S8.

3. We then aggregate the trajectories t_{gd} several different ways, depending on the wind exposure measure. For our main measure, we create a time-invariant aggregation that sums up exposure across June through August for 1940, the earliest available data prior to the end of the Shelterbelt program. For robustness (e.g., Figures S14-S15) we sum up exposure across June through August for all years 1940-1965. We also create: 1) an annual aggregation that sums up exposure for June through August for each year, 2) a monthly aggregation that sums up for each summer month by year, and finally, 3) a daily aggregation that calculates wind exposure for each summer day and year separately. For seasonal robustness checks, we also aggregate wind exposure for different seasons, following the same logic. For each aggregation, we do the following:

   a) We overlap each trajectory with the counties it intersects. Specifically, we convert each hourly position to a point and assign it to a county polygon.

   b) For each county i and day d, a county's raw exposure is equal to the total count of hourly trajectory points falling within its boundaries during that window.

   c) Lastly, we area-adjust by county land area and normalize by the maximum value.

   The above steps create a continuous wind exposure metric between 0 to 1. The last panel of Figure S7 shows the wind exposure resulting from this region of the Shelterbelt for nearby non-Shelterbelt counties.

Figure S7: Shelterbelt wind exposure steps

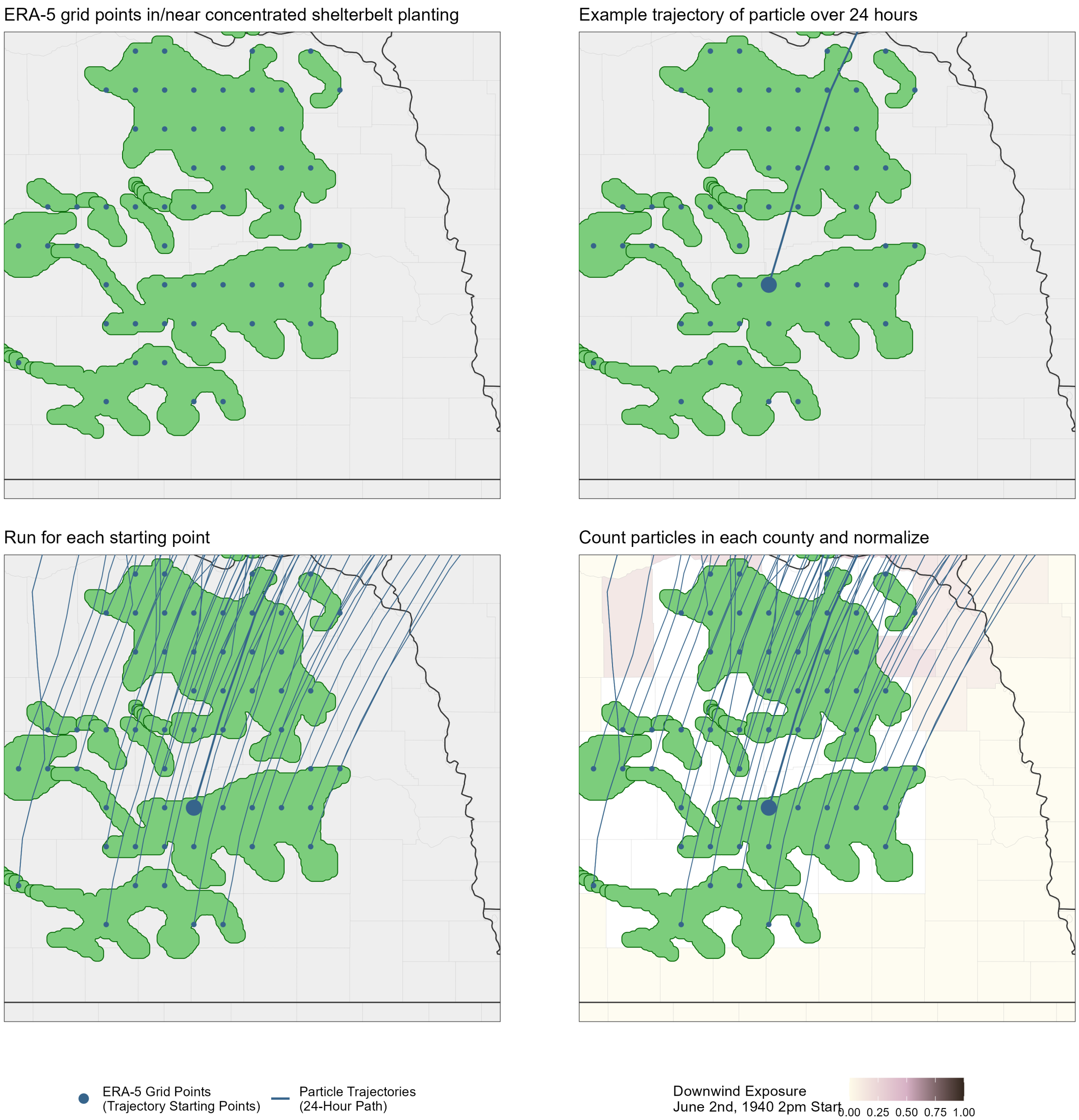

Notes: Figure demonstrates the main steps of our wind exposure metric construction for an area of the Shelterbelt in South Dakota and Nebraska. Shaded green area shows concentrated Shelterbelt planting.

Figure S8: Shelterbelt wind exposure three-dimensional path

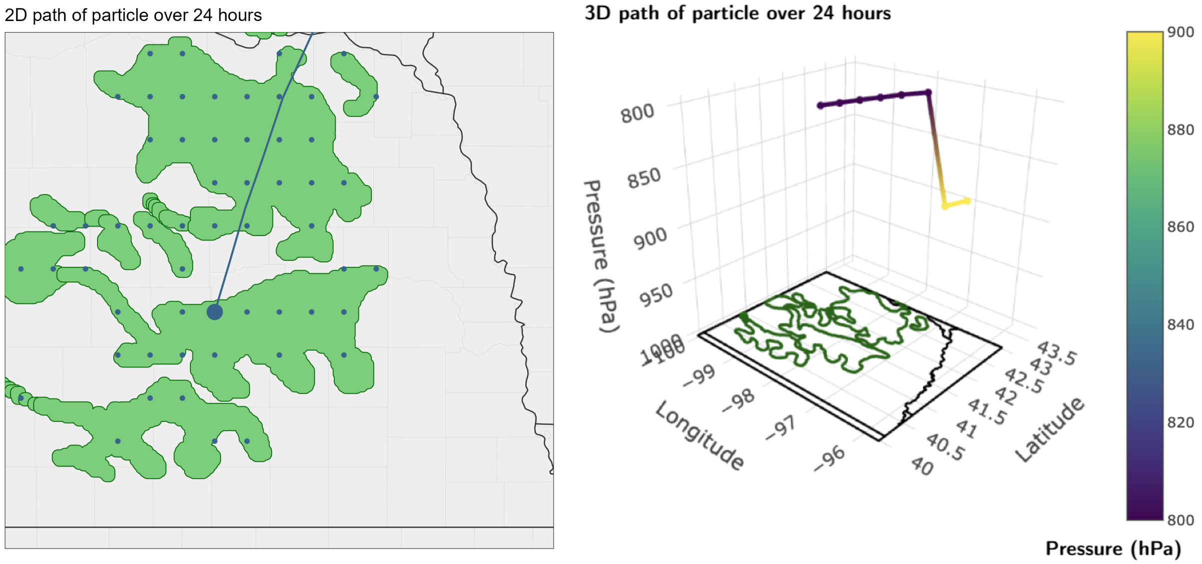

Notes: Figures shows the same particle trajectory in two and three dimensions. In the left panel, the path of an imaginary particle is illustrated in two dimensions, as in Figure S7. The right panel shows the vertical path of the same particle, which starts at 800 hPa and moves closer to ground level. Only the first seven hours (out of 24) are shown in this illustration.

S.3 Climate data construction

S.3.1 Main climate data construction

We build our main weather data from daily station data using a methodology inspired by Schlenker and Roberts (2006). We use NOAA's Global Historical Climatology Network daily (GHCNd) data to create a balanced panel of stations with availability between 1930 and 1965. We take the following steps to construct our county-level daily data.

1. Start with precipitation and temperature stations from the GHCNd stations that are available for 1930 through 1965 (1,977 and 1,479 precipitation and temperature stations, respectively).

2. Select a constant set of stations based on availability. Keep stations with less than 5% missing observations for June 1st through August 31st between 1930 and 1965 (1,100 and 774 precipitation and temperature stations, respectively).

3. Fill in missing observations for this set of constant stations.

   a. For each station, S_i, find the 10 closest stations in the data.

   b. For each of the 10 nearby stations, calculate the percentile of the daily precipitation and maximum and minimum temperatures readings for each day, based on the entire available distribution of weather measures at the appropriate station.

c. For each missing observation for station S_i, calculate the average percentile reading of the 10 closest stations (e.g., 71st percentile).

d. Then, fill in the missing observation using the corresponding value from the distribution of S_i (e.g., if the 71st percentile corresponds to 20mm of precipitation at station S_i, the missing value will be filled in with 20mm).

4. Calculate degree days at each station.

5. Interpolate all variables to a 0.1 degree grid.

6. Average gridded values at the county level.

S.3.2 Additional climate data

In addition to our main weather data described above, we construct various other weather datasets used for additional analyses and robustness checks. For these datasets, we use the same steps as above, except with the following modifications.

- **Alternative time periods (1910–1965 and 1930–2002)**: We repeat the same steps as above, except in steps 1 and 2 we use GHCNd stations that are available for these alternative time periods. We keep stations with less than 5% missing observations for the appropriate time periods. There are fewer stations with available data in these early years (623 precipitation and 491 temperature stations).

- **Non-summer months (1930–1965)**: We repeat the same steps as above. We use the same set of stations as in the main climate data construction (steps 1 and 2) to base station availability and consistency on our main period of interest (the summer). We fill in missing observations for other seasons the same way (step 3).

- **PRISM data:** We use 4km gridded daily minimum temperature, maximum temperature, and precipitation from the PRISM Climate Group at Oregon State University, which makes steps 1–3 and 5 above unnecessary, as the data are already gridded and gap-free, and each grid cell is assigned to the county that contains it. We compute degree days at the grid cell–day level using the same method as in step 4, and then average all variables across the grid cells within each county (step 6).

- **NClimDiv data:** We use NOAA NCEI's nClimDiv county-level monthly climate data (available from 1895), which interpolates GHCN station records to a grid and aggregates them to counties using a different interpolation method than ours, and so we take these data as given rather than repeating any of the steps above. Because the data are reported at the monthly rather than daily level, they provide precipitation and mean, minimum, and maximum temperature, but no degree days.

S.4 Identification assumptions

As described in Section 4, our preferred empirical specification is a difference-in-differences model with a continuous treatment variable: wind exposure (Equation 1). In such model, the main coefficient of interest β has a clear interpretation as the marginal effect of wind exposure, if we assume a constant marginal effect (Callaway et al. 2024). (Under a constant marginal effect, the "strong parallel trends assumption" is mechanically satisfied.) Given that the interpretation of β is difficult absent this assumption, we also present results from a classic binary DiD specification. For either the continuous DiD with constant marginal effects or the binary DiD, the key identifying assumption is the classic parallel trends assumption: that units would have had the same trends in their (climate and economic) outcomes absent the Shelterbelt tree-planting. While this cannot be tested, one can provide suggestive evidence by formally testing for differential pre-trends during the baseline period. Section S.4.1 describes this test.

Finding diverging baseline trends in outcomes across counties with different wind exposure does not imply that our results are incorrect. Two different approaches can be adopted. One can verify empirically whether the baseline pre-trends are strong enough to overcome the main results, if one assumes that the baseline pre-trends continue throughout the period. This is the "Honest DiD" method from Rambachan and Roth (2023), which we describe in section S.4.2. One can also choose a different control group, for which the baseline outcomes' trends are parallel to the treatment group. It requires using a binary treatment variable (for instance, above- or below-median wind exposure) rather than a continuous one, but ensures by design that the baseline trends are parallel. This is the "Synthetic DiD" method from Arkhangelsky et al. (2021). In section S.4.3, we describe both the binary DiD specification and the synthetic DiD method. The results from these various tests and specifications are reported in section S.4.4.

S.4.1 Baseline pre-trends

To test for differential trends during the baseline period, we estimate the following Equation:

$$y_{it} = \alpha^{\text{pre-trend}} t + \beta^{\text{pre-trend}} t \times w_i + \gamma^{pt}(X_i \times Y_t) + \delta_{st}^{pt} + \epsilon_{it}, \text{ for } t \leq 1942 \tag{3}$$

Where w_i is the wind exposure measure, y_{it} the outcome of interest, t covers the baseline years (until 1942) and $\beta^{\text{pre-trend}}$ is the coefficient of interest: whether the baseline time trend in the outcomes' residuals differs with the level of wind exposure. Given that our preferred specification of interest includes state-by-year fixed effects and a set of controls interacted with year fixed effects, we include these controls here as well.

While not necessary for identification, one can similarly test the baseline balance in the outcomes' residuals:

$$y_{it} = \beta^{balance} w_i + \gamma^{bal}(X_i \times Y_t) + \delta_{st}^{bal} + \epsilon_{it}, \text{ for } t \leq 1942 \tag{4}$$

S.4.2 "Honest" difference-in-differences.

We acknowledge that the parallel trends assumption may be violated for some outcomes in our study setting, and provide confidence sets for the downwind effects of the Shelterbelt tree-planting that are robust to deviations from this assumption. We implement the approach developed by Rambachan and Roth (2023): we re-estimate the effects by allowing for the existence of a linear differential trend in outcomes across counties. This is similar in spirit to the approach adopted in applied work from Bhuller et al. (2013) or Goodman-Bacon (2018), who estimate a linear pre-trend and use it to de-trend the post-treatment outcomes. The confidence sets obtained through the Rambachan and Roth (2023) method are typically wider than the confidence intervals on classic DiD estimates as it accounts for the statistical uncertainty in the estimation of the event-study coefficients, and guarantees uniformly robust inference.

S.4.3 Binary treatment and synthetic difference-in-differences

We implement a "synthetic difference-in-differences" analysis to address potential concerns related to spatially-differential climate trends and mean reversion. While our main empirical specifications use a continuous measure of wind exposure as treatment variable, implementing the synthetic difference-in-differences methods based on Arkhangelsky et al. 2021 requires a binary treatment variable. We therefore convert our continuous downwind exposure measure to a binary treatment indicator for being highly exposed. We first detail the classic difference-in-differences estimator with the binary treatment variable, before describing the synthetic difference-in-differences method in more details. We show that the results using both methods are qualitatively similar to our main results using a continuous treatment variable.

Figure S9: Shelterbelt neighbor wind exposure

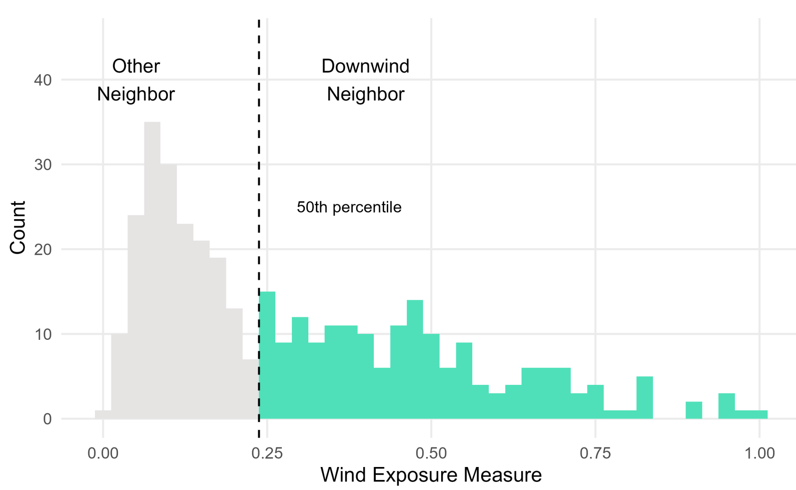

Notes: Figure shows histogram of the wind exposure measure for counties within 200km of afforested areas. Counties with wind exposure above the median measure (black dashed line) are classified as downwind neighbor counties, while the rest are classified as other neighbors.

Discretized wind exposure details To create a binary or discretized wind exposure measure, we still use our main wind exposure measure, but now classify counties outside the Shelterbelt area into the following groups:

i) Downwind neighbor counties, with centroids within 200km of Shelterbelt counties, and above median wind exposure from the afforested areas

ii) Other neighbor counties, with centroids within 200km of Shelterbelt counties and below median wind exposure from afforested areas

iii) Pure control counties, with centroids 200-300km away from Shelterbelt counties

Figure S9 shows a histogram of our continuous wind exposure measure and how we divide counties into the above-median (downwind) and below-median (other control) groups. Figure S10 shows maps of the resulting treatment categories.

Figure S10: Shelterbelt binary treatment categories

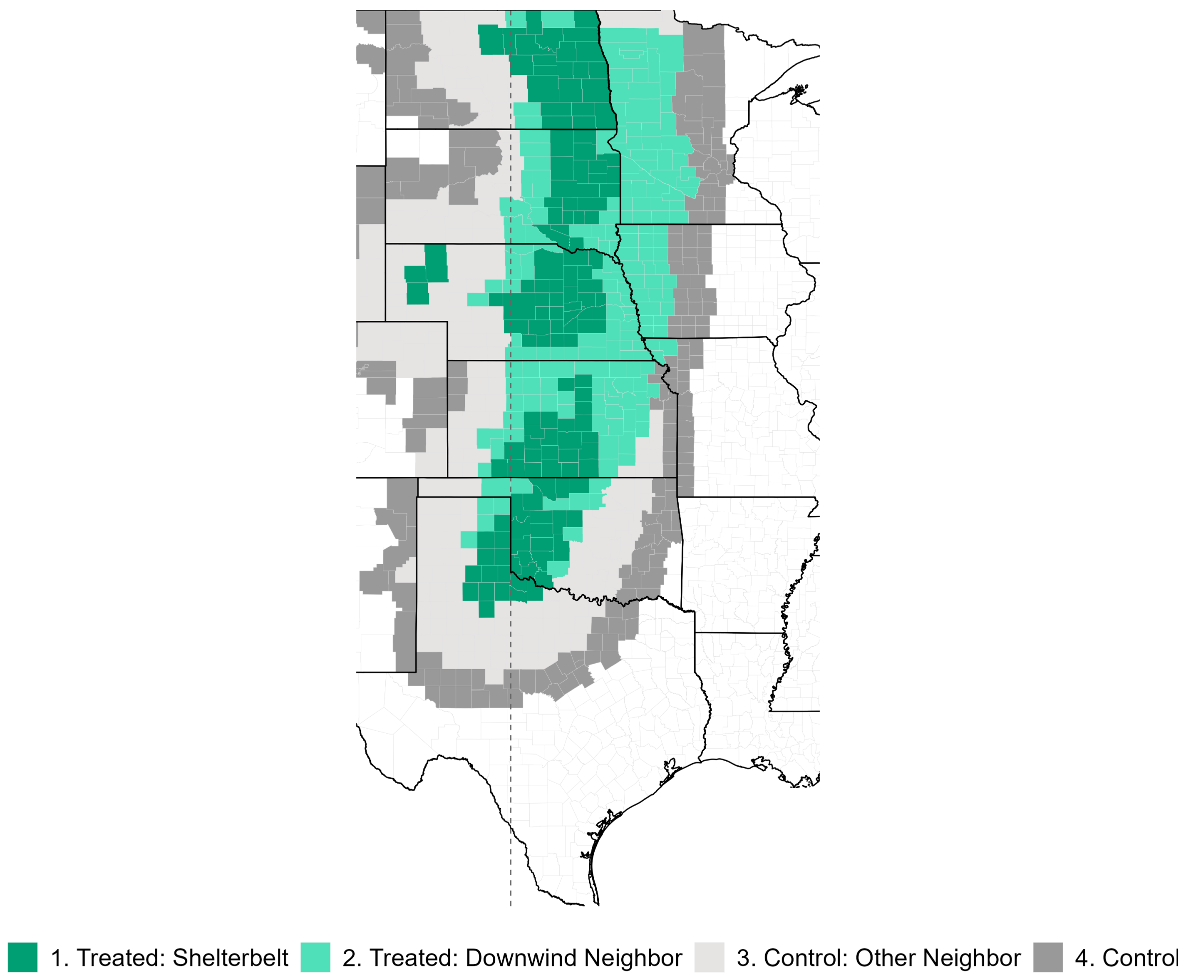

Notes: Figure shows maps of the binary treatment categories resulting from dividing non-Shelterbelt counties within 200km of the Shelterbelt based on wind exposure above and below the median measure into downwind and other neighbors.

Binary treatment empirical strategy We replicate our main results using the binary treatment measure. Although this approach cannot take advantage of all the variation in the wind exposure measure, it allows us to produce an estimation with a clear interpretation (cf. Section 4.3 for a discussion on the interpretation of the coefficient from a continuous DiD specification) as well as to carry out helpful placebo exercises. We compare climate and economic outcomes across these groups of counties. We define the regional effects as the impacts on the neighboring downwind counties. While some climate effects might be present in the other counties (since some counties with below-median wind exposure might still be exposed to non-negligible wind exposure), we expect these effects to be limited relative to those in the downwind counties.

We estimate the following difference-in-differences Equation:

$$y_{it} = \beta_D(D_i \times P_t) + \beta_U(U_i \times P_t) + \gamma(\mathbf{X}_i \times Y_t) + \gamma_{st} + \nu_i + \epsilon_{it} \tag{5}$$

where D_i is an indicator for downwind neighbor counties and U_i is an indicator for other neighbor counties. As in our main specification, we add time-invariant county-level controls interacted by year, as well as state-by-year (γ_{st}) and county (ν_i) fixed effects.

Note that Equation 5 includes two levels of treatment (downwind neighbors and non-downwind neighbors), which are each compared to a control group. One could also run the simplest specification of comparing "treatment" versus "control" on a sample that includes only the downwind neighbors and the control counties. The results are similar in these two cases (not reported for brevity).

Synthetic difference-in-differences To address possible concerns with the parallel trends assumption, we then repeat our difference-in-differences with binary treatment variables analyses using a synthetic difference-in-differences approach.

The synthetic difference-in-differences method, described by Arkhangelsky et al. (2021), combines features of the synthetic control and difference-in-differences methods. The synthetic difference-in-differences method weakens reliance on parallel trends by reweighing and matching pre-treatment trends. The method then uses the resulting weights in a two-way fixed effects regression to estimate the average causal effect of exposure to the treatment. We use the synthetic difference-in-differences method to compare, in turn, the downwind neighbor counties to a synthetic control and the other neighbor counties to another synthetic control. As possible contributors to the synthetic controls, we choose all counties with centroids between 108°West and 88°West who are neither Shelterbelt counties nor have centroids within 200km of a Shelterbelt county (i.e., who are not what we have defined thus far as "Shelterbelt neighbors"). These are counties in the US Great Plains, which potentially share common features to the treated counties of interest.

Formally, consider a balanced panel with N total counties (e.g., the downwind Shelterbelt neighbor counties plus the pool of potential contributing counties, or the other Shelterbelt neighbor counties plus the pool of potential contributing counties) indexed by i and U periods indexed by t. Like before, treatment exposure is denoted by $(T_i \times P_t) \in \{0, 1\}$, where T_i

indicates treatment status and P_t treatment timing. The synthetic differences method finds weights $\hat{\omega}^{sdid}$ and $\hat{\lambda}^{sdid}$ to align pre-treatment trends in treated and unexposed counties as well as to balance pre-exposure periods with post-exposure ones. These weights are used in the following two-way fixed effects regression

$$(\hat{\tau}^{sdid}, \hat{\mu}, \hat{\alpha}, \hat{\beta}) = \arg\min \{ \sum_{i=1}^{N} \sum_{t=1}^{U} (y_{it} - \mu - \alpha_i - \beta_t - (T_i \times P_t)\tau)^2 \hat{\omega}_i^{sdid} \hat{\lambda}_t^{sdid} \}. \qquad (6)$$

Equation 6 is similar to a standard two-way fixed effects regression with binary treatment variables, such as the one we use in Section S.4.3, but includes the unit and time weights ($\hat{\omega}^{sdid}$ and $\hat{\lambda}^{sdid}$). Since the weights are already determined to create a synthetic control for each group of treated counties, we do not need to include our time-varying controls, or the state-by-year fixed effects, to achieve it. As such, our synthetic difference-in-differences only has the standard time and unit fixed effects. In addition, since the synthetic method creates a different synthetic control for each group of treated units (the downwind neighbors, and the non-downwind neighbors), we estimate their treatment effects separately—while our classic binary specification, presented in Equation 5, was estimating them jointly.

Due to these differences in specifications, we do not expect the results of the classic and synthetic binary difference-in-differences to be exactly the same. However, unless the baseline parallel trends were an issue, we still expect them to yield qualitatively similar insights.

S.4.4 Results

Climate outcomes Table S1 reports results for the climate outcomes. Panel A presents the sample mean of our four climate variables of interest (precipitation, mean temperature, maximum temperature, and 29C degree days) together with the estimated point estimate and p-value from the balance test (Equation 4). Once we include controls, Shelterbelt wind exposure is not correlated with any of the climate outcomes at baseline. This isn't required for identification but can prove useful to interpret the variation we are leveraging: we are comparing areas that have varying degrees of exposure to winds blowing through the Shelterbelt but a similar climate to begin with.

Panel B reports the estimated point estimate and p-value from the pre-trends test (Equation 3) using the continuous wind exposure measure (Columns 1 and 2). It also reports the 90% confidence intervals from our preferred DiD specification (Equation 1, Column 3) and from the Honest DiD specification (Column 4). Likewise, Panel C reports the estimated point estimate and p-value from the pre-trends test using the binary wind exposure measure (Columns 1-2), the associated point estimate and p-value from our binary DiD specification (Equation 5, Column 3) and from the Synthetic DiD specification (Column 4). While we find significant pre-trends for precipitation and mean temperature, the estimated effects of Shelterbelt wind exposure are consistent across all specifications (continuous DiD, binary DiD, honest DiD, synthetic DiD), indicating that the small existing pre-trends are not driving the results.

Table S1: Baseline pre-trends and balance: Climate outcomes

Panel A: Balance by wind exposure

Outcome	Sample Mean	Without Controls		With Controls	
	(1)	(2)	(3)	(4)	(5)
Precipitation (cm)	7.2	1.563	< 0.001	0.327	0.302
Mean Temp (C)	24.4	1.848	< 0.001	0.364	0.187
Max Temp (C)	31.9	1.113	< 0.001	0.330	0.333
Degree Days (29C)	36.9	11.907	< 0.001	3.973	0.138

Panel B: Baseline pre-trends and honest DiD (continuous wind exposure)

	Pre-trend		Classic DiD	Honest DiD
Outcome	β	P-Val.	90% CI	90% CI
	(1)	(2)	(3)	(4)
Precipitation (cm)	-0.173	< 0.001	[0.87, 1.76]	[3.79, 5.71]
Mean Temp (C)	-0.022	0.005	[-0.69, -0.39]	[-0.42, 0.01]
Max Temp (C)	0.003	0.789	[-0.94, -0.58]	[-1.32, -0.63]
Degree Days (29C)	-0.162	0.109	[-11.63, -7.99]	[-4.83, 0.38]

Panel C: Baseline pre-trends and synthetic DiD (binary wind exposure)

	Pre-trend		Classic DiD	Synthetic DiD
Outcome	β	P-Val.	$\hat{\beta}$ (p)	$\hat{\beta}$ (p)
	(1)	(2)	(3)	(4)
Precipitation (cm)	-0.047	< 0.001	0.423 (< 0.001)	0.682 (< 0.001)
Mean Temp (C)	-0.008	0.008	-0.140 (< 0.001)	-0.234 (< 0.001)
Max Temp (C)	0.004	0.418	-0.187 (< 0.001)	-0.289 (< 0.001)
Degree Days (29C)	-0.026	0.452	-2.476 (< 0.001)	-2.637 (< 0.001)

Notes: The table reports baseline balance and pre-trends for the four climate outcomes (June–August monthly averages) over the climate sample. Panel A reports, for each outcome, its sample mean over the 1930–1942 baseline period (Column 1) and the coefficient and p-value from a regression of the baseline outcome on wind exposure w_i, without controls except state-by-year FEs (Columns 2–3) and with additional controls for elevation, ruggedness, and Ogallala-aquifer share each interacted with year (Columns 4–5). Panel B reports the slope of the linear pre-trend in wind-exposure effects over the 1930–1942 baseline period and its p-value (Columns 1–2), the 90% confidence interval from the classic difference-in-differences estimator (Column 3), and the 90% confidence interval from the Rambachan and Roth (2023) "honest DiD" method allowing bounded violations of parallel trends (Column 4). *Panel C* reports the same linear pre-trend slope and p-value using the binary (above-median) wind-exposure measure for downwind neighbors (Columns 1–2), the classic binary difference-in-differences estimate and its p-value (Column 3), and the synthetic difference-in-differences estimate of Arkhangelsky et al. (2021) and its p-value (Column 4). Standard errors are clustered by county; the synthetic DiD uses jackknife standard errors.

Economic outcomes Table S2 reports results for the economic outcomes. While the climate variables are available annually, the economic variables are available roughly every five years (each agricultural census year). As such, for the economic outcomes, we only have three data points per county for the baseline period. This limits our ability to meaningfully test for pre-trends, as well as to implement the Honest DiD and Synthetic DiD approaches. While we acknowledge lower data quality for earlier periods, we therefore extend the baseline to start in 1910 (or the earliest census year with available data for each variable, if later than 1910). Each agricultural outcome studied in the paper has up to two rows in Table S2: one with the earlier baseline (the exact start year being reported in Column 1), and one with the 1930 baseline; outcomes first observed in 1930 have a single row.

For each, the table reports the point estimate and p-value from our headline continuous DiD specification (Column 2), the p-value from the associated pre-trend test (Column 3) and the associated Honest DiD 90% confidence sets (Column 4). It also reports results from the binary specification, with the point estimate and p-value (Column 5), the p-value from the associated pre-trend test (Column 6), and the synthetic DiD point estimate and p-value (Column 7). Column (8) summarizes the robustness of the headline DiD results (from the continuous DiD specification with a 1930 baseline start) to the Honest DiD and Synthetic DiD specifications with the earliest baseline date.

Placebo outcomes The binary and synthetic difference-in-differences specifications support a falsification exercise. We test whether the "other neighbor" counties—those within 200km of the Shelterbelt but with below-median wind exposure—show effects they should not. Figure S11 reports these non-downwind coefficients for our six main outcomes under both the binary DiD (Equation 5) and the synthetic DiD (Equation 6). For precipitation the placebo estimates are small (an order of magnitude smaller than the corresponding downwind effects) and centered at zero. The extreme temperature outcomes show some positive placebo estimates—significant for maximum temperature under the synthetic DiD and for 29°C degree days under the binary DiD—but these run opposite in sign to the downwind cooling we document, so they cannot account for it and if anything widen the downwind–non-downwind gap. The corn production placebo estimates are also very small and centered at zero under both estimators. For the share of small farms, the non-downwind synthetic DiD estimate is close to the downwind one, but the binary DiD is not statistically significant and smaller in magnitude.

Table S2: Baseline pre-trends and robustness: Economic outcomes

		Continuous wind exposure			**Binary wind exposure**			
Outcome	Baseline (1)	DiD $\hat{\beta}$ (p) (2)	PT p (3)	HonestDiD CI (4)	DiD $\hat{\beta}$ (p) (5)	PT p (6)	Synth. $\hat{\beta}$ (p) (7)	Robustness (8)
Table 3A: Corn production								
Log Corn Production	1925	+1.36 (<.001)	0.003	[-0.25, +1.60]	+0.23 (0.015)	<.001	+0.813 (<.001)	Robust (part.)
vs. 1930	1930	+1.67 (<.001)	0.043	[+3.48, +6.72]	+0.35 (<.001)	0.057	+0.809 (<.001)	
Log Corn Acreage	1925	+1.12 (0.002)	0.008	[+0.35, +1.76]	+0.21 (0.013)	<.001	+0.676 (<.001)	Robust (full)
vs. 1930	1930	+1.40 (<.001)	0.147	[+2.89, +5.35]	+0.30 (<.001)	0.211	+0.696 (<.001)	
Log Corn Yield	1925	+0.24 (0.010)	0.024	[+0.03, +0.96]	+0.02 (0.394)	0.006	-0.012 (0.680)	Robust (part.)
vs. 1930	1930	+0.27 (0.010)	0.017	[+0.76, +2.12]	+0.04 (0.133)	0.015	-0.010 (0.748)	
Table 3B: Other crop activities								
Log Wheat Acreage	1910	-0.76 (<.001)	<.001	[-0.57, +0.36]	+0.04 (0.547)	0.361	-0.089 (0.175)	Not robust
vs. 1930	1930	-0.45 (0.010)	0.005	[-0.93, +0.76]	+0.03 (0.599)	<.001	-0.150 (0.018)	
Log Irrigated Area	1910	+1.03 (<.001)	<.001	[+0.40, +0.91]	+0.15 (0.001)	<.001	+0.068 (0.178)	Robust (part.)
vs. 1930	1930	+0.95 (<.001)	0.004	[-0.44, +0.27]	+0.14 (0.001)	0.113	+0.069 (0.164)	
Log Crop Failure	1925	+0.01 (0.965)	<.001	[-2.27, -0.67]	-0.01 (0.854)	0.005	+0.262 (<.001)	n/a
vs. 1930	1930	-0.42 (0.122)	0.001	[-3.07, -1.23]	-0.06 (0.347)	0.032	+0.139 (0.109)	
Table 3C: Animal husbandry								
Log Cattle	1910	-0.13 (0.068)	0.020	[-0.13, +0.30]	+0.01 (0.654)	0.125	+0.048 (0.073)	n/a
vs. 1930	1930	-0.02 (0.768)	0.316	[-0.14, +0.48]	+0.03 (0.255)	0.722	+0.046 (0.084)	
Log Pigs	1910	+0.62 (<.001)	<.001	[+0.69, +1.25]	+0.01 (0.811)	<.001	+0.180 (<.001)	Robust (full)
vs. 1930	1930	+0.81 (<.001)	0.070	[+0.53, +1.68]	+0.09 (0.006)	0.005	+0.213 (<.001)	
Log Chickens	1910	+0.73 (<.001)	0.029	[+0.78, +1.16]	+0.05 (0.145)	0.703	+0.203 (<.001)	Robust (full)
vs. 1930	1930	+0.64 (<.001)	0.063	[+0.57, +1.01]	+0.06 (0.089)	0.890	+0.200 (<.001)	

Notes: Continued on the next page, where full notes are provided.

Table S2: Baseline pre-trends and robustness: Economic outcomes (continued)

		Continuous wind exposure			Binary wind exposure			
Outcome	Baseline (1)	DiD $\hat{\beta}$ (p) (2)	PT p (3)	HonestDiD CI (4)	DiD $\hat{\beta}$ (p) (5)	PT p (6)	Synth. $\hat{\beta}$ (p) (7)	Robustness (8)
Table 4: Farmland use								
Log Land in Farms	1930	-0.10 (0.004)	<.001	[-0.13, +0.09]	-0.01 (0.647)	0.013	-0.019 (0.137)	Not robust
Log Cropland	1925	+0.39 (<.001)	0.001	[+0.36, +0.59]	+0.11 (<.001)	0.209	+0.087 (<.001)	Robust (full)
vs. 1930	1930	+0.36 (<.001)	<.001	[+0.30, +0.55]	+0.11 (<.001)	0.008	+0.079 (<.001)	
Log Pasture Land	1925	-0.50 (<.001)	<.001	[+0.00, +0.35]	-0.10 (<.001)	0.233	-0.063 (0.070)	Robust (part.)
vs. 1930	1930	-0.40 (<.001)	<.001	[+0.08, +0.48]	-0.10 (<.001)	0.011	-0.107 (0.003)	
Log Woodland	1930	-0.45 (0.001)	0.176	[-1.18, -0.11]	-0.11 (0.010)	0.379	-0.098 (0.020)	Robust (full)
Log Other Land	1930	+0.52 (<.001)	0.119	[-0.20, +0.88]	+0.06 (0.072)	0.832	+0.068 (0.071)	Robust (part.)
Table 5: Farm consolidation								
Total Farms	1910	+523 (<.001)	0.122	[+314, +665]	+82.00 (0.017)	0.238	+133 (<.001)	Robust (full)
vs. 1930	1930	+425 (<.001)	0.680	[+337, +780]	+84.48 (0.010)	0.001	+110 (<.001)	
Log Avg. Farm Size	1930	-0.47 (<.001)	<.001	[-0.69, -0.47]	-0.06 (<.001)	0.421	-0.079 (<.001)	Robust (full)
Share Farms 0-99ac	1910	+0.12 (<.001)	<.001	[+0.08, +0.14]	+0.03 (<.001)	0.007	+0.024 (<.001)	Robust (full)
vs. 1930	1930	+0.09 (<.001)	0.995	[+0.08, +0.16]	+0.02 (<.001)	0.408	+0.024 (<.001)	
Share Farms 100-499ac	1910	-0.02 (0.593)	0.034	[-0.02, +0.06]	-0.05 (<.001)	0.635	-0.037 (<.001)	n/a
vs. 1930	1930	-0.03 (0.311)	0.238	[-0.07, +0.02]	-0.04 (<.001)	0.923	-0.033 (<.001)	
Share Farms 500ac+	1910	-0.10 (0.004)	<.001	[-0.18, -0.10]	+0.01 (0.081)	0.005	+0.015 (0.022)	Robust (part.)
vs. 1930	1930	-0.05 (0.064)	0.170	[-0.12, -0.04]	+0.02 (0.002)	0.415	+0.012 (0.071)	

Notes: Continued on the next page, where full notes are provided.

Table S2: Baseline pre-trends and robustness: Economic outcomes (continued)

		Continuous wind exposure			Binary wind exposure			
Outcome	Baseline (1)	DiD $\hat{\beta}$ (p) (2)	PT p (3)	HonestDiD CI (4)	DiD $\hat{\beta}$ (p) (5)	PT p (6)	Synth. $\hat{\beta}$ (p) (7)	Robustness (8)
Table 6A: Aggregate values								
Log Land Value	1910	-0.21 (0.001)	0.011	[-0.17, +0.20]	-0.03 (0.203)	0.007	-0.098 (<.001)	Robust (part.)
vs. 1930	1930	-0.15 (0.014)	0.390	[-0.11, +0.35]	-0.02 (0.445)	0.325	-0.106 (<.001)	
Log Crop Value	1910	+0.78 (<.001)	0.004	[+0.17, +1.14]	+0.18 (0.007)	0.011	+0.106 (0.042)	Robust (full)
vs. 1930	1930	+0.43 (0.004)	0.004	[-1.04, +2.84]	+0.09 (0.083)	0.035	+0.082 (0.143)	
Log Animal Revenue	1910	-0.05 (0.615)	0.132	[-0.59, +0.41]	-0.03 (0.466)	0.146	+0.020 (0.494)	n/a
vs. 1930	1930	+0.01 (0.867)	0.131	[-0.69, +0.56]	-0.00 (0.944)	0.179	+0.018 (0.562)	
Table 6B: Values per acre								
Log Land Value/Acre	1930	-0.05 (0.340)	0.368	[-0.12, +0.31]	-0.01 (0.571)	0.926	-0.081 (<.001)	n/a
Log Crop Value/Acre	1925	+0.15 (0.239)	0.022	[-0.05, +1.42]	+0.00 (0.958)	0.076	-0.042 (0.374)	n/a
vs. 1930	1930	+0.07 (0.620)	0.016	[-1.44, +2.32]	-0.02 (0.736)	0.074	-0.033 (0.484)	
Log Animal Revenue/Acre	1930	+0.47 (<.001)	–	–	+0.10 (0.007)	–	n/a	Not testable
Table 7: Agricultural inputs								
Log Hired Labor	1910	-0.72 (<.001)	<.001	[-0.96, -0.27]	-0.18 (<.001)	0.023	-0.226 (<.001)	Robust (full)
vs. 1930	1930	-0.50 (<.001)	0.007	[-1.49, +0.32]	-0.11 (0.001)	0.013	-0.217 (<.001)	
Log Hired Machine	1930	-0.41 (<.001)	0.216	[-1.56, +0.49]	-0.07 (0.105)	0.166	-0.202 (<.001)	Robust (part.)
Log Fertilizer	1910	+4.32 (<.001)	<.001	[+3.20, +5.93]	+1.19 (<.001)	<.001	+1.117 (<.001)	Robust (full)
vs. 1930	1930	+6.90 (<.001)	<.001	[+0.70, +8.35]	+1.81 (<.001)	0.001	n/a	

Notes: Table reports baseline pre-trend tests and robustness checks for the economic outcomes of Tables 3–7, for the continuous wind-exposure treatment (w_i, as in Equation 1) and for the binary treatment (downwind-neighbor counties vs. control counties). Each outcome has up to two rows: the earliest credible baseline (1910 or 1925, using pre-period census data extended back from the paper's 1930 start) above the paper's 1930 baseline (Column 1). Outcomes for which no earlier census is comparable have a single 1930 row. *DiD* columns (Columns 2 and 5) report the difference-in-differences coefficient and its cluster-on-county p-value in parentheses; the 1930-baseline continuous coefficients are identical to those reported in Tables 3–7, which also report Conley spatial standard errors. *PT p* (Columns 3 and 6) is the p-value of a linear pre-trend test over the baseline period. *HonestDiD CI* (Column 4) is the 90% confidence interval from the Rambachan and Roth (2023) method at $M = 0$, i.e., linearly projecting the estimated baseline pre-trend forward. *Synth.* $\hat{\beta}$ (Column 7) is the synthetic difference-in-differences estimate (Arkhangelsky et al. 2021) for the downwind-neighbor contrast, with its jackknife-based p-value. *Robustness* (Column 8) is shown on the earliest-baseline row and judged relative to the paper's 1930-baseline continuous DiD: *Robust (full)* if both the HonestDiD interval (excludes zero with the same sign) and the synthetic DiD (significant at the 10% level with the same sign) corroborate it; *Robust (part.)* if exactly one of the two does; *Not robust* if neither; *n/a* when the 1930-baseline DiD is itself not significant at the 10% level.

Figure S11: Binary and synthetic difference-in-differences placebo results, 1930 to 1965

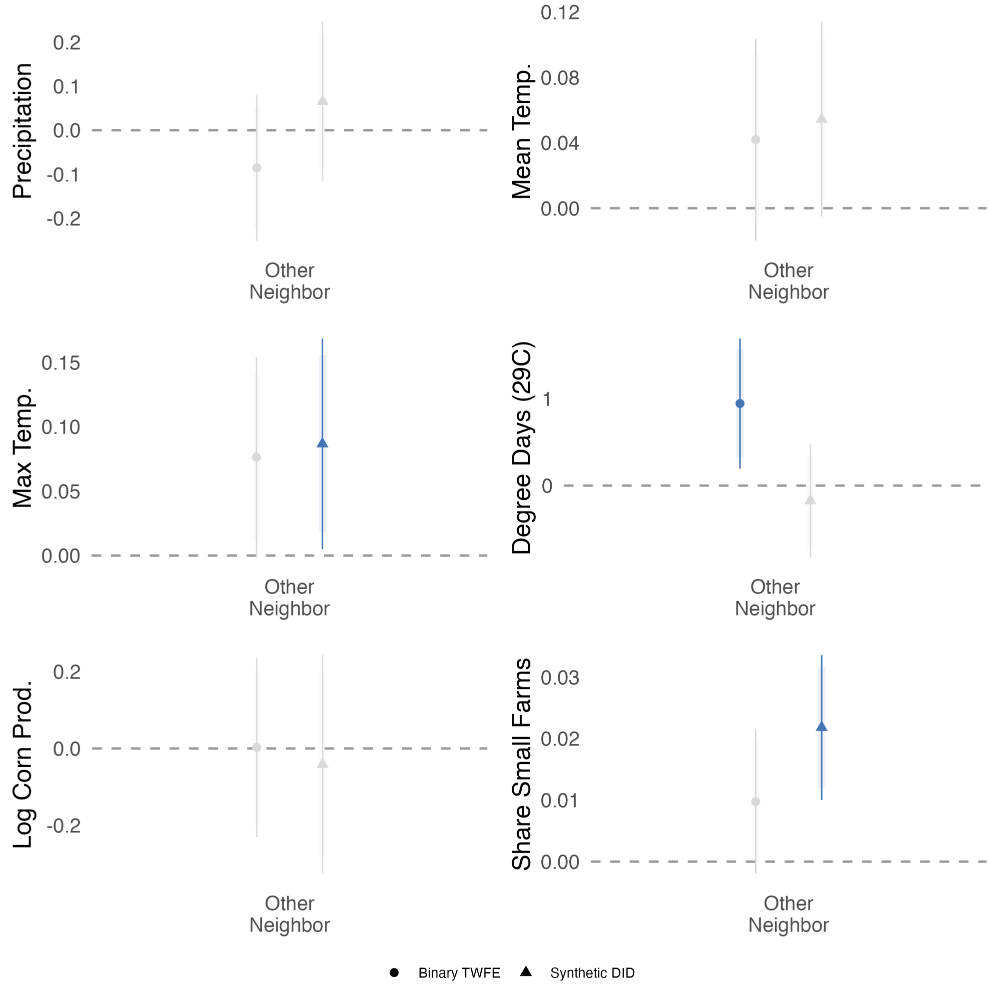

Notes: Figures plot coefficient estimates and 95% (thin line) and 90% (thick line) confidence intervals across two different models: binary difference-in-differences (Equation 5) and synthetic difference-in-differences TWFE (Equation 6) for non-downwind areas (counties within 200km of the Shelterbelt but with below-median wind exposure).

S.5 Details on additional empirical approaches

S.5.1 Instrumental variables approach

This section shows additional details of our instrumental variable approach that addresses the potential threat to our main identification strategy from possible strategic planting behavior of the decision-makers involved with the Shelterbelt project. The motivation for using an IV strategy, as well as the choice of the instrument, are discussed in the paper in Section 5.3.2.

We start with the initial planned location of the Shelterbelt tree-planting program. We find that counties inside and outside the planned area differ in baseline climate, as expected given the way the plans were drawn (as described in Section 5.3.2). However, these differences disappear once we control for longitude quartiles and our main specification's controls (Appendix Table S3, Panel A).

We then reproduce the wind exposure measure construction steps described in Section S.2, except replace the Shelterbelt area with the planned area. This means that we initialize imaginary particles at ERA-5 grid points starting in the planned Shelterbelt area (green shaded area in the left panel of Figure S12) instead of the actual Shelterbelt area. Figure S12 shows the wind exposure instrument next to the actual wind exposure measure. The resulting planned wind exposure measure is orthogonal to our sample counties' baseline climate. Precipitation does not vary with wind exposure in the raw data, while the three temperature variables do not once we include the controls (Appendix Table S3, Panel B). We thus present IV results with and without controls.

Table S3: Balance table for IV

Outcomes	Sample Mean	Without Controls		With Controls	
		Coef.	P-Val.	Coef.	P-Val.
	(1)	(2)	(3)	(4)	(5)
Panel A: Inside vs. outside the planned Shelterbelt area					
Precipitation (cm)	7.1	-0.387	< 0.001	-0.031	0.683
Mean Temp (C)	24.5	0.273	< 0.001	-0.001	0.987
Max Temp (C)	32	0.434	< 0.001	0.083	0.291
Degree Days (29C)	37.8	4.76	< 0.001	0.585	0.354
Panel B: Predicted wind exposure					
Precipitation (cm)	7.2	-0.005	0.99	1.102	< 0.001
Mean Temp (C)	24.4	1.414	< 0.001	0.022	0.945
Max Temp (C)	31.9	1.49	< 0.001	0.087	0.805
Degree Days (29C)	36.9	15.434	< 0.001	-1.333	0.603

Notes: Table shows the balance of baseline climate outcomes with respect to the planned Shelterbelt area, in two panels. In both panels the outcomes are listed on the left, Column 1 reports each outcome's sample average over the baseline period 1930–1942, Columns 2–3 report the OLS point estimate and associated p-value without controls, and Columns 4–5 report them when adding controls. *Panel A* regresses each outcome on an indicator equal to 1 if the county is inside the planned Shelterbelt area; the sample is the 678 counties with centroids within 300km of the centroids of Shelterbelt counties. *Panel B* regresses each outcome on the continuous predicted wind exposure to the planned Shelterbelt area (the instrument used in the IV specification); the sample is the 539 counties within 300km of the centroids of Shelterbelt counties but excluding the Shelterbelt counties themselves, consistent with the IV first stage. The controls in Columns 4–5 are ruggedness, elevation, Ogallala share, and longitude quartile, each interacted with year, plus state-by-year fixed effects. Standard errors are clustered by county.

We use the planned wind exposure measure (w_i^p) as an instrument for the continuous treatment variable (w_i) in our difference-in-differences model. Specifically, we estimate a two-stage least squares (2SLS) regression, where the first stage is:

$$w_i = \xi_1 w_i^p + \theta \mathbf{X}_i + \phi_s^{IV} + e_i \tag{7}$$

where w_i is the actual wind exposure measure for each county, w_i^p is the planned wind exposure measure for each county, $\mathbf{X}_i$ is the set of time-invariant controls, augmented by longitude quartiles, included in our main specification, and ϕ_s is state fixed effects. The model for the second-stage estimation is then:

$$y_{it} = \beta^{IV}(w_i \times P_t) + \gamma^{IV}(\mathbf{X}_i \times Y_t) + \delta_{st}^{IV} + \nu_i^{IV} + \epsilon_{it} \tag{8}$$

where w_i is instrumented by w_i^p, and all other variables are as defined in Equation 1.

The results are presented in Table S4. The instrument is strong in both specifications (Kleibergen-Paap F-statistics of 284 without controls and 344 with controls, Column 5). Without controls, the temperature estimates are similar to our headline DiD specification, while the precipitation estimate is smaller but remains strong and significant (Panel A). With controls—matching our preferred DiD specification—all IV estimates are similar to our main difference-in-differences estimates (Panel B). This indicates that our preferred estimates are not driven by a strategic selection of tree-planting location.

Figure S12: Wind exposure and wind exposure instrument

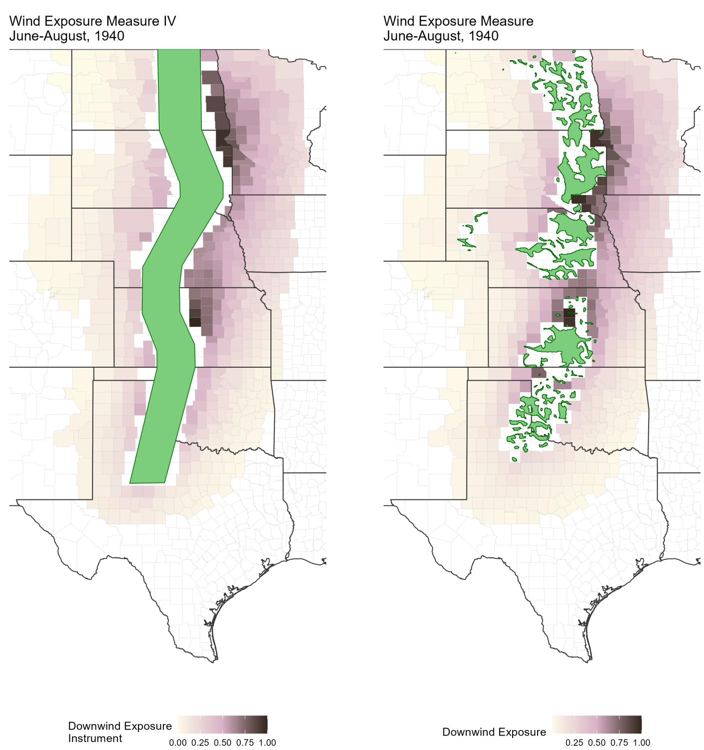

Notes: Left panel shows the instrument for the continuous wind exposure measure constructed based on the planned 100-mile Shelterbelt zone. Right panel shows the final continuous wind exposure measure based on realized Shelterbelt planting. Dark green outlines show planned and realized Shelterbelt areas.

Table S4: Impact of Great Plains Shelterbelt on summer county climate, 1930 to 1965 (instrumental-variable estimates)

	Dependent variable:				
	Precip. (cm)	Mean Temp (C)	Max Temp (C)	Degree Days (29C)	Wind Exposure
	(1)	(2)	(3)	(4)	(5)
Panel A: Without controls					
Wind Exp.:Post 1942	0.790***	−0.560***	−0.925***	−10.649***	
	(0.288)	(0.099)	(0.136)	(1.288)	
	[0.007]	[<0.001]	[<0.001]	[<0.001]	
Wind Exp. IV:Post 1942					0.801***
					(0.048)
					[<0.001]
Kleibergen-Paap F-stat	-	-	-	-	284.37
Panel B: With controls					
Wind Exp.:Post 1942	1.245***	−0.623***	−0.964***	−11.537***	
	(0.357)	(0.127)	(0.158)	(1.633)	
	[0.001]	[<0.001]	[<0.001]	[<0.001]	
Wind Exp. IV:Post 1942					0.911***
					(0.049)
					[<0.001]
Kleibergen-Paap F-stat	-	-	-	-	344.31
Sample Mean	7.16	24.43	31.88	36.86	-
Std.Dev.	2.94	2.82	2.92	22.94	-
75th-25th Perc. Wind Exp	0.21	0.21	0.21	0.21	-
Observations	19,404	19,404	19,404	19,404	19,404

Notes: Table shows results for estimating Equation 8 for 539 counties, non afforested but with centroids within 300km of the centroids of Shelterbelt counties. Dependent variables are June - August averages. Main independent variable is wind exposure (w_i), which measures approximate exposure to winds from afforested areas, interacted by a post-treatment dummy. This variable is instrumented by the planned wind exposure measure, which reconstructs the wind exposure measure based on the planned 100-mile wide Shelterbelt zone. First stage is shown in Column 5, with robust Kleibergen-Paap F-statistic reported (adequate for the just-identified heteroskedastic case we are studying). Panel A reports IV estimates without additional controls; Panel B adds county-level elevation, ruggedness, area over the Ogallala aquifer, and longitude-quartile indicators, each interacted with year. "75th-25th Perc Wind Exp" shows the difference between the 75th and 25th percentile of the continuous wind exposure measure. County and state-by-year FE are included. Standard errors clustered at the county level shown in parentheses; p-values shown in brackets (*p<0.1; **p<0.05; ***p<0.01).

S.5.2 Panel evidence from within-county variation

In our main specification, we use cross-sectional variation in wind exposure for causal identification. We are comparing changes in outcomes (before vs. after the Shelterbelt program) across different counties that are generally exposed to more or less wind blowing from the Shelterbelt. Importantly, wind speed and direction vary over time: across days, months, and years. This provides us with an additional source of identifying variation for the effects of tree-planting on the climate. We can indeed implement a two-way fixed effects panel specification on the post-treatment period. (The ERA-5 wind data is available from 1940 onwards, so we cannot run it on the baseline period as a placebo exercise.) That is, we estimate the following regression.

$$weather_{it} = \beta^{TWFE} windexposure_{it} + \delta_t^{TWFE} + \nu_i^{TWFE} + \epsilon_{it} \tag{9}$$

Note that because of the inclusion of the county and time fixed effects, we are essentially identifying the direct short-term effects of being more or less exposed to the Shelterbelt on the climate. The cross-county variation in wind exposure is absorbed by the county fixed effects: we are now identifying the effects of the variation across time within a given county, and across counties within a given time period only. This is a completely different source of identifying variation than our primary specification, and so makes for a robust alternative way of estimating the effects of the Shelterbelt tree-planting on the downwind climate.

The results, reported in Table 2, are consistent whether we use data at the annual (Panel A) or monthly (Panel B) level. In both cases, all four climate outcomes are significant at the 1% level under both clustered and Conley standard errors: higher wind exposure raises precipitation and lowers mean and maximum temperature and 29C degree days. These effects are directly aligned with those from our main identification strategy, corroborating our main results. The coefficients in Table 2 are larger in magnitude than those in Table 1, which reflects the different nature of the identifying variation. After absorbing county and time fixed effects, the residual variation in the time-varying wind exposure measure is approximately one-fifth of the cross-sectional variation in the static measure, scaling up the per-unit coefficient. The signs and statistical significance are consistent across both specifications.

Interestingly, these results also hold at the daily level. There, one needs to be cautious about the specific timing of the events, from being exposed to wind blowing from the Shelterbelt to the impacts on the local weather (precipitation and temperature). We estimate a modified version of Equation 9 that includes 10 days of lags and leads in addition to the contemporaneous wind exposure. The results, reported in Figure S13, are consistent across outcomes and with the results from Table 2. There, we find that in the day following a wind exposure shock (i.e., looking at the 1-day lagged variable), there is a strong and statistically significant increase in precipitation. This is associated with a decrease in temperature, on that day following the wind exposure shock as well as in the 9 following days. Interestingly, the day of the wind exposure shock itself, extreme temperatures are higher. However, the cumulative effect of the lower subsequent days fully offsets and reverses that effect. In other words, we find evidence consistent with warm moist air arriving from the Shelterbelt on the day of the high wind exposure, with the warm moist air leading to rain the next day. That rain cools off the air, which becomes cooler for several days afterwards. These results are consistent with expectations from atmospheric sciences, with our panel TWFE results aggregated at the month or year level, and with our main specification.

While highly useful, both as a robustness check and to provide direct refined evidence on the effects of planting trees on the downwind weather (which can be of separate interest to climate scientists for instance), this is not our preferred specification. It only allows us, indeed, to estimate the short-term effects on the weather (i.e., to study weather shocks driven by shocks to wind exposure)—while we are interested in the effects of the climate (a change in the distribution of the weather shocks).

Figure S13: Panel regression with daily data, 10 lags and leads.

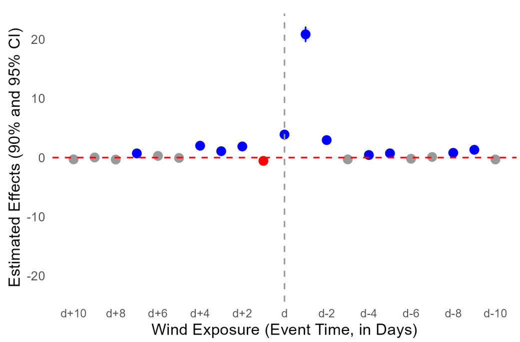

(A) Precipitation

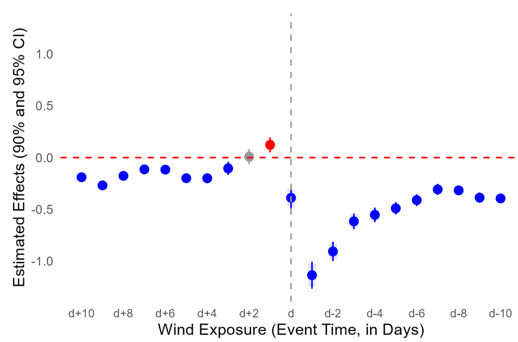

(B) Degree Days 29C

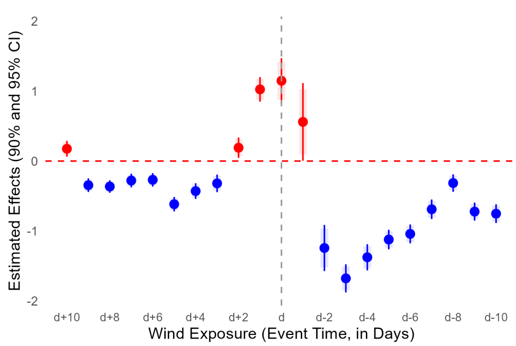

(C) Mean Temperature

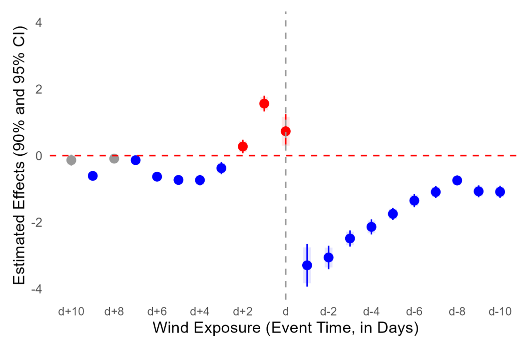

(D) Max Temperature

Notes: Figure shows result from regressing daily weather outcome on wind exposure from the Shelterbelt, including 10 days of leads and lags of the wind exposure measure. Outcome is precipitation (in mm), 29C degree days, mean temperature, and maximum temperature (in degree celsius). Point estimates and associated 90% and 95% confidence intervals (thick and thin bars, respectively) are reported. Statistically significant coefficients at the 5% level are reported in color (blue and red if positive/negative); the others are in grey. The lagged coefficients are reported to the right of the figure, and the lead coefficients to the left. For instance, Panel B reads: on the 9 days following a high Shelterbelt wind exposure day, temperature (measured as 29C degree days) is significantly lower than usual. Standard errors clustered at the county-level.

S.6 Additional results

S.6.1 Alternative controls, fixed effects, regressors

Our main TWFE difference-in-differences results are similar whether we include all of the controls together (elevation, ruggedness, ogallala) as in the main specification, one control at a time, or no control. This holds for the climate outcomes (Figure S14, top panel) and our key economic outcomes (Figure S15, top panel). Note that for brevity, we only report results for corn production and the share of small farms, but results are similar across most of our economic variables. This robustness is also true whether we use state-by-year fixed effects, year fixed effects, or grid-cell by year fixed effects (middle panels of these two figures), though corn production results are somewhat noisier with the grid-cell by year fixed effects. Similarly, results are similar whether we use wind data from 1940 initialized at 800 hPa, wind data from 1940-1965 initialized at 800 hPa, wind data from 1940 initialized at 1000 hPa, or wind data from 1940-1965 initialized at 1000 hPa (bottom panels).

S.6.2 Results by season

Table S5 re-estimates the climate effects by season. Precipitation rises and mean temperature falls in every season, with no significant sign reversals. The cooling of maximum temperature and extreme heat is concentrated in summer, when evapotranspiration peaks. We note that the absence of a significant fall effect on extreme heat is not surprising given that degree days above 29°C outside the summer are largely confined to September and to the southernmost counties of our sample, which are also least exposed to winds from the Shelterbelt, leaving little identifying variation.

S.6.3 Alternative climate data

Table S6 re-estimates our climate effects using two alternative datasets. Panel A uses PRISM data, aggregated from grid cells to counties, with degree days computed at the grid cell–day level using the same method as for our main data. Because PRISM is already gridded and gap-free, it requires none of the station selection, gap-filling, or interpolation steps described in Section S.3, and it draws on all available stations rather than a balanced panel, so it tests both our interpolation choices and our decision to hold the station set fixed. All four of our climate effects replicate with similar magnitudes. Panel B uses NOAA NCEI's nClimDiv county-level dataset, which interpolates GHCN station records to a grid and aggregates them to counties by a different method than ours. Because nClimDiv is reported monthly rather than daily, we cannot compute degree days, but the precipitation increase and the mean- and maximum-temperature decreases all replicate. The fact that our results hold across three datasets built from different station samples and interpolation methods is reassuring and shows they are not artifacts of our particular data construction.

Figure S14: Climate results robustness

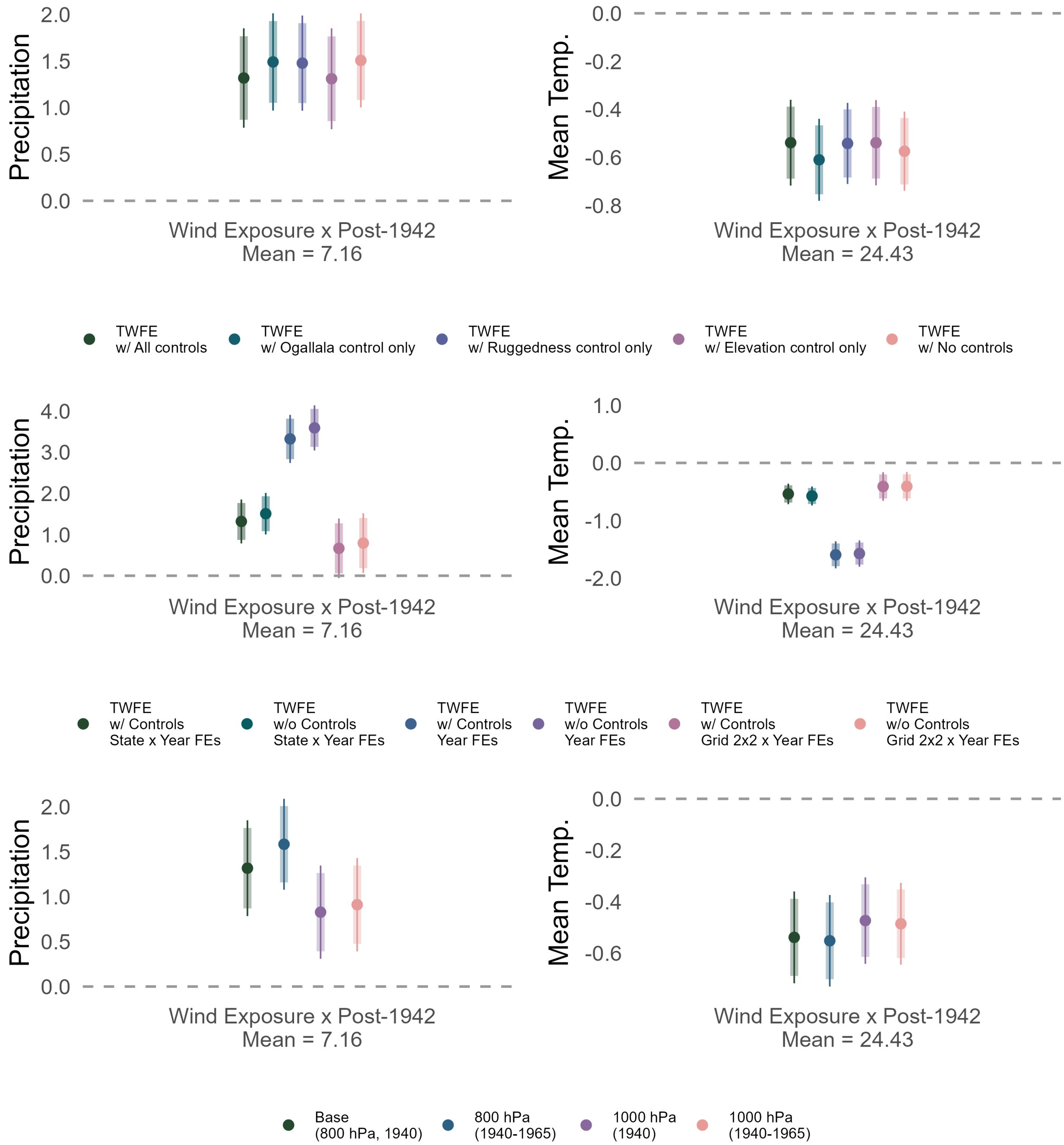

Notes: Figures plot coefficient estimates and 95% (thin line) and 90% (thick line) confidence intervals for mean summer precipitation and mean summer temperatures. In the top panel, we show robustness across five versions of estimating Equation 1 with various controls. In the middle panel, we show robustness across six specifications (based on Equation 1) with various fixed effects. Finally, in the bottom panel we show robustness using alternative wind exposure measures. The patterns of robustness are similar for maximum temperature and 29DD; not reported for brevity.

Figure S15: Economic results robustness

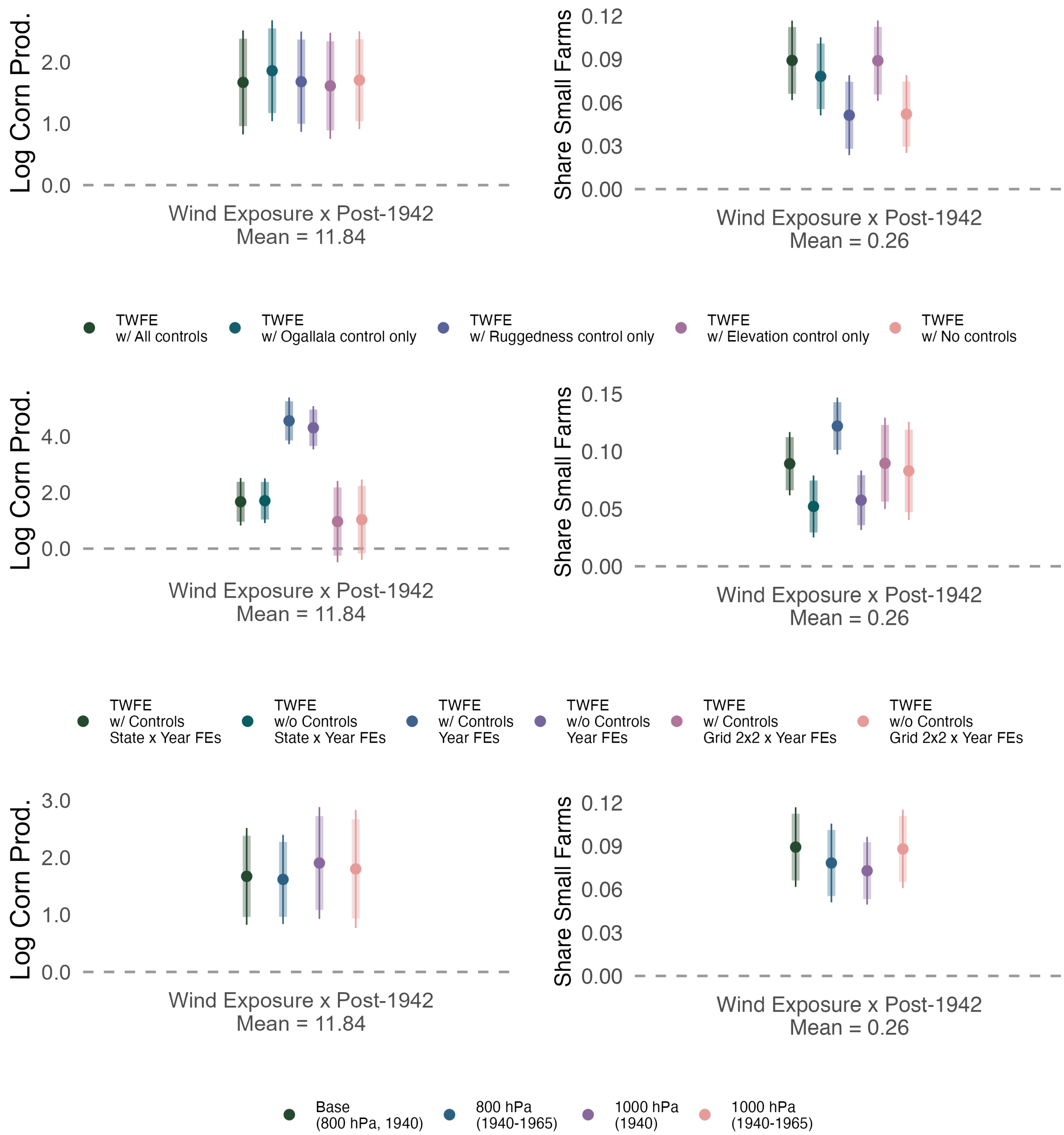

Notes: Figures plot coefficient estimates and 95% (thin line) and 90% (thick line) confidence intervals for corn production and the share of small farms. In the top panel, we show robustness across five versions of estimating Equation 1 with various controls. In the middle panel, we show robustness across six specifications (based on Equation 1) with various fixed effects. Finally, in the bottom panel we show robustness using alternative wind exposure measures. Logged outcomes use $\log(x)$ when zero-free and $\log(x + 1)$ otherwise (zero counts in Table S13).

Table S5: Impacts on the climate by season

	Annual	Winter	Spring	Summer	Fall
	(1)	(2)	(3)	(4)	(5)
Panel A: Precipitation (cm)					
Seasonal Wind Exposure x Post 1942	1.361***	1.315***	1.213***	1.462***	0.808***
	(0.153)	(0.161)	(0.309)	(0.301)	(0.255)
	[<0.001]	[<0.001]	[<0.001]	[<0.001]	[0.002]
Mean Dependent Var.	5.22	2.47	6.02	7.16	5.14
Panel B: Mean Temp (C)					
Seasonal Wind Exposure x Post 1942	−0.565***	−0.744***	−0.580***	−0.598***	−0.281**
	(0.107)	(0.141)	(0.136)	(0.101)	(0.113)
	[<0.001]	[<0.001]	[<0.001]	[<0.001]	[0.014]
Mean Dependent Var.	11.88	-1.3	11.23	24.43	12.79
Panel C: Max Temp (C)					
Seasonal Wind Exposure x Post 1942	−0.463***	−0.384**	−0.352*	−0.847***	−0.134
	(0.124)	(0.153)	(0.182)	(0.122)	(0.126)
	[<0.001]	[0.013]	[0.054]	[<0.001]	[0.291]
Mean Dependent Var.	18.93	5.05	18.34	31.88	20.03
Panel D: Degree Days (29C)					
Seasonal Wind Exposure x Post 1942	−3.671***	0.002	−0.325*	−10.890***	−0.159
	(0.480)	(0.005)	(0.175)	(1.226)	(0.216)
	[<0.001]	[0.717]	[0.065]	[<0.001]	[0.461]
Mean Dependent Var.	11.22	0.01	2.07	36.86	5.62
75th-25th Perc. Wind Exp	0.26	0.24	0.24	0.3	0.28
Observations	19,404	19,404	19,404	19,404	19,404

Notes: Table shows results for estimating Equation 1. Sample of 539 counties outside the Shelterbelt and with centroids within 300km of the centroids of Shelterbelt counties. Column 1 estimates effects at the annual level (using annual wind exposure and annual outcome), Column 2 for the winter (December to February), Column 3 for the spring (March to May), Column 4 for the summer (June to August), and Column 5 for the fall (September to November). Wind exposure is also season-specific, computed by averaging monthly wind exposure for the months in each season (using the 1940 cross-section). Summer results (Column 4) do not exactly match our main results in Table 1 due to different normalization of wind exposures. "75th-25th Perc Wind Exp" shows the difference between the 75th and 25th percentile of the continuous wind exposure measure in the sample. Controls and fixed effects are identical to those described in Figure 3. Standard errors are clustered at the county level, shown in parentheses; p-values shown in brackets (*p<0.1; **p<0.05; ***p<0.01).

Table S6: Impact of Great Plains Shelterbelt on summer county climate, 1930 to 1965

	Dependent variable:			
	Precipitation (cm)	Mean Temp (C)	Max Temp (C)	Degree Days (29C)
	(1)	(2)	(3)	(4)
Panel A: PRISM				
Wind Exposure:Post 1942	1.332***	−0.434***	−0.683***	−8.136***
	(0.387)	(0.082)	(0.099)	(1.045)
	[0.001]	[<0.001]	[<0.001]	[<0.001]
Sample Mean	4.91	24.17	31.51	31.13
Std.Dev.	2.48	2.9	2.91	21
75th-25th Perc. Wind Exp	0.21	0.21	0.21	0.21
Observations	19,368	19,368	19,368	19,368
Panel B: NClimDiv				
Wind Exposure:Post 1942	1.634***	−0.364***	−0.813***	
	(0.281)	(0.078)	(0.103)	
	[<0.001]	[<0.001]	[<0.001]	
Sample Mean	7.16	24.16	31.44	
Std.Dev.	2.95	2.99	3.02	
75th-25th Perc. Wind Exp	0.21	0.21	0.21	
Observations	19,404	19,404	19,404	

Notes: Table shows results for estimating Equation 1 using PRISM data aggregated to county-level (Panel A) and NOAA NClimDiv county-level climate data (Panel B) as alternatives to our main interpolated weather station data. NClimDiv provides monthly county-level precipitation, minimum temperature and maximum temperature (the average of which is taken to be mean temperatures), but not degree days. Sample of 539 counties outside the Shelterbelt and with centroids within 300km of the centroids of Shelterbelt counties (missing PRISM data for one county). Dependent variables are the annual average of each month's average climate for June, July, and August. The "Mean" and "Std. Dev." measures are taken in the pre-1942 period. The main independent variable is wind exposure (w_i), which measures approximate exposure to winds from afforested areas, interacted by a post-treatment dummy. Time-invariant controls (elevation, ruggedness, Ogallala aquifer share), interacted by year. County and state-by-year FE are included. Standard errors are clustered at the county level, shown in parentheses; p-values shown in brackets (*p<0.1; **p<0.05; ***p<0.01).

S.6.4 Differential climate trends and the Dust Bowl

This section presents our additional results reinforcing that the Dust Bowl or longer-time climate trends do not bias our results.

Dropping Dust Bowl years First, we verify the robustness of our main results to omitting the Dust Bowl era, or controlling for Dust Bowl severity. We rerun our analyses separately dropping the project implementation years (1936 to 1942) and peak Dust Bowl years (1934, 1936, 1939) from our baseline period.[39] Tables S7 and S8 show the results are generally consistent with our main findings. We also re-run our analyses on our main sample but add county-level Dust Bowl erosion measures from Hornbeck (2012) as controls, so identification comes from comparing counties with similar Dust Bowl severity. The climate effects, reported in Table S9, are essentially unchanged.

Table S7: Impact of Great Plains Shelterbelt on summer county climate, 1930 to 1965 (Excluding 1936 to 1942)

	Dependent variable:			
	Precipitation	Mean Temp	Max Temp	Degree Days
	(cm)	(C)	(C)	(29C)
	(1)	(2)	(3)	(4)
Wind Exposure:Post 1942	0.757**	−0.612***	−0.739***	−9.969***
	(0.311)	(0.092)	(0.114)	(1.109)
	[0.016]	[<0.001]	[<0.001]	[<0.001]
Sample Mean	6.79	24.63	32.16	38.66
Std.Dev.	2.74	2.79	2.79	22.86
75th-25th Perc. Wind Exp	0.21	0.21	0.21	0.21
Observations	15,631	15,631	15,631	15,631

Notes: Table shows results for estimating Equation 1, excluding the Shelterbelt implementation years (1936–1942) from the sample. The pre-treatment period is therefore 1930–1935 and the post-treatment period is 1943–1965. Sample of 539 counties outside the Shelterbelt and with centroids within 300km of the centroids of Shelterbelt counties. Dependent variables are the annual average of each month's average climate for June, July, and August. For clarity, for the 'Mean' row: (1) precipitation of 6.79cm is the average monthly cumulative rainfall, averaged across June-August; (2) mean temperature of 24.63C is the monthly average of daily mean temperatures, averaged across June-August; (3) max temperature of 32.16C is the monthly average of daily maximum temperatures, averaged across June-August; (4) degree days (29c) of 38.66 is the monthly sum of daily degree days exceeding 29C (i.e., a 32C day would contribute 3 degree days to that month), averaged across June-August. The "Mean" and "Std. Dev." measures are taken in the pre-1936 period. The main independent variable is wind exposure (w_i), which measures approximate exposure to winds from afforested areas, interacted by a post-treatment dummy. Time-invariant controls (elevation, ruggedness, Ogallala aquifer share), interacted by year. County and state-by-year FE are included. Standard errors are clustered at the county level, shown in parentheses; p-values shown in brackets (*p<0.1; **p<0.05; ***p<0.01).

[39] We note that 1935 had very few trees planted as shown in Figure S3, so we keep it in this analysis.

Table S8: Impact of Great Plains Shelterbelt on summer county climate, 1930 to 1965 (Excluding 1934, 1936, and 1939)

	Dependent variable:			
	Precipitation (cm)	Mean Temp (C)	Max Temp (C)	Degree Days (29C)
	(1)	(2)	(3)	(4)
Wind Exposure:Post 1942	2.076***	−0.554***	−0.800***	−10.546***
	(0.306)	(0.085)	(0.104)	(0.968)
	[<0.001]	[<0.001]	[<0.001]	[<0.001]
Sample Mean	7.71	24.12	31.41	32.07
Std.Dev.	2.76	2.59	2.6	17.66
75th-25th Perc. Wind Exp	0.21	0.21	0.21	0.21
Observations	17,787	17,787	17,787	17,787

Notes: Table shows results for estimating Equation 1, excluding peak Dust Bowl years (1934, 1936, and 1939) from the sample. The pre-treatment period is therefore 1930–1933, 1935, and 1937–1938 and the post-treatment period is 1943–1965. Sample of 539 counties outside the Shelterbelt and with centroids within 300km of the centroids of Shelterbelt counties. Dependent variables are the annual average of each month's average climate for June, July, and August. For clarity, for the 'Mean' row: (1) precipitation of 7.71cm is the average monthly cumulative rainfall, averaged across June-August; (2) mean temperature of 24.12C is the monthly average of daily mean temperatures, averaged across June-August; (3) max temperature of 31.41C is the monthly average of daily maximum temperatures, averaged across June-August; (4) degree days (29c) of 32.07 is the monthly sum of daily degree days exceeding 29C (i.e., a 32C day would contribute 3 degree days to that month), averaged across June-August. The "Mean" and "Std. Dev." measures are taken in the pre-treatment period. The main independent variable is wind exposure (w_i), which measures approximate exposure to winds from afforested areas, interacted by a post-treatment dummy. Time-invariant controls (elevation, ruggedness, Ogallala aquifer share), interacted by year. County and state-by-year FE are included. Standard errors are clustered at the county level, shown in parentheses; p-values shown in brackets (*p<0.1; **p<0.05; ***p<0.01).

Table S9: Impact of Great Plains Shelterbelt on summer county climate, 1930 to 1965

	Dependent variable:			
	Precipitation (cm)	Mean Temp (C)	Max Temp (C)	Degree Days (29C)
	(1)	(2)	(3)	(4)
Wind Exposure:Post 1942	1.272***	−0.503***	−0.734***	−9.492***
	(0.272)	(0.088)	(0.108)	(1.070)
	[<0.001]	[<0.001]	[<0.001]	[<0.001]
Sample Mean	7.16	24.43	31.88	36.86
Std.Dev.	2.94	2.82	2.92	22.94
75th-25th Perc. Wind Exp	0.21	0.21	0.21	0.21
DB Erosion Controls	Yes	Yes	Yes	Yes
Observations	18,684	18,684	18,684	18,684

Notes: Table shows results for estimating Equation 1, adding county-level Dust Bowl erosion measures from Hornbeck (2012). Sample of 519 counties outside the Shelterbelt and with centroids within 300km of the centroids of Shelterbelt counties and with available Dust Bowl erosion measures. Dependent variables are the annual average of each month's average climate for June, July, and August. For clarity, for the 'Mean' row: (1) precipitation of 7.16cm is the average monthly cumulative rainfall, averaged across June-August; (2) mean temperature of 24.43C is the monthly average of daily mean temperatures, averaged across June-August; (3) max temperature of 31.88C is the monthly average of daily maximum temperatures, averaged across June-August; (4) degree days (29C) of 36.86 is the monthly sum of daily degree days exceeding 29C (i.e., a 32C day would contribute 3 degree days to that month), averaged across June-August. The "Mean" and "Std. Dev." measures are taken in the pre-1942 period. The main independent variable is wind exposure (w_i), which measures approximate exposure to winds from afforested areas, interacted by a post-treatment dummy. "75th-25th Perc Wind Exp" shows the difference between the 75th and 25th percentile of the continuous wind exposure measure in the sample. Time-invariant controls, interacted by year, include county-level Dust Bowl erosion levels, elevation, ruggedness, and area over the Ogallala aquifer. County and state-by-year FE are included. Standard errors are clustered at the county level, shown in parentheses; p-values shown in brackets (*p<0.1; **p<0.05; ***p<0.01). See Appendix Table S12 for results restricting the sample to county-years with agricultural census data available.

Longer and alternative time periods Next, we rerun our analyses over a longer time period, noting that our main analysis starts in 1930 due to quality concerns for earlier data periods.[40] Nevertheless, replicating our main difference-in-differences analysis on the 1910-1965 sample instead of our preferred 1930–1965 results produces similar results, though somewhat lower in magnitude (Table S10).

Table S10: Impact of Great Plains Shelterbelt on summer county climate, 1910 to 1965

	Dependent variable:			
	Precipitation (cm)	Mean Temp (C)	Max Temp (C)	Degree Days (29C)
	(1)	(2)	(3)	(4)
Wind Exposure:Post 1942	0.943***	−0.171***	−0.393***	−3.992***
	(0.214)	(0.059)	(0.083)	(0.621)
	[<0.001]	[0.004]	[<0.001]	[<0.001]
Sample Mean	7.59	23.76	31.13	31.31
Std.Dev.	2.69	2.64	2.61	17.85
75th-25th Perc. Wind Exp	0.21	0.21	0.21	0.21
Observations	30,184	30,184	30,184	30,184

Notes: Table shows results for estimating Equation 1. Sample of 539 counties outside the Shelterbelt and with centroids within 300km of the centroids of Shelterbelt counties, over 1910-1965. This is the analogue of Table 1, with a sample starting in 1910 instead of 1930. Dependent variables are the annual average of each month's average climate for June, July, and August. For clarity, for the 'Mean' row: (1) precipitation of 7.59cm is the average monthly cumulative rainfall, averaged across June-August; (2) mean temperature of 23.76C is the monthly average of daily mean temperatures, averaged across June-August; (3) max temperature of 31.13C is the monthly average of daily maximum temperatures, averaged across June-August; (4) degree days (29C) of 31.31 is the monthly sum of daily degree days exceeding 29C (i.e., a 32C day would contribute 3 degree days to that month), averaged across June-August. The "Mean" and "Std. Dev." measures are taken in the pre-1942 period. The main independent variable is wind exposure (w_i), which measures approximate exposure to winds from afforested areas, interacted by a post-treatment dummy. "75th-25th Perc Wind Exp" shows the difference between the 75th and 25th percentile of the continuous wind exposure measure in the sample. Time-invariant controls, interacted by year, include county-level elevation, ruggedness, and area over the Ogallala aquifer. County and state-by-year FE are included. Standard errors are clustered at the county level, shown in parentheses; p-values shown in brackets (*p<0.1; **p<0.05; ***p<0.01).

To address potential violations to the parallel trends assumption when extending the start date of our analysis back to 1910, we also replicate our synthetic difference-in-differences analyses (detailed in Section S.4.3). Figure S16 shows the results from the synthetic difference-in-differences analysis, implemented on the periods 1910-1965 and 1920-1965. We find similar effects on downwind precipitation as with our preferred difference-in-differences approach with controls. Temperature results are lower in magnitude, but directionally consistent with

[40] The 1910–1965 station panel is both sparser and less complete than the 1930–1965 panel used in our main analysis. Requiring coverage over the longer window leaves 623 precipitation and 491 temperature stations against 1,100 and 774 for 1930–1965. Among these stations, the share of station-summer-days missing from the raw GHCNd record is highest in the 1910s, at 3.2% for precipitation and 3.3% for temperature, roughly twice the average of any later decade.

our main results too. The one exception is the 1910–1965 panel, which shows an increase in summer temperatures in "other neighbor" counties that do not appear in any other specifications. We attribute it to the quality of the early-century station record as 1910–1919 are the least complete years in the record. For temperature, 3.3% of station-summer-days in the 1910s are absent from the raw GHCNd data, against 1.5–2.7% in each subsequent decade. The additional imputation adds noise to the interpolated county series in the years that distinguish the two samples. The 1920–1965 results closely mirror our main findings.

Figure S16: Synthetic difference-in-differences summer climate results, longer time periods

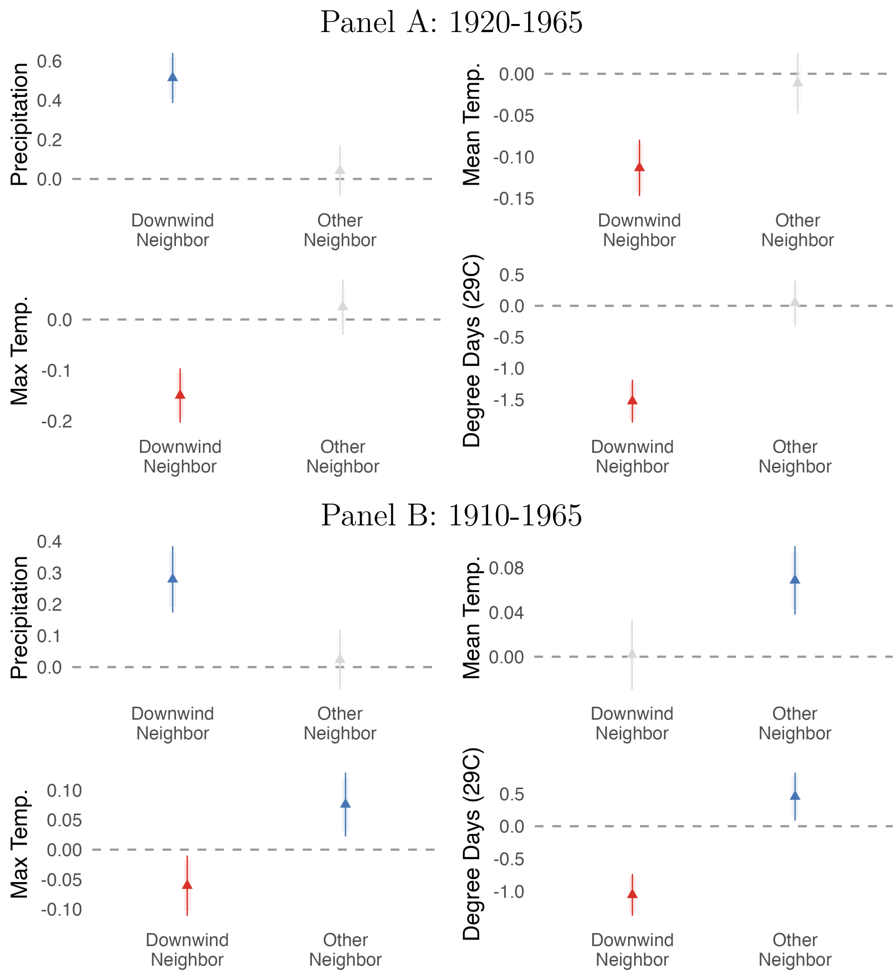

Notes: Figures plot coefficient estimates and 95% (thin line) and 90% (thick line) confidence intervals from the synthetic difference-in-differences estimator (Equation 6), extending the baseline period to 1920 (Panel A) and 1910 (Panel B). Each panel shows results for downwind neighbor and other neighbor counties relative to their synthetic control.

Finally, we conduct long difference estimates (Equation 2) with alternative time periods, comparing time periods with similar characteristics. In Panel A of Table S11, we compare 1925–1930 – instead of 1930-1935 – to 1960–1965, to address concerns that the early 1930s were heavy drought periods. In Panel B, we compare 1930–1935 to 1950–1955 – instead of 1960–1965 – to compare two general drought periods in the Great Plains in the pre- and post-planting periods. The estimates are qualitatively similar to our main long differences results.

Table S11: Impact of Great Plains Shelterbelt on summer county climate

	Dependent variable:			
	Precipitation (cm)	Mean Temp (C)	Max Temp (C)	Degree Days (29C)
	(1)	(2)	(3)	(4)
Panel A: 1925–1930 vs. 1960–1965				
Wind Exposure	2.948***	−0.792***	−0.791***	−11.503***
	(0.460)	(0.130)	(0.176)	(1.634)
	[<0.001]	[<0.001]	[<0.001]	[<0.001]
Sample Mean	6.2	24.25	31.86	37.14
Std.Dev.	2	2.63	2.52	19.8
Panel B: 1930–1935 vs. 1950–1955				
Wind Exposure	1.156***	−0.742***	−1.033***	−13.161***
	(0.408)	(0.107)	(0.153)	(1.347)
	[0.005]	[<0.001]	[<0.001]	[<0.001]
Sample Mean	6.91	24.7	32.22	38.96
Std.Dev.	1.8	2.65	2.5	18.51
75th-25th Perc. Wind Exp	0.21	0.21	0.21	0.21
Observations	539	539	539	539

Notes: Table shows results for estimating Equation 2. Sample of 539 counties outside the Shelterbelt and with centroids within 300km of the centroids of Shelterbelt counties. Dependent variables are the annual average of each month's average climate for June, July, and August. Panel A compares 1925–1930 to 1960–1965; Panel B compares 1930–1935 to 1950–1955. The main independent variable is wind exposure (w_i), which measures approximate exposure to winds from afforested areas, interacted by a post-treatment dummy. "75th-25th Perc Wind Exp" shows the difference between the 75th and 25th percentile of the continuous wind exposure measure in the sample. Controls, interacted by year, include county-level elevation, ruggedness, and area over the Ogallala aquifer. State FE are included. Standard errors are clustered at the county level, shown in parentheses; p-values shown in brackets (*p<0.1; **p<0.05; ***p<0.01).

S.6.5 Agricultural census subsample results

Figure S17 illustrates the geographical coverage of USDA agricultural census (conducted every approximately 5 years) between 1930 and 1964. We use agricultural census data in our main analysis, as it offers a more comprehensive coverage of the region.

Figure S17: Agricultural census data

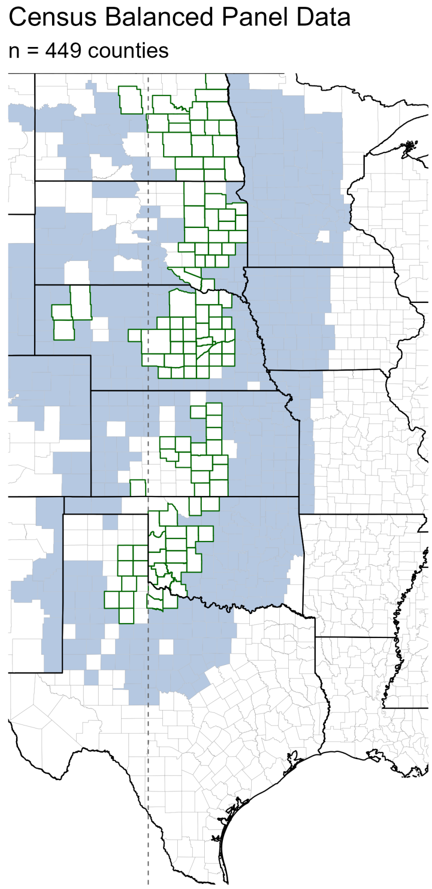

Notes: Figure shows counties for which we have corn yield observations from the agricultural census for every time period between 1930 and 1964. Shelterbelt (directly afforested) counties are shown with green borders.

We can rerun our main climate analysis for only counties and years for which the census data are available. Although the resulting effects shown in Panel A of Table S12 are similar to our main results in Table 1, the precipitation coefficient is no longer statistically significant. However, by decomposing this attenuation, we find that the precipitation effect remains statistically significant within the census-county subsample at full annual frequency (Panel B of Table S12) and is marginally significant within all 539 counties at census-year frequency (Panel C of Table S12). Significance is lost only when both restrictions apply, reflecting a compounded sample-size loss rather than a substantive change in the underlying effect.

Table S12: Impact of Great Plains Shelterbelt on summer county climate: Agricultural census sample

	Dependent variable:			
	Precipitation (cm)	Mean Temp (C)	Max Temp (C)	Degree Days (29C)
	(1)	(2)	(3)	(4)
Panel A: Census Counties, Census Years				
Wind Exposure:Post 1942	0.491	-0.764^{***}	-1.063^{***}	-12.965^{***}
	(0.585)	(0.128)	(0.155)	(1.523)
	[0.402]	[<0.001]	[<0.001]	[<0.001]
Sample Mean	7.81	24	31.26	32.92
Std.Dev.	3.01	2.43	2.48	16.96
Observations	3,592	3,592	3,592	3,592
Panel B: Census Counties, All Climate Years				
Wind Exposure:Post 1942	0.784^{***}	-0.525^{***}	-0.754^{***}	-8.769^{***}
	(0.290)	(0.095)	(0.116)	(1.167)
	[0.008]	[<0.001]	[<0.001]	[<0.001]
Sample Mean	7.43	24.51	31.9	36.78
Std.Dev.	2.99	2.71	2.85	22.96
Observations	16,164	16,164	16,164	16,164
Panel C: All Counties, Census Years				
Wind Exposure:Post 1942	0.930^{*}	-0.713^{***}	-0.992^{***}	-12.998^{***}
	(0.532)	(0.112)	(0.137)	(1.325)
	[0.081]	[<0.001]	[<0.001]	[<0.001]
Sample Mean	7.45	23.95	31.28	33.15
Std.Dev.	2.99	2.55	2.58	17.23
Observations	4,312	4,312	4,312	4,312

Notes: Table shows results for estimating Equation 1, for three restrictions of the main sample based on counties and years. (Table 1 reports results from the main sample.) Panel A restricts the sample to counties and years where agricultural census data is available (Panel A). Panel B restricts the sample to the 449 counties (out of 539 in the main sample) where agricultural census is available, but includes all years from 1930 to 1965. Panel C uses all 539 counties, but restricts the sample to the years in which the agricultural census was conducted. Everything else is as in Table 1.

We note that temperature results are significant across all subsamples, likely due to the fact that precipitation is much less spatially correlated than temperatures (National Center for Atmospheric Research Staff 2014), so our interpolation may lead to more noise in precipitation than temperature.

Zeros in logged outcomes A number of the agricultural outcomes we study in logs take a value of zero for some county-years, which requires a choice about how to handle them. Table S13 shows the number of zeros for each variable in the agricultural census data that enters Tables 3-7 with a log transformation. Most variables have no or very few zeros. For variables with positive shares of zeros, the log transformation used in tables and figures is $\log(x + \varepsilon)$ with $\varepsilon = 1$; all other outcomes use $\log(x)$. We also rerun our main results shown in Tables 3–7 with the inverse hyperbolic sine (*asinh*) transformation and find very similar results (not reported for brevity). Finally, for the two variables with a meaningful share of zeros (irrigated farmland and fertilizer spending), we also estimate the downwind effects of the Shelterbelt on the likelihood of recording a zero value of the variable (not reported for brevity). For both variables, we find no statistically significant effect on this likelihood, indicating that the estimated effects stem from intensive margin responses.

Table S13: Zero counts for log-transformed outcomes

	N	# Zeros	% Zeros
Corn production (Table 3, Panel A)			
Corn production (bushels)	3,592	0	0.00
Corn area harvested (k acres)	3,592	0	0.00
Corn yield (bu/acre)	3,592	0	0.00
Other crop activities (Table 3, Panel B)			
Wheat acreage (k acres)	3,592	60	1.67
Irrigated farmland (k acres)	3,592	1,959	54.54
Crop failure (k acres)	2,245	1	0.04
Animal husbandry (Table 3, Panel C)			
Total cattle (head)	3,592	0	0.00
Number of pigs (head)	3,592	0	0.00
Number of chickens (head)	3,592	0	0.00
Farmland use (Table 4)			
Land in farms (k acres)	3,592	0	0.00
Total cropland (k acres)	3,592	0	0.00
Total pasture (k acres)	3,143	0	0.00
Woodland not pastured (k acres)	3,143	79	2.51
Other land (k acres)	3,143	0	0.00
Farm consolidation (Table 5)			
Average farm size (acres)	3,592	0	0.00
Aggregate values (Table 6, Panel A)			
Land + building value (USD)	3,592	0	0.00
Crops sales value (USD)	3,143	0	0.00
Animal sales value (USD)	3,143	0	0.00
Values per acre (Table 6, Panel B)			
Land + building value per acre (USD/acre)	3,592	0	0.00
Crop sales value per acre (USD/acre)	3,143	0	0.00
Animal sales value per acre (USD/acre)	2,694	0	0.00
Inputs (Table 7)			
Hired labor spending (USD)	2,694	0	0.00
Hired machine spending (USD)	2,694	0	0.00
Fertilizer spending (USD)	1,632	151	9.25

Notes: Table shows the number of zeros for each variable that enters Tables 3–7 with a log transformation. The sample in this table is the balanced panel of 449 non-Shelterbelt counties in the regression samples of Tables 3–7. Input variables (Table 7) have smaller N because they are not reported in every census year. Throughout the paper, logged outcomes use $\log(x)$ when zero-free and $\log(x+1)$ otherwise. One outcome only is reported for Table 5, as the others are not logged.

S.7 Irrigation

Irrigation is another major land use choice that has the potential to affect the climate, both locally and downwind (see e.g., Lobell et al. 2008; DeAngelis et al. 2010; Mueller et al. 2016; Braun and Schlenker 2023). We therefore consider whether irrigation might confound our main estimated effect, which could happen if an expansion of irrigation happened in the same place and time as the Shelterbelt tree-planting (section S.7.1). In addition, we test whether irrigation is complement or substitute to the downwind climate change induced by the Shelterbelt program, and its importance for the external validity of our results (section S.7.2).

S.7.1 Irrigation as potential confound

Irrigation strongly expanded in the US Midwest after World War II. If this expansion of irrigation happened in the same areas as where the Shelterbelt tree-planting happened, then our results might be biased: there could have been a change in the climate downwind from the Shelterbelt areas, even absent the tree-planting. However, this potential concern is not warranted empirically.

First, historical sources (e.g., Barton 1936) describe precisely the cultivation of the trees planted under the Shelterbelt project. He describes everything from the preparation of the ground to enhance rainfall capture to post-planting weeding—without any mention of irrigation. This contemporaneous account shows windbreaks were very unlikely to be irrigated, as water was scarce and irrigation did not expand in earnest until the post-war period.

Second, we do not find the expansion of irrigation over our study period to be correlated with the areas of Shelterbelt planting. Figure S18 plots the expansion of irrigated farmland between the start and end of our main study period (1930 - 1964) against (to the left) the area of concentrated Shelterbelt planting from the Read 1958 maps and (to the right) the area of Shelterbelt trees from the Snow 2019 shapefiles. The sample consists of all counties which we classify in this study as "Shelterbelt counties", meaning counties with at least 5% of their surface covered by "areas of concentrated Shelterbelt planting". For the Read 1958 measure of concentrated planting, we find no correlation between tree-planting intensity and irrigation expansion ($\beta = 0.007$, $p = 0.76$); for the Snow 2019 measure, the correlation is negative ($\beta = -4.72$, $p = 0.02$). Counties with denser shelterbelt planting saw, if anything, a relatively smaller expansion of irrigation. Importantly, only a positive correlation between planting and irrigation expansion would generate our downwind results absent the tree-planting; a negative one would, if anything, attenuate our estimates. In addition, we also consider all counties classified in this study as either "Shelterbelt counties" or their neighbors (i.e., all counties with a centroid within 200km of the centroid of a Shelterbelt county), and regress the 1930–1964 increase in irrigation on an indicator variable for being a Shelterbelt county (as opposed to a Shelterbelt neighbor). We find that the increase in irrigation (as a share of the total county area) was neither statistically nor economically significantly different for Shelterbelt counties than for their neighbors (coef. = 0.005, p-value = 0.459, not reported in an exhibit).

As such, since the Shelterbelt trees were not irrigated themselves, and irrigation expanded, if anything, less in the areas of dense Shelterbelt planting, the potential concern that the substantial expansion of irrigation post-WWII might be confounding our results is not warranted.

Figure S18: Irrigation and Shelterbelt planting

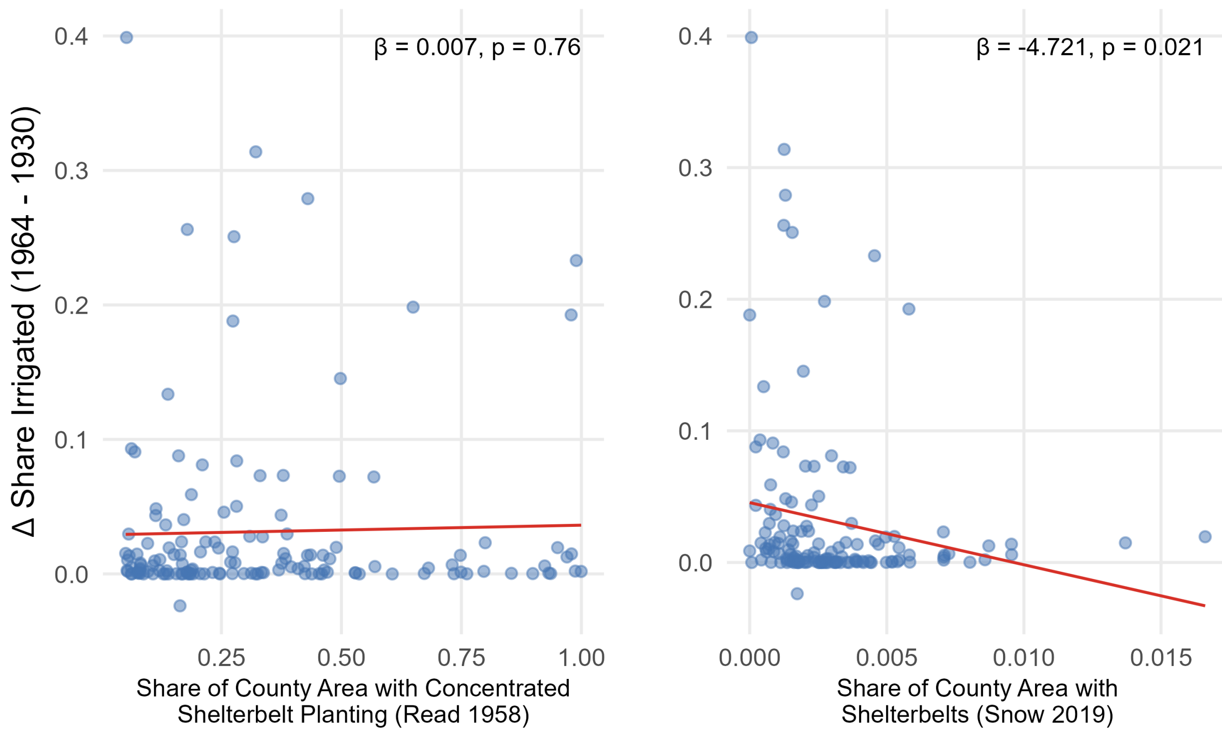

Notes: Scatterplots of the expansion of irrigated farmland (as a share of total county area, from 1930 to 1964) against the extent of Shelterbelt tree-planting (as share of total county area). The left panel uses the area of concentrated tree-planting from Read (1958) to measure tree-planting, while the right panel uses the area of the shelterbelts' polygons from Snow (2019). Sample of counties with some concentrated Shelterbelt planting ("Shelterbelt counties" throughout the paper). The OLS point estimate and associated p-value from the corresponding regression, with heteroskedastic robust standard errors, are reported in each panel.

S.7.2 Irrigation as an outcome

Irrigation is an important instrument to reduce the vulnerability of agricultural output (Hornbeck and Keskin 2014; Edwards and Smith 2018). As such, it is important to consider whether the increase in precipitation and reduction in extreme temperatures downwind from the Shelterbelt tree-planting led to changes in irrigation: are irrigation and the climate complement, substitutes, or unrelated?

Importantly, irrigation can be based on surface water (with water drawn from nearby rivers and streams, for instance) or groundwater (with wells to access water from the aquifer). Our study area, the US Midwest, is characterized by a rich heterogeneity in the potential for groundwater irrigation: areas over the Ogallala aquifer have the potential to irrigate by drawing water from that aquifer at a low cost; while areas located outside the Ogallala aquifer do not have the possibility to access groundwater and need to rely on surface water irrigation.

The overall effects of the Shelterbelt tree-planting on downwind irrigation are reported in Table 3 (Panel B, Column 2), while Appendix Table S14 reports their heterogeneity by Ogallala status (being over the aquifer or not). While the Shelterbelt increases aggregate irrigation downwind, the results are strongly heterogeneous. For counties that are *not* located over the aquifer, we find that the increased precipitation induced by upwind Shelterbelt planting is associated with a significant increase in irrigated farmland area (whether we consider it in logs or in levels). By contrast, for counties over the aquifer, we find significantly different effects: the irrigation response is negative or zero, depending on the specification.

This pattern of results can be explained by the fact that for counties that are not located over an aquifer, the availability of surface water is key for the availability of surface-water irrigation, leading to the strong estimated complementarities between irrigation and increased precipitation. Counties over the Ogallala aquifer already have access to cheap irrigation through groundwater and were using it: they had a ten-fold larger level of irrigated farmland at baseline. For them, the availability of rain water changing the water flows in rivers and streams was not required to attain their desired irrigation level. Consistent with this, we find no irrigation response for these counties. Some specifications suggest a decline, which would indicate substitution away from groundwater, but that result is not robust to controls.

This result is especially important in the context of global climate change, since irrigation is often presented as a major adaptation tool for farmers.

Consistent with evidence that irrigation is used to buffer crops against drier conditions (Hornbeck and Keskin 2014; Fishman 2018; Russo and Lall 2017), we find that areas over the aquifer that experience a wetter and cooler climate use irrigation less. This is the same substitution observed in the opposite direction, and under a durable change in climate rather than transitory weather. However, we show that in settings where groundwater is not readily available (either because a county is not located over an abundant aquifer, or potentially in the future when aquifers become depleted), surface water irrigation itself requires the availability of rainfall—and so wouldn't be sufficient to adapt to a decrease in precipitation. We leave the detailed exploration of these ideas for future work.

Could irrigation then drive some of the equilibrium effects that we observe? We find irrigation and climate improvements to be complement over the non-Ogallala counties, and we know from prior work that irrigation can itself have a local (and downwind) effect on the climate. Then, the overall effect of tree-planting on the climate downwind from the Shelterbelt areas would be a combination of the direct effect from the trees and the irrigation response. This is not an issue for the internal validity of the results as it is an equilibrium response, but would be important for external validity (i.e., whether we expect places to respond with irrigation or not would have an effect on the total climate effects) and for comparison with scientific model outputs.

Table S15 is informative: we do not find statistically significantly different effects of the

Table S14: Impact of Great Plains Shelterbelt on irrigation, by groundwater irrigation potential

	Dependent variable:			
	Irrigated Farmland Area			
	Log		Level	
	(1)	(2)	(3)	(4)
Wind Exposure:Post 1942	0.626^{***}	0.645^{***}	18.786^{***}	17.763^{***}
	(0.147)	(0.141)	(5.416)	(5.403)
	[<0.001]	[<0.001]	[0.001]	[0.002]
Wind Exposure:Post 1942:Ogallala	-1.296^{***}	-0.636	-50.812^{***}	-21.937^{**}
	(0.388)	(0.415)	(13.172)	(10.485)
	[0.001]	[0.127]	[<0.001]	[0.037]
Post 1942:Ogallala	1.267^{***}	0.876^{***}	32.357^{***}	15.651^{***}
	(0.117)	(0.138)	(6.536)	(4.594)
	[<0.001]	[<0.001]	[<0.001]	[0.001]
Controls	No	Yes	No	Yes
Coef. sum (rows 1 + 2)	-0.67	0.009	-32.026	-4.174
P-value sum	0.063	0.983	0.001	0.651
Mean in Ogallala	0.53	0.53	7.46	7.46
Mean outside Ogallala	0.08	0.08	0.84	0.84
Observations	4,304	4,304	4,304	4,304

Notes: Table shows results for estimating a version of Equation 1 with a triple interaction of wind exposure, Post-1942, and Ogallala indicator. The Ogallala indicator equals 1 when at least part of the county is located over the Ogallala aquifer, a major source of potential groundwater irrigation. Sample of 539 counties outside the Shelterbelt and with centroids within 300km of the centroids of Shelterbelt counties, from 1930 to 1965. Dependent variables are the area of irrigated farmland (in thousands of acres), and its logged value, using $\log(x+1)$ (so counties with no irrigation enter as zero). The "Mean" measures are taken in the pre-1942 period, and are reported separately for the Ogallala and non-Ogallala counties. The main independent variable is wind exposure (w_i), which measures approximate exposure to winds from afforested areas, interacted by a post-treatment dummy. "Coef. sum" corresponds to the point estimate of the Wind Exposure X Post 1942 for the Ogallala counties, and "P-value sum" the corresponding p-value. Columns 2 and 4 include time-invariant controls for elevation and ruggedness, interacted by year. County and state-by-year FE are included. Standard errors are clustered at the county level, shown in parentheses; p-values shown in brackets (*p<0.1; **p<0.05; ***p<0.01).

Shelterbelt on the downwind climate for Ogallala and non-Ogallala counties. As such, while irrigation does increase downwind outside the Ogallala, the magnitude of the effect is not large enough to drive a significant change in the local climate. We can therefore interpret our climate effects as being driven primarily by the tree-planting itself, rather than from a second-order effect through an irrigation response.

Table S15: Impact of Great Plains Shelterbelt on summer county climate, by groundwater irrigation potential

	Dependent variable:			
	Precipitation	Mean Temp	Max Temp	Degree Days
	(cm)	(C)	(C)	(29C)
	(1)	(2)	(3)	(4)
Wind Exposure:Post 1942	1.083***	−0.445***	−0.772***	−9.167***
	(0.280)	(0.109)	(0.131)	(1.348)
	[<0.001]	[<0.001]	[<0.001]	[<0.001]
Wind Exposure:Post 1942:Ogallala	0.345	−0.104	0.317	0.896
	(0.565)	(0.160)	(0.226)	(2.069)
	[0.542]	[0.518]	[0.162]	[0.665]
Post 1942:Ogallala	0.264*	−0.135**	−0.269***	−2.399***
	(0.152)	(0.053)	(0.082)	(0.670)
	[0.083]	[0.011]	[0.002]	[<0.001]
Coef. sum (rows 1 + 2)	1.428	-0.549	-0.455	-8.271
P-value sum	0.007	0	0.021	0
Mean in Ogallala	5.87	24.61	32.75	40.11
Mean outside Ogallala	7.71	24.36	31.52	35.48
Observations	19,404	19,404	19,404	19,404

Notes: Table shows results for estimating Equation 1, with a triple interaction of wind exposure, Post-1942, and ogallala indicator. The Ogallala indicator equals 1 when at least part of the county is located over the Ogallala aquifer, a major source of potential groundwater irrigation. Sample of 539 counties outside the Shelterbelt and with centroids within 300km of the centroids of Shelterbelt counties, from 1930 to 1965. Dependent variables are the annual average of each month's average climate for June, July, and August. The "Mean" measures are taken in the pre-1942 period, and are reported separately for the Ogallala and non-Ogallala counties. The main independent variable is wind exposure (w_i), which measures approximate exposure to winds from afforested areas, interacted by a post-treatment dummy. "Coef. sum" corresponds to the point estimate of the Wind Exposure X Post 1942 for the Ogallala counties, and "P-value sum" the corresponding p-value. Time-invariant controls, interacted by year, include elevation and ruggedness. County and state-by-year FE are included. Standard errors are clustered at the county level, shown in parentheses; p-values shown in brackets (*p<0.1; **p<0.05; ***p<0.01).